DOE-HTGR-90257
Revision 0

MHTGR FUEL PROCESS AND QUALITY CONTROL DESCRIPTION

AUTHORS/CONTRACTORS

GENERAL ATOMICS

ISSUED BY GENERAL ATOMICS
FOR THE DEPARTMENT OF ENERGY
CONTRACT DE-AC03-89SF17885

SEPTEMBER 1991

DOE-HTGR-90257
Revision 0

CAUTION

Do not publicly release this document.

This technical report is being transmitted in advance of DOE patent clearance and no further dissemination or publication shall be made of the report without prior approval of the DOE Patent Counsel.

This document will be returned upon request or when no longer needed, unless notification has been received that this document has been cleared for release or publication.

REV. 0
DOE PATENT
10-25-91

MHTGR FUEL PROCESS AND QUALITY CONTROL DESCRIPTION

APPLIED TECHNOLOGY

Any Further Distribution by any Holder of this Document or Data Therein to Third Parties Representing Foreign Interest, Foreign Governments, Foreign Companies, and Foreign Subsidiaries or Foreign Divisions of U.S. Companies Shall be Approved by the Associate Deputy Assistant Secretary for Reactor Systems, Development and Technology, U.S. Department of Energy. Further, Foreign Party Release May Require DOE Approval Pursuant to Federal Regulation 10 CFR Part 810, and/or May Be Subject to Section 127 of the Atomic Energy Act.

Issued By:
General Atomics
P.O. Box 85608
San Diego, California 92186-9784

DOE CONTRACT DE-AC03-89SF17885

GA Project 6300

SEPTEMBER 1991

GENERAL ATOMICS

GA 1485 (REV. 9/89) ROLL 2233

ISSUE/RELEASE SUMMARY

☐ R&D ☒ DV&S ☐ DESIGN	APPVL LEVEL	DISC.	QA LEVEL	SAFETY	SYS	DOC. TYPE	PROJECT	DOCUMENT NO.	REV
	5	N	N/A	N/A	11	RGE	6300	DOE-HTGR-90257	0
			SEISMIC N/A	ELECTRICAL N/A					

TITLE: 450 MW(t)
MHTGR FUEL PROCESS AND QUALITY CONTROL DESCRIPTION

CM APPROVAL/ DATE	REV	PREPARED BY	APPROVAL(S) ENGINEERING	QA	PROJECT	REVISION DESCRIPTION/ W.O. NO.
INFO 1 SEP 27 1991	0	S.Bresnick	R.Turner R.Klapka Interface Assurance	R.Maxwell	F.S.Ople	Initial Issue 7617115002 WBS 1711.5 M/S C17115.04

CONTINUE ON GA FORM 1485-1

*See list of effective pages

NON-CONTROLLED COPY
VERIFY ISSUE STATUS
WITH DOCUMENT CONTROL
PRIOR TO USE

NEXT INDENTURED DOCUMENT(S)

DOE-HTGR-90011

LIST OF EFFECTIVE PAGES

Page Number	Page Count	Revision
Issue Summary	1	0
i through ix	9	0
1-1 through 1-10	10	0
2-1 through 2-7	7	0
3-1 through 3-22	22	0
4-1 through 4-4	4	0
5-1 through 5-41	41	0
6-1 through 6-33	33	0
7-1 through 7-32	32	0
8-1 through 8-7	7	0
9-1 through 9-31	31	0
10-1 through 10-4	4	0
A-1 through A-19	19	0
B-1 through B-2	2	0
Total Pages	222	

CONTENTS

FIGURES

FIGURES (Continued)

TABLES

1. EXECUTIVE SUMMARY

This document describes the fabrication processes and the quality control techniques that will assure highly reliable performance of Modular High-Temperature Gas-Cooled Reactor (MHTGR) fuel. This information is provided in support of MHTGR performance and safety evaluations.

A key MHTGR concept is the coated particle fuel, which serves as a miniature fission product containment vessel. The refractory nature of the fuel materials assures a high degree of fission product retention and passive safety under severe service and accident conditions.

Successful operation of the MHTGR is dependent on predictable performance of the fuel. The fuel must generate the required nuclear fission heat and retain fission products during its lifetime while limiting coating failures to levels within the design envelope. Manufacturing and inspecting the fuel are critical steps in assuring the performance necessary for the success of the reactor system.

The development and demonstration of MHTGR fuel concepts has taken place over the past three decades through private and governmental programs at General Atomics and at other organizations throughout the U.S., Europe (UK, FRG, France), and Japan. The current fuel design and manufacturing processes represent an evolution and refinement of the specification, manufacturing processes, and inspection methods, based on the development, manufacturing, and irradiation performance experience of the past 30-plus years.

1.1. PROCESS SUMMARY

MHTGR fuel is manufactured in four sequential stages:

- Fuel kernel manufacture
- Coating the fuel kernels
- Compacting coated particles
- Assembling fuel blocks

These four stages are summarized below.

1.1.1. Fuel Kernel Manufacture

Spherical ceramic nuclear materials are fabricated by a process that yields kernels with high density and highly uniform shape and composition.

The process commences with formation of uniform size droplets through vibrating needles, each droplet containing a precise amount of heavy metal. The process includes gelation of the droplets by the diffusion of a chemical reactant (ammonia) from outside the spherical droplets into the body of the droplet. An alternate process not described in this report, internal gelation, requires a hardener reactant inside the droplet.

The droplets are countercurrently washed in solutions that complete the gelling process and remove undesirable byproducts. After the washing process is completed, the gelled microspheres are dried in a rotary oven and then undergo a controlled heat treatment that sinters the microspheres into dense ceramic spheres.

Two variations of the same process are used to produce fissile and fertile kernels. The gel supported precipitate (GSP) process is used to manufacture uranium oxycarbide (UCO) fissile kernels. These kernels are

a two-phase mixture containing 85% UO_2 and 15% UC_2. The sol-gel process is used to manufacture thorium oxide (ThO_2) fertile kernels.

In the GSP process, a water soluble polymer is added to increase the viscosity of the droplets. The polymer is also the source of carbon that drives the carbothermic reduction of UO_3 feed to UO_2 and partially reacts with UO_2 to form UC_2. A change in pH of the droplets caused by reaction with ammonia causes precipitation of the substrate within the polymer matrix. Gelled microspheres are heat treated to obtain hard, dense ceramic kernels.

In the thorium sol-gel method, denitration of thorium nitrate forms a stable sol in spherical droplets that are gelled in the presence of ammonia. Then the kernels are heat treated to obtain dense microspheres.

1.1.2. Coated Fuel Particles

Uranium oxycarbide (UCO) or thorium oxide (ThO_2) kernels are coated with eight layers of pyrolytic carbon (PyC) and silicon carbide (SiC) to make up the TRISO coating. TRISO is a name selected early in the HTGR development for fuel particle coatings consisting of three materials: low-density buffer PyC, high-density PyC and SiC. This ceramic coating acts as a miniature containment vessel for fission products.

1.1.2.1. Coating Methods. Coatings are applied in a high-temperature fluid bed system in a sequential process, with quality control verification after each coating step. The eight coating layers from the kernel out are:

1. PyC buffer
2. PyC seal coat
3. Inner PyC (IPyC)
4. SiC

5. Outer PyC (OPyC)
6. PyC seal coat
7. Protective low-density PyC (PPyC)
8. PyC seal coat

Two coating methods are used, depending on the material applied:

1. PyC coating is accomplished by flowing acetylene, propylene, or mixtures of those gases into the coater hot zone, where they decompose and deposit PyC on the fluidized particles.

2. SiC coating is accomplished by the thermal decomposition of methyltrichlorosilane, which is carried into the coater as a vapor with a hydrogen stream.

During coating layer deposition, carrier gas specified as hydrogen or argon fluidizes the bed while the temperature is raised to the proper level. For IPyC and OPyC coating, a diluent gas of helium or hydrogen is introduced to control the deposition rate.

1.1.2.2. Coating Functions and Characteristics. Each coating layer performs a specific function, and therefore requires certain characteristics as described below.

The PyC buffer (layer 1) provides void volume to collect fission products and allow for dimensional changes in the kernel during irradiation. Buffer coating porosity is the critical parameter in this layer.

Seal coatings (layers 2, 6, and 8) are applied between the buffer and IPyC, between the OPyC and the PPyC, and on the exterior of the finished particle. The first seal coating separates the buffer and IPyC to facilitate measurement of the IPyC coating density. The second seal coating protects the OPyC from failure induced by shrinkage and failure

of the PPyC. The third seal coating facilitates flow of the particles through metering and blending equipment during compact formation.

The IPyC (layer 3) provides a high-density coating to protect the kernel from HCl attack during SiC deposition. It also provides a secondary protective layer between the kernel and the SiC coating. High density is required to ensure good irradiation performance and to prevent HCl formed during the subsequent SiC coating process from reaching the fuel assemblies. Therefore, dense impermeable structures are desired.

The SiC (layer 4) is the primary load bearing member and fission product diffusion barrier in the fuel particle system. It requires high strength to resist stresses imposed by the internal gas pressure generated as the result of fissioning.

The OPyC (layer 5) coating provides a secondary barrier to the release of fission gases, protects the SiC from external gas reaction, and provides compressive prestressing of the SiC layer to improve its function as the primary pressure boundary. The OPyC layer must assure as low a permeability as possible to fission gasses while maintaining structural integrity during irradiation.

The outer PPyC (layer 7) provides an interface layer between the coated particle and the compact matrix to prevent damaging the OPyC or SiC during compact formation. This low-density layer cushions the inner layer from compressive loads; it is not required as a fission-protective barrier.

1.1.3. Fuel Compacts

For handling and performance considerations, the coated fuel particles are incorporated into small solid cylinders, called fuel compacts, for placement within the fuel assmblies. The particles are bound

together in each compact with a carbonaceous matrix binder. The manufacturing process involves several steps for combining the fuel particles and other raw materials and forming them into compacts. The matrix is first formulated by mixing heated petroleum pitch, graphite filler, and selected additives, then granulating the cooled and hardened matrix cakes. Fuel and graphite shim particles are accurately weighed and blended, then loaded into steel mold cavities where the heated, fluidized matrix is pressure injected to form green rods. A two-step, inert gas heat treatment drives off matrix volatiles and achieves first carbonization, then a limited graphitization of the compact binder.

The goal of the compact manufacturing process is to incorporate fuel particles into the compacts without damaging particles or introducing contaminants into the reactor. Experience and testing have shown the relationship between key process parameters and compact product attributes. Accordingly, key parameters such as injection pressure, speed and temperature, as well as heat treatment time and temperature, are specified and controlled to minimize mechanical loads applied to particles. Process temperatures, furnace heating rates, and gas flows are likewise controlled to avoid thermal shocks and adverse chemical reactions.

1.1.4. Fuel Block Assembly

As the final stage in fuel assembly, stacks of compacts are installed in a machined, hexagonal, nuclear grade graphite block. The graphite block is cleaned and heated to drive off moisture. Aluminum tubes are used to stack the compacts and transfer them into predrilled holes in the block. Once all holes in the block have been filled, the compacts are sealed in place with graphite plugs and the entire assembly is cured. The block is then packaged for shipment.

1.2. PRODUCTION QUALITY CONTROL

Nearly all MHTGR fuel product attribute specifications and the quality control methods employed to determine conformance of MHTGR fuel to these specifications are based on statistical sampling and analyses. This approach is dictated by the large size of the fuel product populations (e.g., kernels, coated particles, and compacts), and by the destructive test methods used to measure many of the specified properties. (A reactor core contains about 10 billion coated fuel particles in two million fuel compacts.)

The quality control approach employed to determine the acceptability of the fuel with respect to a particular product specification (except for those few for which 100% inspection is performed), is to (1) collect a sample representative of the population, (2) measure the property of interest, and (3) apply a statistical test to determine the acceptability of the population based on the test results for the sample. Given this approach, the following are vital to assure that MHTGR fuel meets the requirements of the Fuel Product Specification:

- Sampling techniques which assure that the samples obtained for quality control testing are representative of the parent populations.

- Test methods that accurately measure the specified properties of the fuel.

- Sound statistical methods which can be used to demonstrate that population properties meet specification requirements at the specified confidence levels based on test results from samples.

To maintain uniformity of the fuel and reduce quality control costs, the practice of compositing is utilized in MHTGR fuel manufacturing. A composite is a homogeneous blend of two or more batches of

kernels and or particles. The kernel/coated-particle composite and the compact lot are the basic units of MHTGR fuel subject to acceptance testing. Samples are randomly selected from these production units using technically sound compositing and sampling techniques that have been demonstrated to yield representative samples through long use in Fort St. Vrain (FSV) fuel manufacturing. These techniques include particulate sampling methods such as riffle, rotary, and 10-way splitting.

As with the sampling techniques, most quality control test methods employed to characterize the fuel have been thoroughly demonstrated through long use in FSV fuel manufacturing. With the exception of a few techniques unique to quality control of MHTGR fuel, these methods are either direct applications of American Society for Testing Materials (ASTM) methods, or adaptations of ASTM methods. Control standards traceable to National Institute of Standards and Technology (NIST) or the New Brunswick Laboratory (NBL) are used to ensure the accuracy of applicable quality control test methods.

Each specified fuel property is one of two types, attribute or variable. An attribute property is a discrete property in the sense that the product is either good or bad. The acceptance criteria for an attribute property are stated in terms of an allowable fraction of defects.

A variable property is defined by a continuous distribution of values. The acceptance criteria for a variable property are stated in terms of the population mean and/or the population dispersion. For the population mean, the criterion is that the mean must lie within a specified interval. For population dispersion, the criterion is that no more than a specified fraction of the population be greater and/or less than certain specified values, called critical limits for the population.

Sampling plans and acceptance tests for attribute properties are based on the binomial or the hypergeometric distribution. Sampling

plans and statistical acceptance tests for variable properties are based on the normal distribution.

When using statistical acceptance testing, there is a chance of making a wrong decision concerning the acceptability of the population. Two types of wrong decisions can be made. The first is when a population that does not meet the specifications is accepted (false acceptance). The second is when a population that does meet the specifications is rejected (false rejection). The risk of false acceptance (i.e., the consumer's risk) is limited by the Fuel Product Specification, which imposes a 95% confidence requirement on virtually all statistical specifications. The risk of false rejection (i.e., the manufacturer's risk) is not fixed; it is affected by the sample size and the quality of the fuel relative to the specification limits.

The manufacturer must target a product quality level that significantly exceeds specification requirements; develop a process capable of meeting these quality goals, and implement statistical process control (SPC) as part of the manufacturing process to maintain average product quality at the desired level. These considerations are important to the consumer as well as to the manufacturer because, from a practical standpoint, the use of sampling inspection and statistical methods virtually guarantees the consumer an average fuel quality that exceeds that required by the Fuel Product Specification.

1.3. REPORT CONTENTS

This report is not intended as a stand-alone design document, but rather to inform technically cognizant personnel on matters related to fuel manufacturing and inspection. The report consists of 10 sections. This section provides a report overview. Section 2 provides a general description of the MHTGR and an introduction to the fuel. Section 3 discusses design and fuel quality requirements.

Section 4 contains process flow diagrams for the four major fuel operations (kernel manufacturing, coating, compacting, and fuel assembly). Sections 5 through 8 provide detailed information on the manufacturing processes for kernels, coated particles, compacts, and fuel assemblies.

Section 9 explains the quality control methods used to assure that high-quality fuel is produced, and that only fuel which meets or exceeds the specification is released for reactor use. Because of the important role of statistical sampling in the quality control of MHTGR fuel, a discussion of the statistical approach and background is also provided in Section 9, with supplementary information on attribute and variable sampling provided in Appendix A.

Section 10 lists references for the entire report. A list of acronyms and abbreviations with their meanings is provided in Appendix B.

2. INTRODUCTION

A clear goal of the United States Department of Energy's Reactor Development Program is to enhance public acceptability of nuclear energy by providing an economic power source with intrinsic safety. The MHTGR is an advanced reactor concept under development in a cooperative program involving the U.S. Government, the nuclear industry and a group of supporting utility companies.

The design of the MHTGR has been guided by specific quantified requirements as defined by utility-user specifications (Ref. 2-1) and top-level regulatory requirements (Ref. 2-2). Stringent safety requirements have led to a design that uses high temperature ceramic materials and passive safety features to assure radionuclide retention at the source of fission.

Thus, the MHTGR containment system is composed of multiple barriers from the core out to the reactor building. This system of barriers places primary emphasis on the ceramic coated fuel particles within the reactor core.

The reference MHTGR plant consists of four identical reactor modules, each sized for a nominal power of 350 MW(t). Each module is housed in a vertical cylindrical concrete enclosure that is fully embedded in the earth. The primary components of a module are the steel reactor vessel, a steam generator vessel and a connecting coaxial cross vessel, as shown in Fig. 2-1. The reactor vessel contains the core, graphite reflectors, metallic core support structures and top penetrations in which the control rod drive mechanisms and refueling machines are inserted.

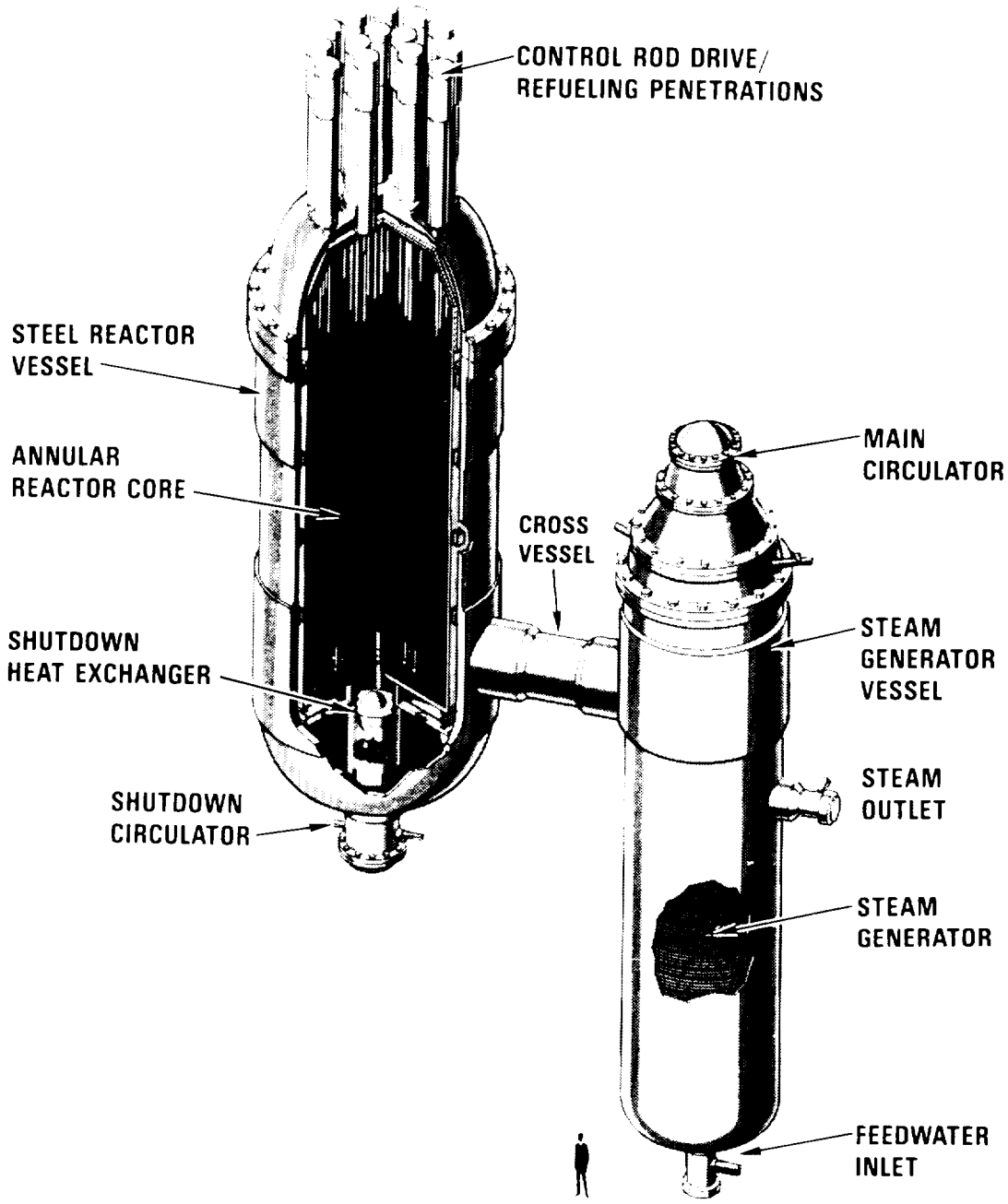

Fig. 2-1. Components of the modular HTGR

The graphite-moderated, helium cooled reactor core utilizes prismatic hexagonal fuel elements (Fig. 2-2) as employed in the FSV reactor. The fuel consists of coated particles of 19.8% enriched fissile UCO and fertile particles containing thorium oxide (Ref. 2-3). The coated particles are bonded within fuel compacts that are contained inside drilled vertical holes within the hexagonal graphite blocks. The active core for a 350 MW(t) module contains 660 fuel elements in 66 columns.

The MHTGR design depends upon the superior material properties of the coated particle fuel. The objectives for development of low-defect fuel for the MHTGR were defined by a disciplined functional analysis approach which began with the top-level plant requirements. A safe and economical plant has been designed through the pursuit of four fundamental goals:

Goal 1. Maintain Plant Operation
Reliably maintain the functions necessary for normal plant operations, including the plant states of energy production, shutdown, refueling, and startup/shutdown operations.

Goal 2. Maintain Plant Protection
Assume that despite the care taken to maintain plant operation, failures will occur; then provide additional design features or systems to ensure availability and investment protection by preventing plant damage.

Goal 3. Maintain Control of Radionuclide Release
Provide additional design features or systems to assure containment of radionuclides in the event normal operating conditions cannot be maintained and/or plant protection cannot be assured.

Goal 4. Maintain Emergency Preparedness
Maintain adequate emergency preparedness to protect the

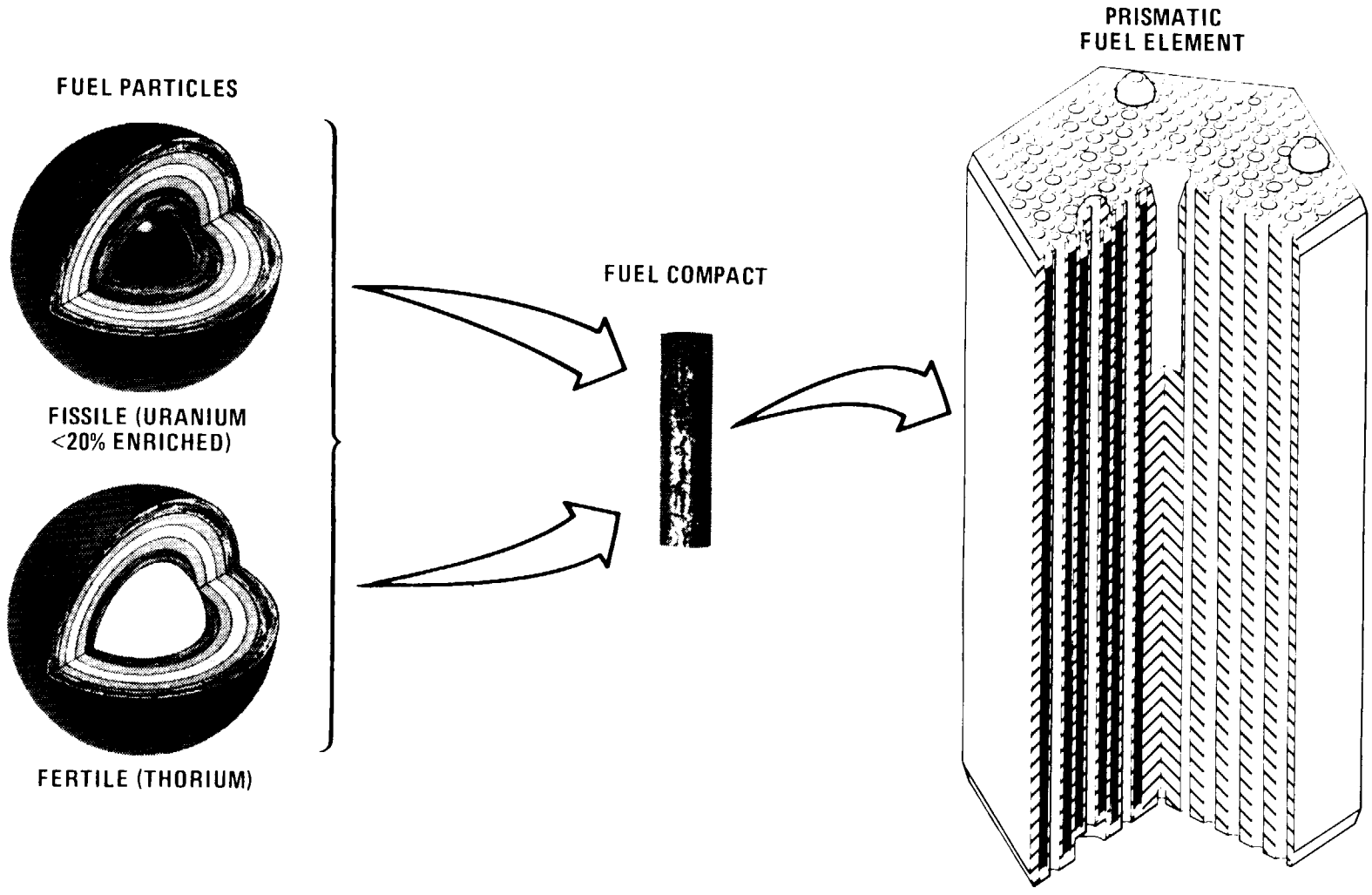

Fig. 2-2. Modular HTGR fuel components

health and safety of the public in the event control of radionuclide release is not accomplished.

To achieve the regulatory criteria for Goals 1 and 2, the design of the MHTGR incorporates inherent characteristics for assuring that normal operational, or any accidental, radionuclide releases of primary circuit activity are low, and that worker exposures are minimized. These techniques have proven effective in other gas-cooled reactors, as demonstrated by low radionuclide releases and worker exposures measured during plant operations in the U.S., Germany, and England.

The unique aspect of the MHTGR design, however, is the approach taken to achieve Goal 3, Control of Radionuclide Release During Abnormal Conditions. To accomplish this goal with high assurance, MHTGR design philosophy places primary emphasis on control of radionuclide releases by retention within the coated fuel particles. The approach minimizes reliance on active design features or operator actions.

The refractory-coated fuel particle has demonstrated its capability to retain fission products under even severe conditions during over 30 years of use. During this period, process optimization and experience with the technology have resulted in continuous product improvement.

A very large quantity of coated particle fuel has been fabricated in the United States and Germany for use in gas-cooled reactors. General Atomics (GA) has operated fuel development and manufacturing facilities in San Diego, California in support of fuel assemblies for Peach Bottom I, Nerva, Rover, UHTREX, FSV, Compact Nuclear Power Source (CNPS), and the New Production Reactor (NPR). Since 1962, approximately 50,000 kgs of coated particle fuels have been fabricated in the Sorrento Valley Fuel Facility at GA.

Substantial quantities of coated particle fuels have been fabricated by NUKEM Company in Germany since 1965. More than 10,000 kgs of coated

particles were made for the AVR and THTR reactors before the NUKEM facility was decommissioned in 1990. At NUKEM, approximately 250 kgs of coated fuel particles were made to the high quality level required for the MHTGR.

The evolution of HTGR fuel quality is shown graphically in Fig. 2-3. The ordinate, which is the measure of accessible uranium by a burn-leach technique, is plotted for significant lots of coated particle fuel fabricated in the U.S. and Germany since 1970. The burn-leach measurement is a direct indicator of the potential fission gas release from fabricated fuel assemblies. The components of leachable U are the sources in defective SiC coatings and distributed contamination. As Fig. 2-3 indicates, there has been continuous quality improvement in both the U.S. (at GA) and the German (at NUKEM) programs.

Two campaigns of high quality MHTGR-type fuel have been fabricated in the developmental facilities at GA. In 1986-87, 44 kgs of coated particles were fabricated to low defect levels. Of this material, 2 kgs were fabricated into fuel compacts for irradiation tests. Fuel from this campaign is in the HRB-21 capsule test, which began operation in the High Flux Isotope Reactor (HFIR) at Oak Ridge National Laboratory (ORNL) in June 1991. The second campaign of high quality fuel was completed at GA in May 1991 for the NPR Test Fuel Program. This fuel showed the lowest defect levels measured on coated particle fuel in the U.S., at a level of 3×10^{-6} fraction of defective SiC layers and uranium contamination. NPR fuel began irradiation testing in the HFIR in July 1991, and is scheduled for irradiation in the Advanced Test Reactor at Idaho Nuclear Engineering Laboratory in Fall 1991.

In 1991, GA and Babcock & Wilcox Naval Nuclear Fuel Division formed a general partnership, TRISO, whose primary product will be the supply of both high and low enriched coated particle fuel for the NPR-MHTGR and the commercial MHTGR.

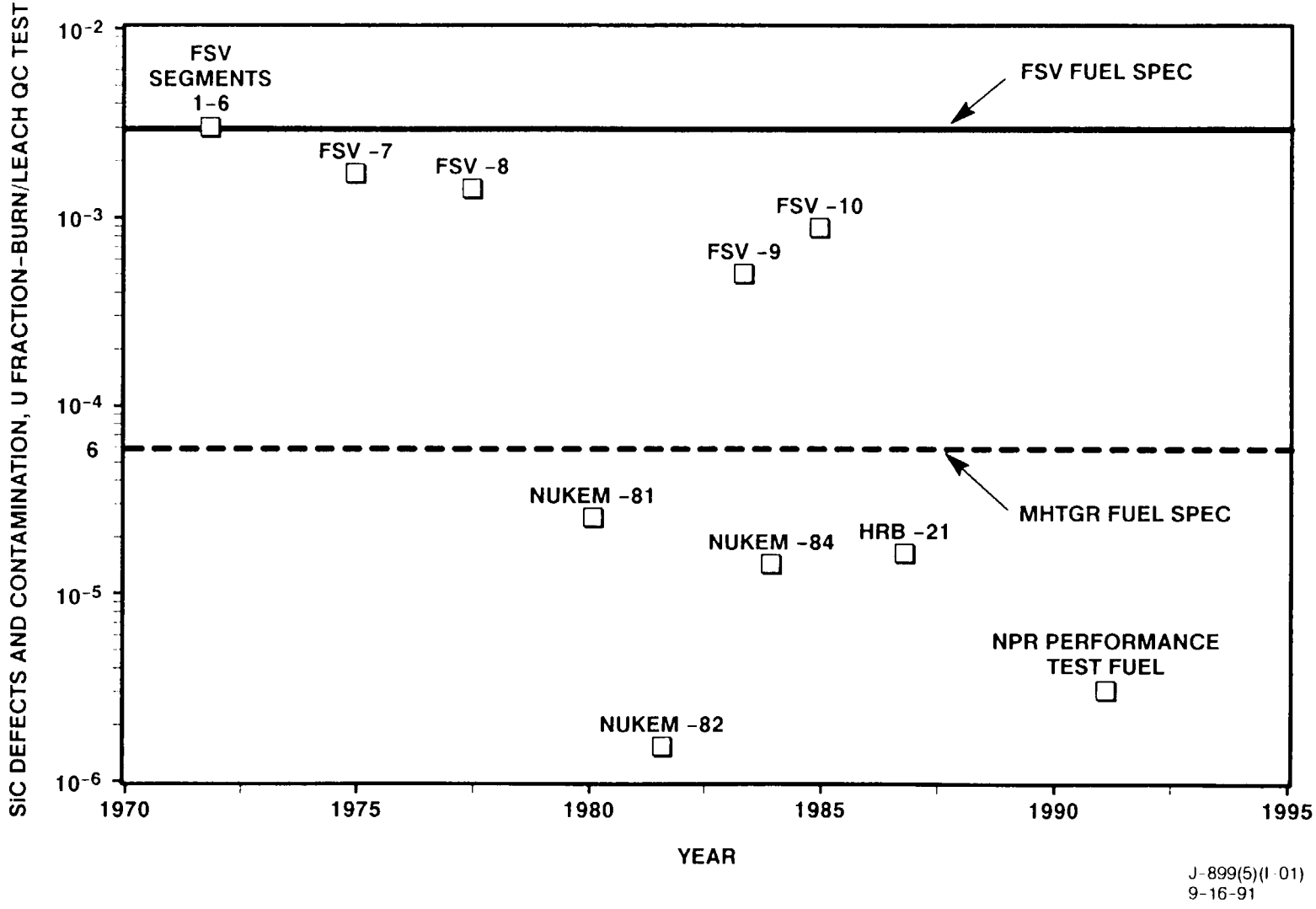

Fig. 2-3. Evolution of HTGR fuel quality

3. FUEL PRODUCT REQUIREMENTS

3.1. SELECTION OF RADIONUCLIDE BARRIERS

The Fuel Product Requirements have been defined using the functional analyses approach as applied to the design of the total reactor plant. The radionuclide containment system design has included quantified limits on the performance of barriers from the core to the offsite environment.

The five principal radionuclide release barriers are: (1) the fuel kernel, (2) the particle coatings, particularly the SiC coating, (3) the fuel-element structural graphite, (4) the primary coolant pressure boundary and (5) the reactor building. Of these multiple barriers, the particle coatings are by far the most important because they provide the largest attenuation factor for the holdup of radionuclides. The in-reactor performance characteristics of the coated-particle fuel are governed by the as-manufactured attributes and the levels of quality control. The quality requirements for the fuel are documented in the Fuel Product Specification for the MHTGR (Ref. 3-1).

The fuel requirements are fundamental to allocating retention factors for radionuclide barriers. The fuel barrier limits were arrived at from iteration of the following: (1) fuel performance under normal and accident conditions as calculated in fuel performance models, (2) practical limitations on the capability of fuel process technology to produce fuel materials with optimum properties, and (3) plant design criteria, which are defined on the basis of optimizing plant performance within material design constraints. Figure 3-1 shows the logic for interactions among the primary areas required to define the fuel and plant components design. The component allocations for both fuel and

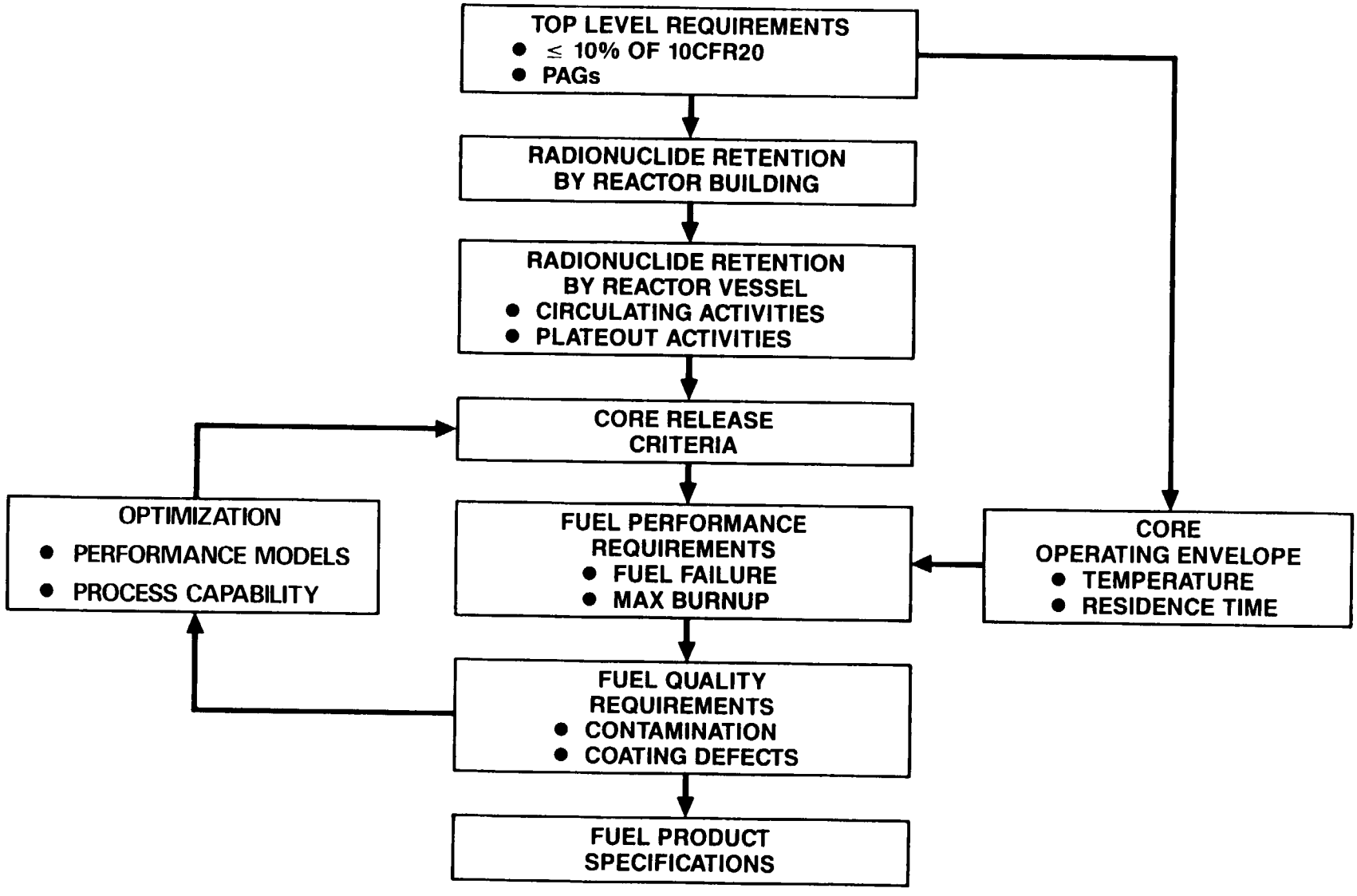

Fig. 3-1. Interactions to define fuel/plant components

plant systems are examined in the sequence shown, then selected in the optimization step.

Key top-level requirements which define radionuclide control requirements are summarized in Table 3-1. The most constraining radionuclide control requirement for the MHTGR is to comply with the dose limits specified in the Environmental Protection Agency Protective Action Guides (PAGs) at the Exclusion Area Boundary (EAB). This allows the Emergency Planing Zone (EPZ) to be located at the EAB, precluding the need for public sheltering and evacuation plans. The PAGs limit both whole body and thyroid doses; these dose limits were used to derive allowable environmental releases of noble gases and iodines, respectively, during Licensing Basis Events (LBEs). The intent of the plant design and the fuel specification is to meet the PAG limits with margin.

The second, most constraining, top-level radionuclide control requirement is to limit the occupational exposure to <10% of 10CFR20. In the derivation, the <10% of the 10CFR20 requirement was analyzed to be met if the gamma radiation fields around the primary circuit due to fission product plateout were limited to <10 mR/hr for scheduled maintenance activities, such as in-service inspection, and to <100 mR/hr for unscheduled maintenance activities, such as steam generator tube plugging. These limits on gamma dose rates were in turn used to set best-estimate limits on primary circuit plateout activity, particularly the cesium and silver isotopes.

3.2. FUEL QUALITY REQUIREMENTS

While each of the barriers contributes to the capability of the plant to meet top-level requirements, the TRISO fuel particle is the critical component. The viability of the MHTGR design fundamentally depends on the ability to mass-produce high-integrity, coated-particle fuel, and to demonstrate that the fuel maintains its high integrity sufficiently during normal operation and LBEs. Fuel behavior in the reactor is evaluated with performance models based on mathematical

TABLE 3-1
KEY TOP-LEVEL REQUIREMENTS WHICH DEFINE RADIONUCLIDE CONTROL

TOP-LEVEL REGULATORY REQUIREMENTS

1. 10CFR50, Appendix I, Limits for Radionuclides in Plant Effluents:
   a. Whole Body Dose ≤5 mrem/year
   b. Thyroid Dose ≤15 mrem/year
2. 10CFR20 Occupational Dose Limits:
   a. Whole Body Dose ≤5 rem/year
   b. Thyroid Dose ≤15 rem/year
3. 10CFR100 Offsite Dose Limits for Licensing Basis Events:
   a. Whole Body Dose ≤25 rem/event
   b. Thyroid Dose ≤300 rem/event
4. EPA-520 Protection Action Guides (PAGs) for Radioactive Release for Public Sheltering and Evacuation:
   a. Whole Body Dose ≤1 rem/event
   b. Thyroid Dose ≤5 rem/event
5. NRC Safety Risk Limits

UTILITY/USER REQUIREMENTS

1. Achieve Occupational Exposures ≤10% of 10CFR20 Limits:
   a. Whole Body Dose ≤0.5 mrem/year
   b. Thyroid Dose ≤1.5 mrem/year
2. Meet Top-Level Regulatory Criteria, including PAGs at the Exclusion Area boundary for all events with a frequency ≥ 5 x 10-7/year

correlations from fuel tests and reactor experience. These models predict coating failure rates as a function of the as-manufactured fuel attributes and the environmental conditions prevailing in the core during normal operation and LBEs. The required as-manufactured key attributes and variables for MHTGR fuel are quantified with confidence statements on all parameters important to performance (Ref. 3-1).

The fuel specifications have been defined through experience with fuel developed and tested for the FSV reactor, the Arbeitsgemeinschaft Versuch Reaktor, the Thorium High Temperature Reactor and the U.S. DOE Base Technology Program. The fuel specifications address the requirements to limit potential fuel failure mechanisms that have been characterized in tests. The bases for the fuel specification values which eliminate or control the fuel failure mechanisms are presented in the Technical Support Document for the MHTGR Fuel Product Specification (Ref. 3-2).

3.3. COATED FUEL PARTICLE DESIGN

Figure 3-2 shows the coated fuel particle design features for the MHTGR. The design has evolved after 30 years of development for the MHTGR (Ref. 3-3). The fuel kernel of UCO or ThO_2 provides fission energy and retains short-lived fission products. The function performed by each of the coating layers is identified in Fig. 3-2.

The silicon carbide layer is the primary barrier to fission product release from the particles. It is also the predominant structural member that bears the loads from internal gas pressures. The outer dense pyrocarbon is a structural member and a barrier to gaseous fission product release. In those small fractions of coated particles where the SiC layer is defective, the intact outer PyC continues to be an effective barrier for gaseous fission products such as krypton or iodine. A laminar PyC seal coat over the structural outer PyC forms a crack-arresting boundary between the dense PyC and the protective layer. The protective low density PyC is a sacrificial layer that absorbs local

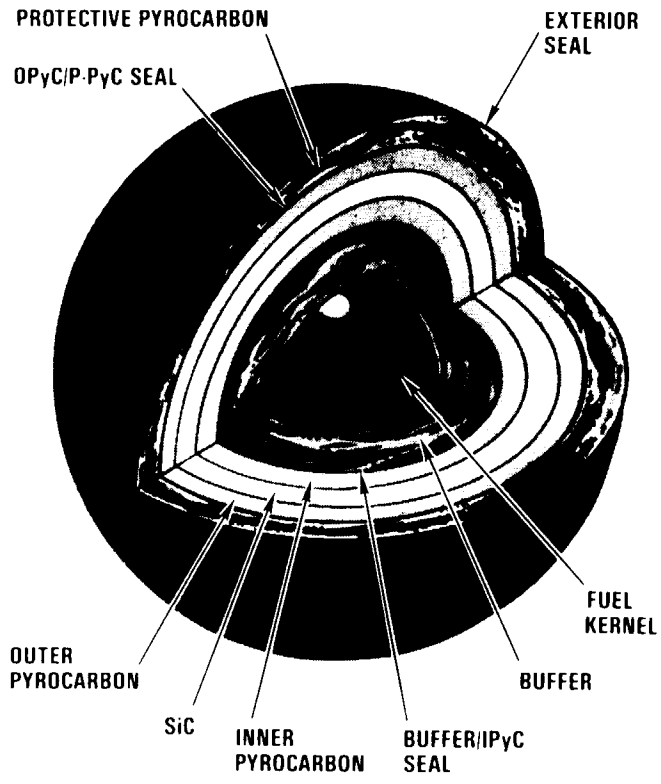

K 185
8 9 91

- FUEL KERNEL
  - PROVIDE FISSION ENERGY
  - RETAIN SHORT LIVED FISSION PRODUCTS
- BUFFER LAYER (POROUS CARBON LAYER)
  - ATTENUATE FISSION RECOILS
  - VOID VOLUME FOR FISSION GASES
- BUFFER/IPyC SEAL
  - FACILITATE IPyC REMOVAL FOR DENSITY MEASUREMENT
- INNER PYROCARBON (IPyC)
  - PROVIDE SUBSTRATE FOR SiC DURING MANUFACTURE
  - PREVENT Cl ATTACK OF KERNEL DURING MANUFACTURE
- SILICON CARBIDE (SiC)
  - PRIMARY LOAD BEARING MEMBER
  - RETAIN GAS AND METAL FISSION PRODUCTS
- OUTER PYROCARBON (OPyC)
  - PROVIDE FISSION PRODUCT BARRIER IN PARTICLES WITH DEFECTIVE SiC
- OPyC/P-PyC SEAL
  - MINIMIZE MECHANICAL COUPLING BETWEEN LAYERS
  - SERVE AS CRACK ARRESTER
- PROTECTIVE PYROCARBON (P-PyC)
  - PROVIDE SOFT, CRUSHABLE LAYER TO PREVENT PARTICLE DAMAGE DURING COMPACT FABRICATION
  - PROVIDE BONDING SURFACE
- EXTERIOR SEAL
  - IMPROVE "FLOWABILITY" OF PARTICLES
  - MINIMIZE MATRIX INTRUSION INTO P-PyC

Fig. 3-2. MHTGR fuel particle design

crushing loads during compact fabrication and provides a bonding surface for the fuel compact matrix. The exterior PyC seal coat prevents ablation of the protective layer during process handling and limits the flow of matrix during fabrication of compacts.

Through testing programs on fuel in the U.S. and Germany, a total of six specific potential failure mechanisms have been identified for the TRISO coated fuel particles. These mechanisms are shown in Table 3-2. The control measures for assuring that these failure mechanisms would be eliminated under the MHTGR conditions are also identified in Table 3-2. The performance of the coated fuel particles is evaluated by analytical models (Ref. 3-4).

3.4. FUEL PRODUCT PROPERTIES REQUIRED DURING MANUFACTURE

The quality of the fuel is assured by a fuel fabrication process in which statistical quality control is maintained for each unit operation. To assure the correct fuel loadings and fuel quality levels for the finished product, more than 80 separate properties must be controlled during manufacture. Property values specified quantitatively must be proven to meet the specifications at a confidence level of 95% or higher. This confidence level was selected to be consistent with the Nuclear Regulatory Commission Standard Review Plans. The following paragraphs describe the limits on the property values and the bases for setting the limits. The limits are discussed separately for the fuel kernels, the TRISO coated particles and the fuel compacts. These properties are consistent with the attributes and variables specified in the Fuel Product Specification (Ref. 3-1). The fuel product units processed at each stage of operation are defined in Fig. 3-3.

3.4.1. Fuel Kernel Requirements

Table 3-3 lists the product qualities to be controlled during kernel fabrication and the limiting values for acceptance of UCO kernels. Table 3-4 lists product qualities for ThO_2 fertile kernels.

TABLE 3-2
POTENTIAL FUEL FAILURE MECHANISMS ELIMINATED BY DESIGN

Failure Mechanism	Control Measures
Pressure-induced failure	Particle mechanical design specifications
	Missing buffer specification
	Kernel composition specification
Irradiation-induced outer pyrocarbon (OPyC) failure	OPyC microporosity specification
Heavy-metal dispersion [defective inner pyrocarbon (IPyC) coating]	IPyC defect specification
SiC/fission product interactions (corrosion)	Core design (time at temperature)
	Kernel composition specification
SiC thermal decomposition	Plant/core design (time at temperature)
Kernel/coating interaction ("Amoeba")	Kernel composition specification
Coating interactions with impurities	Specification of limits on transition metal impurities

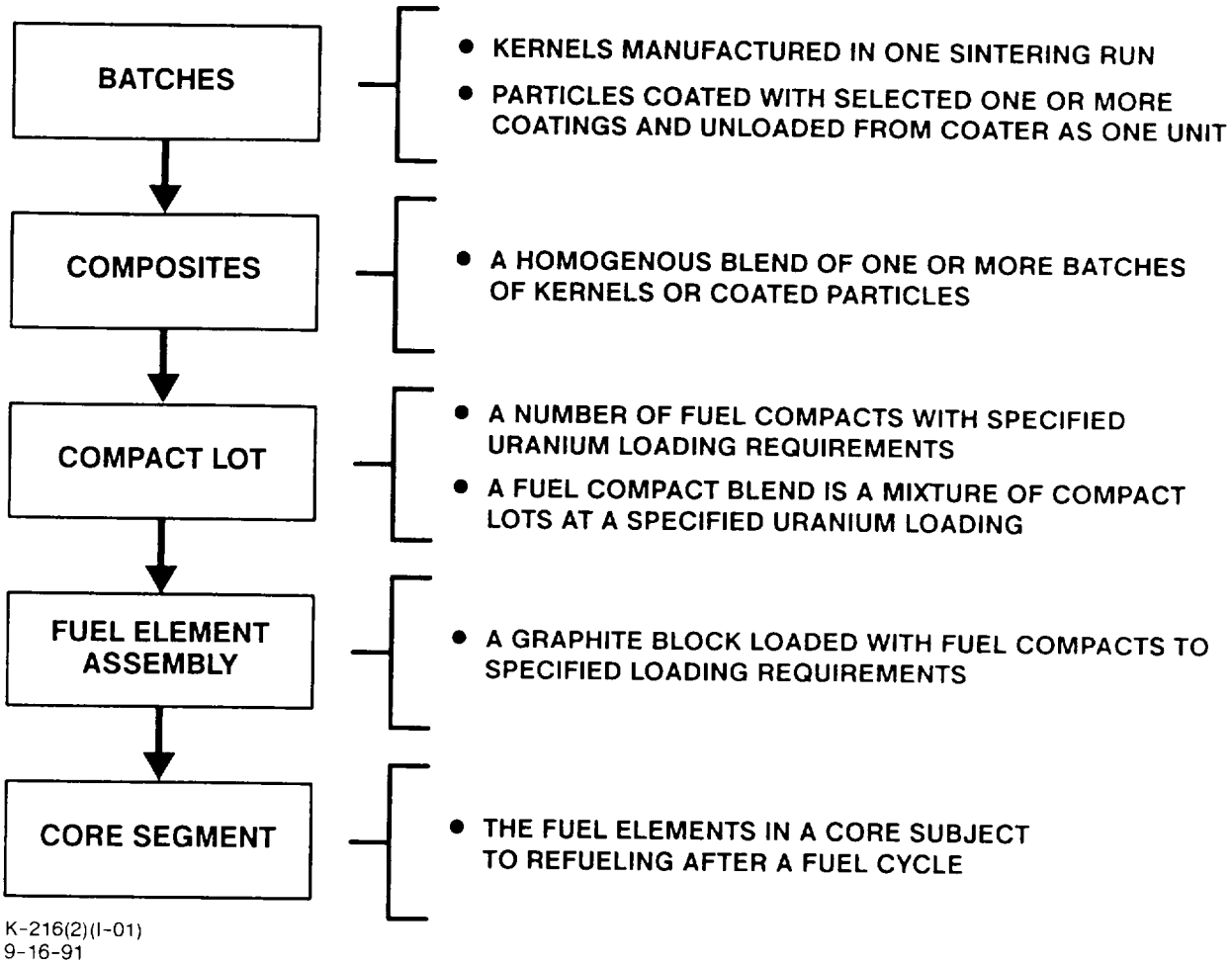

Fig. 3-3. Fuel Product Specification units

TABLE 3-3
UCO KERNEL PARAMETERS

Property	Value[a]	Basis for Limits
Total uranium	≥87.0 wt%	Meet loadings defined by physics analysis
Fissile U-235 enrichment	19.7 to 19.9 wt%	Meet loadings defined by physics analysis
Impurities, each for Al, Ca, Cr, Fe, Mn, Na, Ni, P and Si	≤100 ppm each	Assure chemical stability and limit neutron capture
Carbon/uranium (atomic ratio)	≤0.4	Limit CO generation and kernel migration
Oxygen/uranium (atomic ratio)	1.6 to 1.8	Limit fission product transport and corrosion reactions
Density, Mg/m^3	≥10.5	Assure fission product retention and U loading
Diameter, μm	≤360 μm for lot and ≤0.01 fraction ≥400	Meet design configuration to assure fuel loading and fission product retention

[a]The above limits, current as of the date of this report, are provided for illustration. The official specification limits are contained in the latest revision of Ref. 3-1.

TABLE 3-4
ThO_2 KERNEL PARAMETERS

Property	Value[a]	Basis for Limits
Total thorium	≥87 wt%	Assure loadings from physics analysis
Impurities, each for Al, Ca, Cr, Fe, Na, Ni, Mn, P, and Si	≤100 ppm	Assure chemical stability and limit neutron capture
Density	≥9.50 Mg/M^3	Assure fission product retention and Th loading
Diameter	≤510 μm for lot and ≤0.01 fraction ≥565 μm	Meet design configuration to assure fuel loading and fission product performance

[a]The above limits, current as of the date of this report, are provided for illustration. The official specification limits are contained in the latest revision of Ref. 3-1.

3.4.2. Coated Fuel Particle Requirements

The feed materials for the coated particle operation are the spherical kernels, as described in Section 3.4.1, along with standard coating gases. The coating gases to be used for the various coating layers are listed in Table 3-5.

The coating gases are purchased to well developed procurement specifications, which are the same as used for FSV core fabrication. The chemical composition and level of impurities are controlled to assure reproducible performance in the coater.

Table 3-6 lists product quality requirements at the TRISO coated particle stage for the fissile UCO material. These parameters are defined for a composite of one or more batches discharged from a coating furnace. The normal charge into a coater is 5 Kg of UCO or ThO_2. The fuel manufacturer is permitted to specify the number of coater batches to combine into a composite. All of the parameters in Table 3-6 are established to assure that the coating failure fractions during reactor operation and accidents will meet the design goals. An important aspect of defining fuel quality is to limit the number of coated particles in a composite having dimensions or properties that are outside a specified band or critical limit within a total population. A common term for such coated particles is that they are "tails" in a distribution curve. The last column in Table 3-6 shows the maximum fractions of particles that can exceed the critical limits. The critical limits assure boundaries to the distribution of variables in a population.

Table 3-7 presents the comparable list of product quality parameters for TRISO coated fertile particles.

3.4.3. Fuel Compact Requirements

The feed materials for the fuel compacting step are the coated fuel particles described in Section 3.4.2, the graphite shim particles and

TABLE 3-5
COATING GASES FOR TRISO COATED PARTICLES

Coating Layer	Diluent/Levitation Gas	Active Coating Gas
Buffer PyC	Argon	Acetylene
Seal PyC layers	Argon	Propylene
Inner isotropic PyC	Argon and hydrogen	Acetylene and propylene
Silicon carbide	Hydrogen	Methyltrichlorosilane
Outer isotropic PyC	Argon and hydrogen	Acetylene and propylene
Outer protective PyC	Argon	Acetylene

TABLE 3-6
TRISO COATED LEU FISSILE UCO PARTICLE PARAMETERS

Property	Coating	Limiting Values[a]		
		Composite Mean	Critical Limit	Allowable Fraction Outside Critical Limit
Thickness, μm	Buffer	90-110	≤50	≤0.01
	Seal	(a)	>5	≤0.10
	Inner isotropic	40-60	≤25	≤0.01
	Silicon carbide	≥30	≤20	≤0.01
	Outer isotropic	≥30	≤21	≤0.01
	Seal	2-5	>5	≤0.10
	Protective	35-45	≤20	≤0.01
	Seal	(b)	>5	≤0.10
Density, Mg/m^3	Buffer	0.80-1.10	(b)	(b)
	Inner isotropic	1.85-1.95	≤1.80	≤0.02
	Silicon carbide	≥3.18	<3.17	≤0.01
	Outer isotropic	1.80-1.95	(b)	(b)
	Seal-protective-seal	0.80-1.10	(b)	(b)
Microporosity, ml/m^{-2}-OPyC layer	Outer isotropic	0.9-2.3	(b)	(b)
Anisotropy, BAF_o[c] units	Inner isotropic	≥1.100 ≤1.160	(b)	(b)
	Outer isotropic	(b)	≥1.080	≤0.01
Faceting aspect ratio	Total coated particle	(b)	≥1.20	≤0.10
		Defect		Core Segment Mean
Defective particles fraction	Total coated particle	Missing or incomplete buffer		$\leq 5.0 \times 10^{-5}$
		Missing or incomplete outer isotropic coating		$\leq 1.0 \times 10^{-4}$
		Missing or incomplete protective coating		$\leq 1.0 \times 10^{-3}$

[a]The above limits, current as of the date of this report, are provided for illustration. The official specification limits are contained in the latest revision of Ref. 3-1.

[b]Not specified.

[c]Bacon anisotropy factor.

TABLE 3-7
TRISO COATED FERTILE PARTICLE PARAMETERS

Property	Coating	Limiting Values[a]		
		Composite Mean	Critical Limit	Allowable Fraction Outside Critical Limit
Thickness, μm	Buffer	55-75	≤30	≤0.01
	Seal	(b)	>5	≤0.10
	Inner isotropic	40-60	≤25	≤0.01
	Silicon carbide	≥30	≤20	≤0.01
	Outer isotropic	≥30	≤21	≤0.01
	Seal	2-5	>5	≤0.10
	Protective	35-45	≤20	≤0.01
	Seal	(b)	>5	≤0.10
Density, Mg/m^3	Buffer	0.80-1.10	(b)	(b)
	Inner isotropic	1.85-1.95	≤1.80	≤0.02
	Silicon carbide	≥3.18	<3.17	≤0.01
	Outer isotropic	1.80-1.95	(b)	(b)
	Seal-protective-seal	0.80-1.10	(b)	(b)
Microporosity, ml/m^{-2}-OpYC layer	Outer isotropic	0.9-2.3	(b)	(b)
Anisotropy, BAF_o units	Inner isotropic	≥1.100 ≤1.160	(b)	(b)
	Outer isotropic	(b)	≥1.080	≤0.01
Faceting aspect ratio	Total coated particle	(b)	≥1.20	≤0.10
		Defect		Core Segment Mean
Defective particles fraction	Total coated particle	Missing or incomplete buffer		$\leq 5.0 \times 10^{-5}$
		Missing or incomplete outer isotropic coating		$\leq 1.0 \times 10^{-4}$
		Missing or incomplete protective coating		$\leq 1.0 \times 10^{-3}$

[a]The above limits, current as of the date of this report, are provided for illustration. The official specification limits are contained in the latest revision of Ref. 3-1.

[b]Not specified.

the matrix constituents. Table 3-8 lists the properties required for the shim particles. This material is added solely to fill the space between coated fuel particles before the finer matrix material is injected. The properties required for the matrix constituents are presented in Table 3-9. This is the same matrix formulation that was specified for FSV fuel compacts.

The requirements on fuel quality for heat treated fuel compacts are listed in Table 3-10. Each fuel compact contains approximately 6000 coated fuel particles. Therefore, for a parameter such as the defective SiC layer fraction of 5×10^{-5}, a defective particle would occur in less than one out of three fuel compacts.

3.4.4. Fuel Element Assembly Requirements

There are two types of fuel assemblies in the reactor core: the standard fuel element and the neutron control fuel element. In the total core for the 350 MW(t) MHTGR, there are 540 standard and 120 neutron control fuel elements. The dimensions of the fuel blocks are shown in Fig. 3-4. The only difference between the two types of fuel assemblies is that neutron control fuel elements each have a 3.75-in. diameter hole extending vertically through the assembly. This hole forms a receptacle for the reserve shutdown absorber balls normally held in hoppers above the reactor core.

The heat-treated fuel compacts are loaded into the machined graphite blocks during final assembly. The compacts are loaded into elements in sets requiring a common loading of uranium and thorium. Three axial and three radial fuel loadings are required for a core segment; therefore, a total of nine distinct loading configurations are required for a set of 330 reload elements.

After the fuel compacts are loaded into the graphite blocks, similar compacts containing particles of boron carbide are placed in holes in

TABLE 3-8
GRAPHITE SHIM PARTICLE REQUIREMENTS

Graphite Property	Acceptance Criteria[a]
Grade	Crushed Great Lakes H-451 or National TS-1240, or equivalent
Particle size distribution	99 wt % <1.19 mm (ASTM screen E-11-60-T-1190 μm); 95 wt % >0.59 mm (ASTM screen E-11-60T-595 μm)
Particle shape	Visual standard of approximately cubic shape

[a]The above limits, current as of the date of this report, are provided for illustration. The official specification limits are contained in the latest revision of Ref. 3-1.

TABLE 3-9
MATRIX CONSTITUENTS PROPERTIES

Property	Limiting Values
Pitch and filler grades	Qualified petroleum or coal-tar-derived pitch and graphite filler particles[a]
Matrix additives	Octadecanol and polystyrene
Filler crystallite size	Mean >1000 angstroms
Filler particle size	100 wt % <35 μm
	95 wt % <15 μm
	75 wt % >2 μm

[a]Qualified grades are Ashland Oil Company A240 Grade petroleum pitch and Allied Chemical Company Grade 15V coal-tar-derived pitch, Asbury Mills Grade 6353 natural graphite flake filler, and Lonza KS-15 synthetic graphite filler.

TABLE 3-10
HEAT-TREATED FUEL COMPACT PARAMETERS

Property	Limiting Value[a]	Bases for Limits
Dimensions:		
Diameter (mm)	12.55 ± 0.17	Fit in block and assure heat transfer
Length (mm)	49.3[b]	Assure fuel loading and allow for differential shrinkage
Coke content (g coke/g coke plus filter)	≥0.26 and ≤0.40 for 95% of compacts	Assure irradiation stability and limit matrix/coating interactions
Macroporosity (% matrix void)	≥45 for 95% of compacts	Assure irradiation stability and adequate thermal conductivity
Mean heavy metal contamination fraction:[c]		
(g leached U/g U in compact)	$\leq 1.0 \times 10^{-5}$ mean	Meet goal for radionuclide retention
(g leached Th/g Th in compact)	$\leq 1.0 \times 10^{-5}$ mean	Meet goal for radionuclide retention
Mean defective SiC coating fraction:[c]		
(g leached U/g U in compact)	$\leq 5.0 \times 10^{-5}$ mean	Control metallic fission product release
(g leached Th/g Th in compact)	$\leq 5.0 \times 10^{-5}$ mean	Control metallic fission product release
Mean defective IPyC coating fraction (heavy metal dispersion)		
(Fraction total particles)	$\leq 4.0 \times 10^{-5}$ mean	Meet goal for migration of U during SiC coating
Mean impurities burnable:[c]		
B, Cd, Eu, Gd, Li, Sm (ppm B equivalent)	≤5 mean	Allow acceptable neutron losses to meet core reactivity
Li (ppm B equivalent)	≤1 mean	Limit formation of tritium

TABLE 3-10 (Continued)

Property	Limiting Value	Bases for Limits
Nonburnable:[c] Na, S, Ca, Yb, Ti, V, Cr, Lu, Mn, Fe, Co, Al, Dy, Ni, Cu, Zn, Hf, Mo, Ag, In, Ta, Ca, La, Ce, W, Pr, Nd, Tb, Ho, Er, Tm, (ppm boron equivalent)	≤1	Allow acceptable neutron losses to meet core reactivity
Iron content[c] (μg outside of SiC/g burned back particles)	≤20 mean; ≤50 in ≤1% of compacts	Limit degradation of SiC layers from Fe reaction
Transition metal[c] (Cr, Mn, Co, and Ni) content (ppm in fire compact)	≤55 each metal; ≤240 total metals in ≤1% of compacts	Limit degradation of SiC layers from transition metal reactions
Hydrogen (ppm of rod weight)[c]	≤200 mean	Limit the potential for reactivity change and hydrogen embrittlement to metallic components
Chlorine outside SiC (ppm of rod matrix weight)[c]	≤30	Limit Cl reactions with metals in primary circuit
Sulphur content outside SiC (ppm of matrix plus shim)[c]	≤1200	Limit sulphur reactions with metals in reactor and steam generator

[a]The above limits, current as of the date of this report, are provided for illustration. The official specification limits are contained in the latest revision of Ref. 3-1.

[b]There is no tolerance on the length of individual compacts; combinations of compacts are selected for a stack length of 745 mm ± 7 mm.

[c]Required for a segment lot.

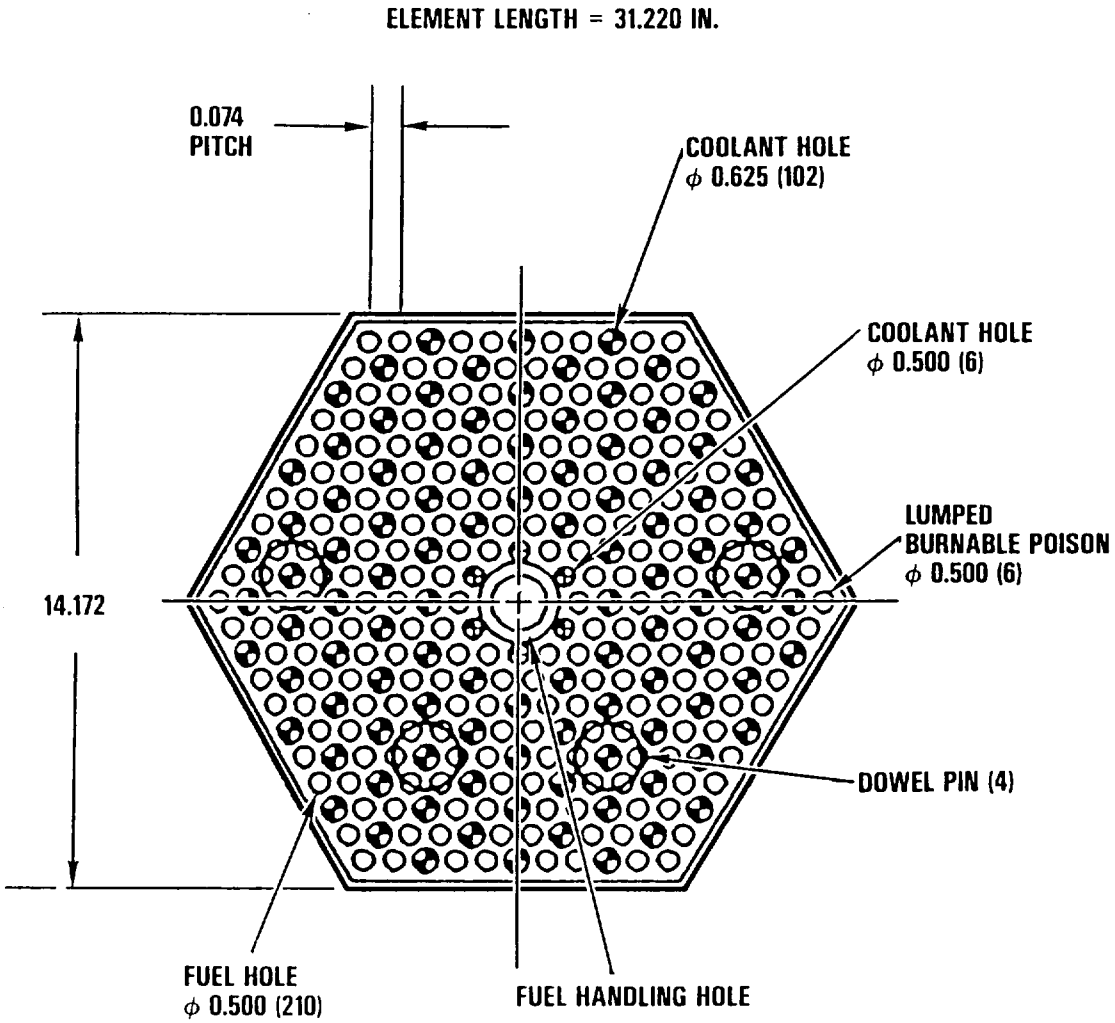

Fig. 3-4. Fuel block dimensions

the six corners of the hexagonal blocks. These burnable poison compacts are designed to limit the core reactivity with the control rods removed. The boron carbide particles are nominally 300 microns in size, and are coated with a two-layer buffer and isotropic pyrocarbon structure. The coated boron carbide particles are molded into compacts formulated from the same matrix material as the fuel compacts.

A total reactor core segment specification package includes drawings of the fuel elements, the fuel product specification document, tables of the fuel loading quantities for each fuel element, and the required loading of burnable poison.

The fuel loading step includes documentation of the quantities of uranium and thorium loaded into each fuel element assembly. Fuel loadings within each fuel element assembly must be independently verified. A serial number is permanently engraved on the side of each fuel element assembly. The fuel materials in each fuel element assembly are traceable back to the starting materials for each fuel kernel batch.

4. PROCESS FLOW DIAGRAMS

The figures in this section provide overall materials and components flow descriptions for fuel processing operations. Figure 4-1 shows the steps in making fuel kernels. Figure 4-2 shows the steps for application of all coating layers. Figure 4-3 shows the steps in compacting and final assembly. Detailed narrative descriptions of these processes are provided in Sections 5 through 8. Section 9 describes the Quality Control inspections and tests performed during fuel processing.

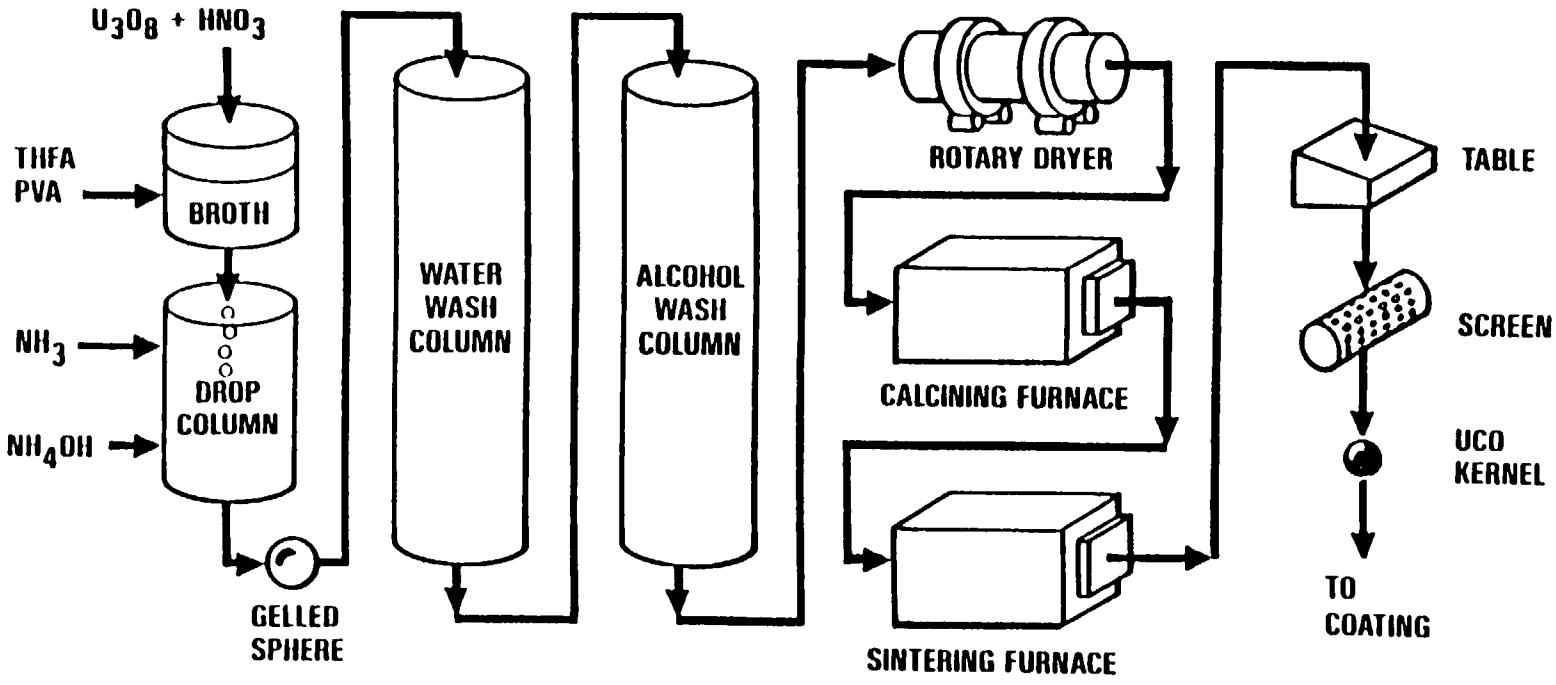

Fig. 4-1. Kernel fabrication (external sol gelation) process flow

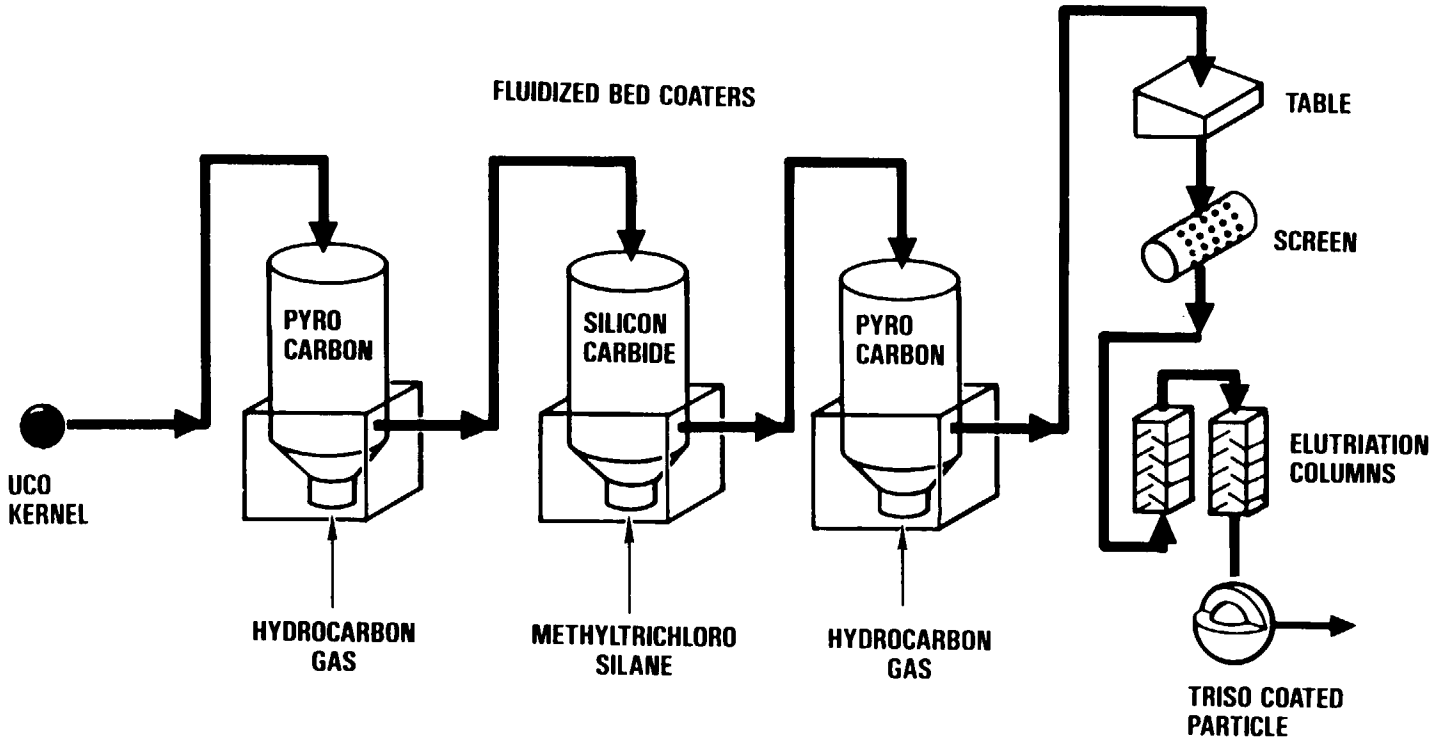

J 909(7)
1-31-91

Fig. 4-2. Coating process flow

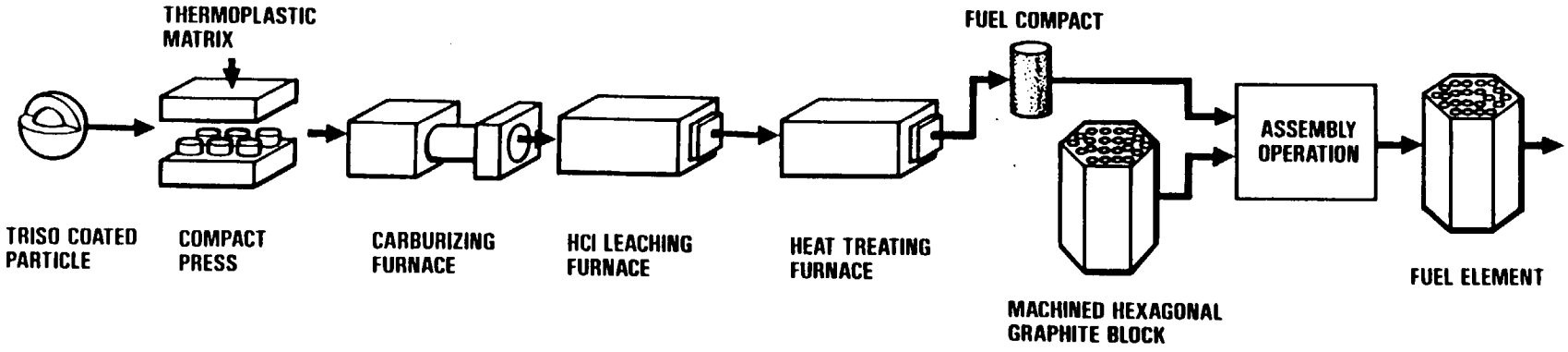

Fig. 4-3. Compacting and assembly process flow

5. FUEL KERNEL FABRICATION

5.1. INTRODUCTION

Spherical ceramic kernels for a range of chemical compositions have been developed using gel formation, where spherical kernels are formed from droplets of aqueous metallic solutions.

External gelation, the process described herein, causes gel formation by diffusing a chemical reactant from outside of the spherical droplets into the body of the droplets. Two important industrial variations of external gelation are the gel-supported precipitation (GSP) and the sol-gel processes.

In the GSP method, a water-soluble organic polymer is added to a uranyl nitrate solution to increase the viscosity of spherical droplets. A change in pH of the droplets caused by reaction with an external additive causes precipitation of the substrate within the organic polymer matrix.

In the sol-gel method, the heavy metal is dispersed as a stable sol in spherical droplets that are gelled by an external additive.

UCO microspheres are produced using a GSP process patterned after the SNAM process (Refs. 5-1 and 5-2) developed in Italy for production of UO_2 kernels. The procedure has been modified to incorporate carbon into the UO_2 matrix, which results in a UO_2-UC_2 two-phase mixture. This process is somewhat similar to the German (NUKEM) process for making sintered UCO kernels.

UCO microspheres made from uranium enriched to 19.8% U-235 are used as fissile kernels. The same type of microspheres, made from either depleted or natural uranium, have been used as fertile uranium kernels.

The papers (Refs. 5-3 through 5-12) that describe the GSP process for fabricating ceramic nuclear fuel emphasize the engineering and process parameters required to produce kernel batches of uniform size, composition, density, and surface smoothness.

The reference MHTGR fuel utilizes thorium oxide as the fertile material. Thorium oxide microspheres are produced using sol-gel technology. References 5-13 through 5-16 describe the sol-gel technology.

This section summarizes the GSP and sol-gel processes utilized to produce dense UCO and ThO_2 kernels at GA.

5.2. PROCESS DESCRIPTION

UCO kernels are fabricated in full-scale production equipment with a capacity of 5 kg of product per day. Parallel units of the same size would be used for higher production rates. The values used for process parameters are those developed for unit operations. The final manufacturing plant would require a total process control system.

Figure 5-1 is a detailed process flow diagram for the manufacture of kernels. The basic process steps are:

1. Broth preparation.
2. Sphere formation.
3. Precipitation.
4. Water washing.
5. Isopropyl alcohol washing.
6. Drying.
7. Calcining.

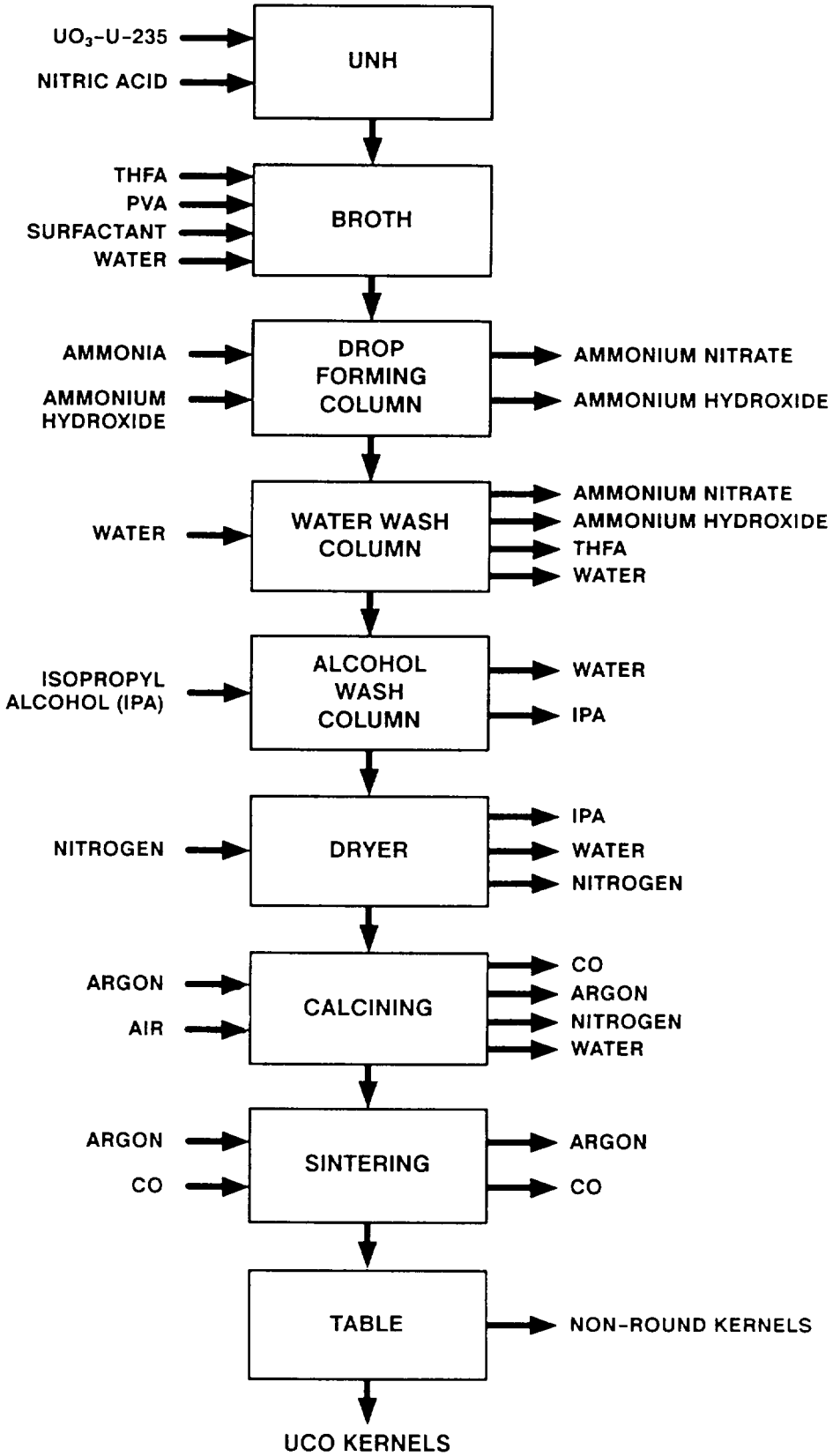

Fig. 5-1. Manufacturing process for MHTGR fuel fissile kernels

8. Sintering.
9. Tabling.

On the process line, each of these steps is performed in a distinct work station and requires a physical transfer of the product from the previous step.

All the modular-sized equipment is of favorable geometry for the reference enrichment of 19.8% U-235. Therefore, the broth tanks, columns, dryer, calciner, sintering furnace, tabler hopper, holding tanks, and transfer containers all have diameters just under the criticality limit of 6 in.

5.2.1. Uranyl Nitrate and Broth Manufacturing

The initial step in manufacturing UCO is converting UO_3 into uranyl nitrate (UNH). UNH is made by dissolving solid UO_3 in nitric acid. The uranium-to-nitrates molar ratio in the feed is 1/1.8. This ratio forms an acid deficient solution that is required for the GSP process. The UNH solution is mixed with tetrahydrofuryfuryl alcohol (THFA). This mixture is added to a polyvinyl alcohol (PVA) dispersion in water to form the broth.

The PVA solution is made in a heated tank. Electrically heated steam in a surrounding jacket is the source of heat. The tank is stirred with a small mixer. The PVA solution is transferred to plastic containers through a valve located at the bottom of the PVA tank.

5.2.2 Drop Formation

The broth is pumped through a drop generator that forms liquid microspheres. The microsphere generator consists of two broth holding tanks, several small diameter needles mounted above a precipitation/extraction column, and an electromagnetic driver that vibrates the needles. A heat exchanger maintains a constant broth temperature.

The broth tank is pressurized to maintain constant broth flow to the needles. The electromagnetic driver vibrates the needle axially, creating periodic instabilities in the laminar jet flow that are required for the production of uniform spheres.

5.2.3. Precipitation and Extraction

The broth droplets fall into a drop-forming column through a distance of approximately 2 ft in air, causing them to spheroidize. The droplets then fall into an ammonia gas (NH_3) atmosphere. An NH_3 exhaust ring prevents the ammonia gas from extending above the air-ammonia gas interface. Figure 5-2 shows the three UCO drop columns for drop forming (ammonia), water washing, and alcohol washing. Figure 5-3 shows additional detail of the ammonia column for drop forming.

The partially gelled kernels land in an aqueous ammonia solution that is continuously circulated upward against the falling spheres. The kernels eventually settle at the bottom of the ammonia column, where the gelation process is completed. After a residence time of approximately 60 min at room temperature, the kernels are pumped in batch mode to the water wash column.

The extraction section of the ammonia column consists of five counter current stages, each with internal recirculation to fluidize the kernels and control the residence time in each stage. To help increase the stage efficiency, the different stages are separated by baffles.

Aqueous ammonia is continuously circulated against the partially gelled kernels. Fresh ammonia feed enters at the bottom of the ammonia column and exits at the top as a mixture of ammonia, ammonium nitrate, and other byproducts.

The ammonia column outlet is connected to two parallel waste liquidcolumns. The same waste liquid columns are used to collect the

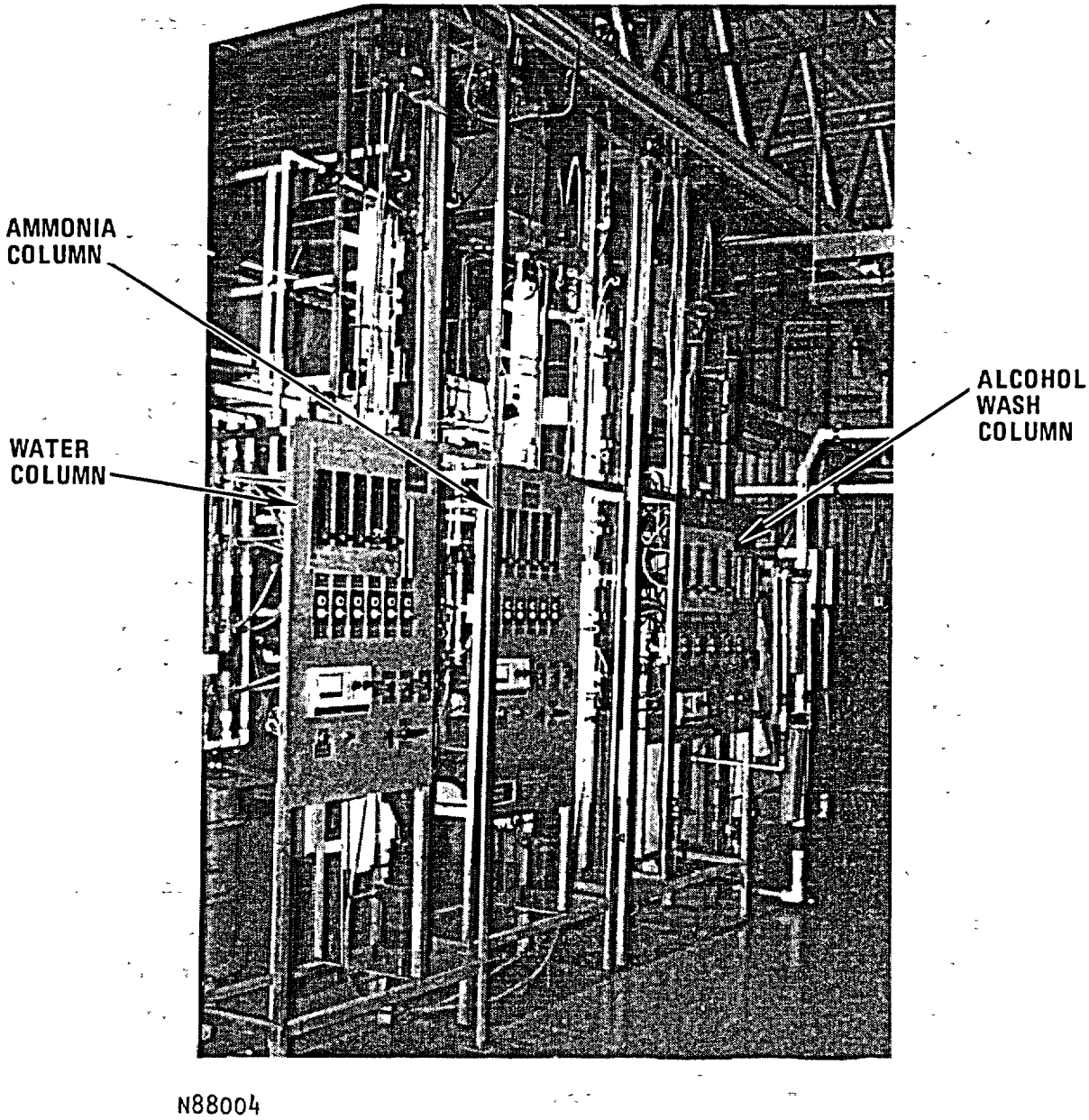

Fig. 5-2. UCO drop columns

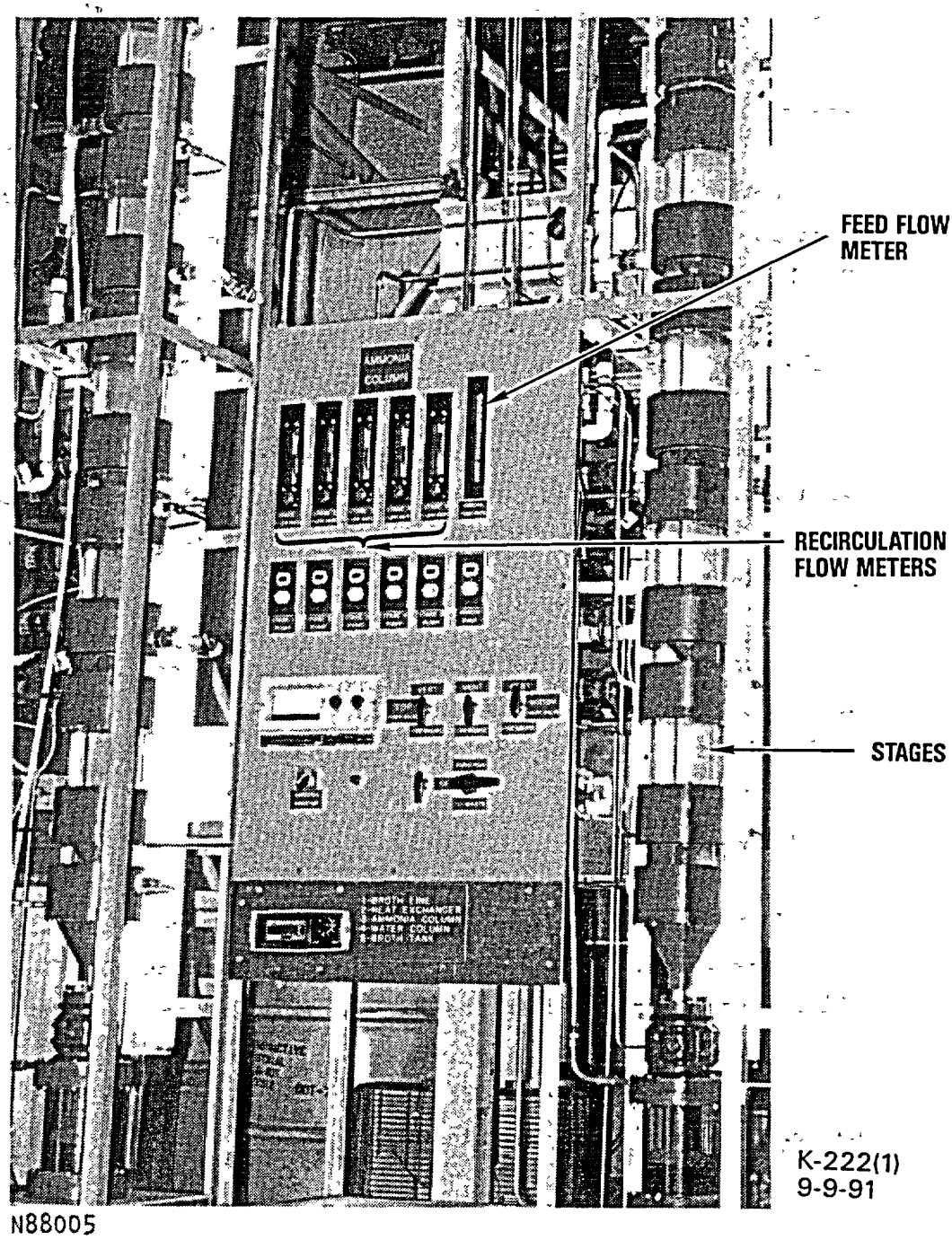

Fig. 5-3. Ammonia column

extraction column, the water column, alcohol column, and dryer outflows. Periodically the liquid waste is pumped to a geometrically safe waste liquid tank located outside the production area.

5.2.4. Water Wash

Kernels are fed to a 6 in. diameter five-stage water wash column. Kernels flow by gravity against a counter flow of deionized water. Fresh water is introduced at the lowest stage and exits at the top of the column. The water wash with excess ammonia, THFA, and nitrates is collected in two waste liquid columns.

The column design, which consists of stages separated by baffles with internal circulation to control the kernel average time, is the same as the drop column. The average residence time in the water wash column is typically 45 min.

Kernels settle into a receiver located at the bottom of the column. The kernels are then transferred in batches to the isopropyl alcohol wash column.

5.2.5. Isopropyl Alcohol Wash

Kernels are fed into the top of a four-stage IPA wash column (Fig. 5-4). Kernels flow by gravity against a counter flow of IPA. The IPA feed is introduced at the bottom of the column and exits at the top.

The average kernel residence time is approximately 45 min at room temperature, and is controlled by the flow rate of recirculating IPA in each stage.

Kernels settle into a receiver located at the bottom of the column. The kernels are then transferred to the dryer feed tank.

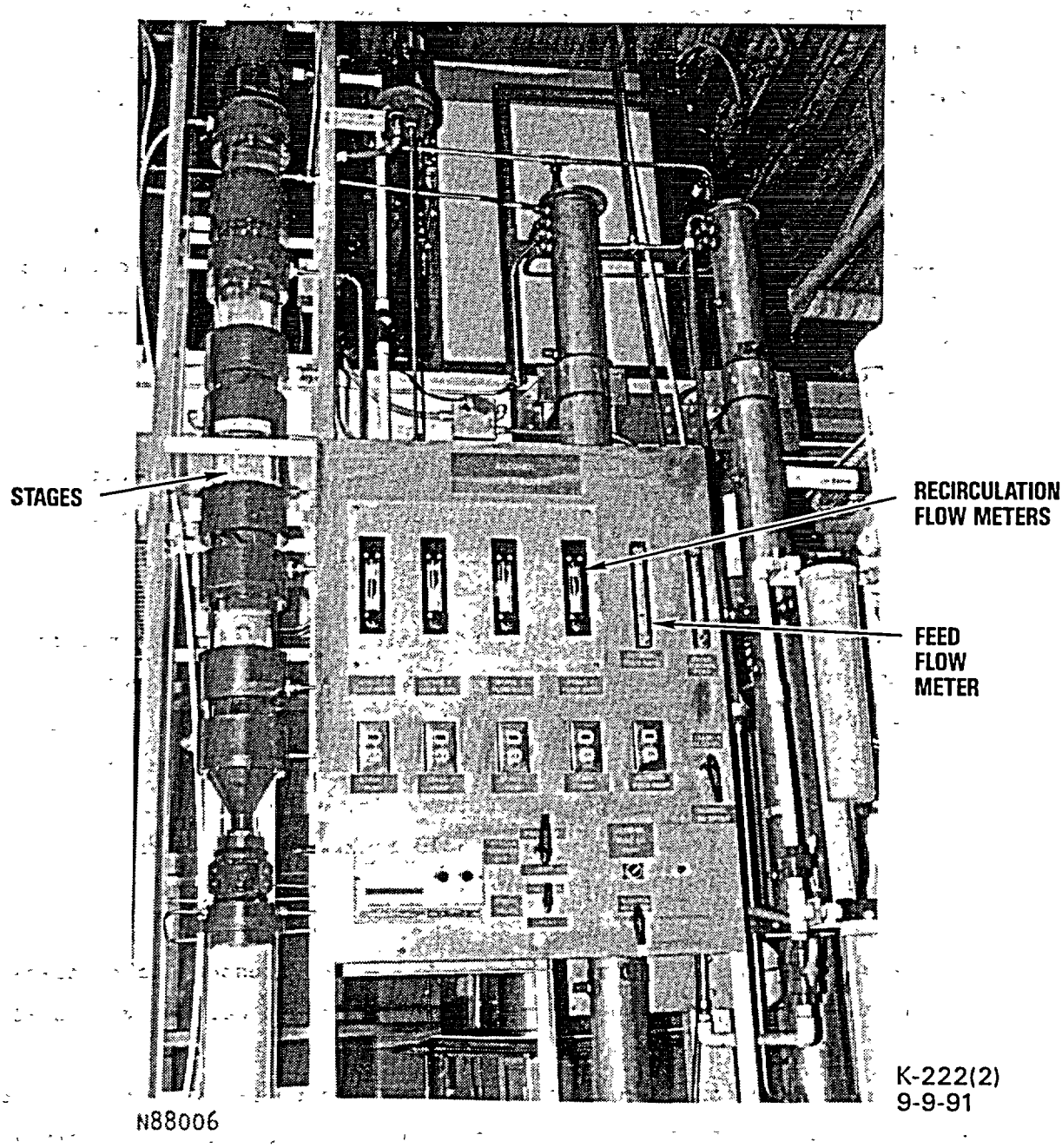

Fig. 5-4. Alcohol wash column

5.2.6. Kernel Drying

Kernels, in alcohol, are transferred by fluid flow from the dryer feed tank into the rotary dryer. Free water and alcohol are removed in the dryer (Fig. 5-5). The tumbling microspheres are dried with hot nitrogen.

The dryer contains a 6 in. diameter, variable speed, rotary basket that holds the kernels. The basket is made of porous stainless steel to allow alcohol and gases to flow through the walls, while ensuring that the kernels are contained within the favorable geometry provided by the basket.

The basket is located inside a cylindrical shell. The outer shell has a drain for removal of water and alcohol. The water/alcohol solution is pumped to the waste liquid columns.

The outer shell is also piped to a nitrogen recirculation system. The tumbling wet microspheres are dried with hot nitrogen. The hot solvent-rich nitrogen that exits the dryer shell is cooled in a heat exchanger to condense water and alcohol. At the end of the heat exchanger, a liquid/gas separator returns dry nitrogen to the dryer, while the liquid is sent to a small hold tank. The small hold tank is connected to the waste liquid system.

The nitrogen carrier gas flows through a compressor, to an electrical heater, through the rotary furnace and to an outer dryer shell.

Kernels are considered dry when alcohol stops flowing from the condensing heat exchanger. A significant volume shrinkage of the kernels occurs during drying. The volume of dry kernels is about 44% of the volume of the wet microspheres.

At the end of the heating cycle, when the system is vented, the outflowing gases are piped to the building filtering system.

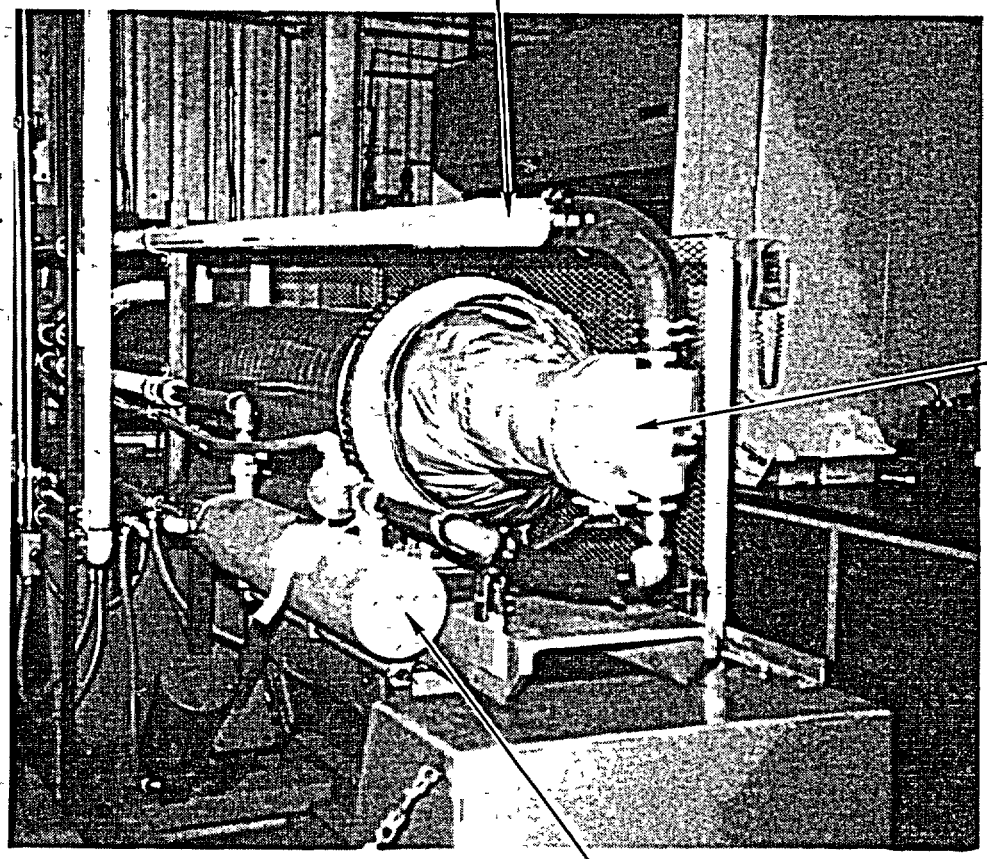

850232-12

K-222(5)
9-9-91

Fig. 5-5. Dryer

5.2.7. Calcining

The rotary furnace used for calcining is shown in Fig. 5-6. The calcining heat treatment is characterized by the mildly exothermic decomposition of the PVA. This reaction occurs between 280° to 300°C, but the heating cycle extends to 700°C. The thermal decomposition occurs in two stages. In the first stage, dehydration and the formation of some volatile products occur. The second stage produces carbon and volatile hydrocarbons.

During calcining, free and chemically bound water and ammonia are driven off. The uranium oxide compound is reduced with the evolution of CO. The calcination of ammonium uranate (AU) occurs in several stages before the final reduction to UO_2. Between 20° and 200°C, dehydration occurs. Thermal decomposition of AU occurs between 200° and 350°C with loss of water and some ammonia. Between 350° and 450°C, ammonia retained in the solid reduces UO_3 to U_3O_8 and U_4O_9. The final reduction occurs above 500°C.

At the end of the heating/cooling cycle, a hydraulic system tilts one end of the calciner to allow kernels to flow out. Kernels are collected in a 5-in. diameter canister.

5.2.8. Sintering

The final heat treatment of the UCO kernels is performed in a rotary sintering furnace (Fig. 5-7).

The total cycle time for the sintering furnace is approximately 24 hr for a 5-kg batch of UCO kernels.

The rotary sintering furnace contains a 6-in. diameter graphite retort. Heating is provided by six banks of resistance heaters divided into three independent heating zones. An insulated box surrounds the heaters and retort.

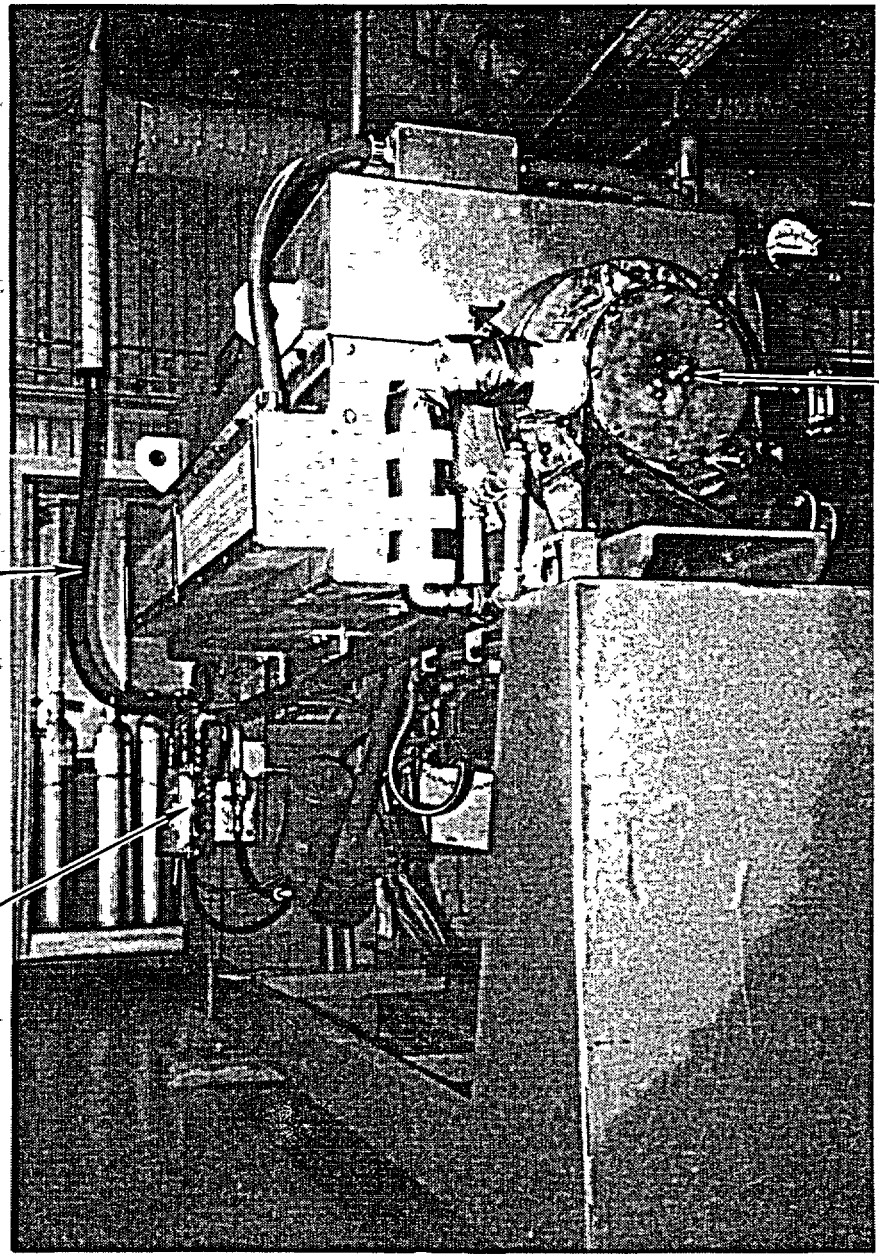

850232-11

K-222(4)
9-9-91

Fig. 5-6. Calciner

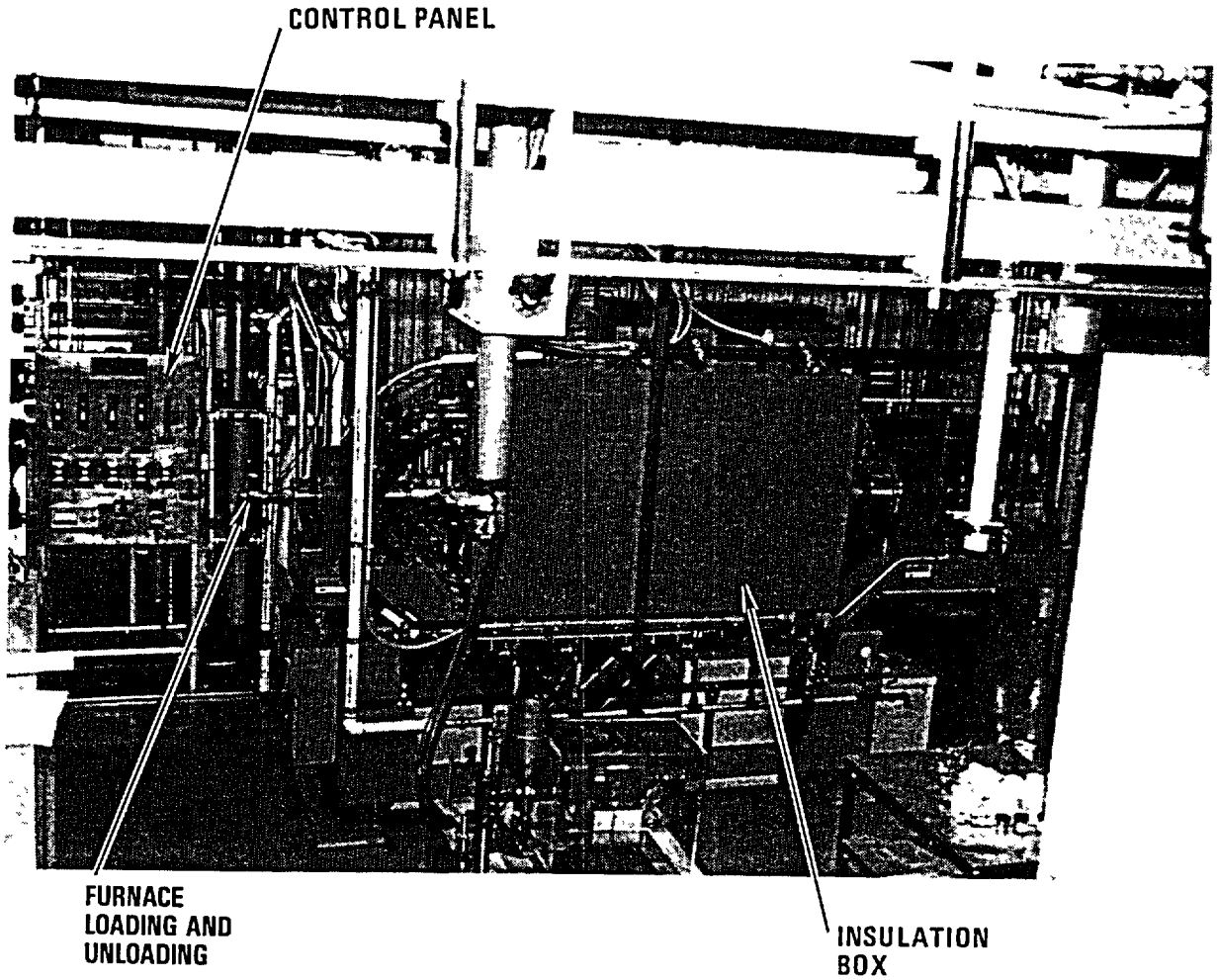

K-222(7)
9-9-91

Fig. 5-7. Sintering furnace

The insulated box is maintained under argon atmosphere. The retort is piped to have an atmosphere of argon, nitrogen, CO, or combinations of these gases.

A hydraulic system tilts the furnace to unload kernels into canisters.

5.2.9. Tabling

A vibrating table separates round from nonround kernels (Fig. 5-8). The table is slightly inclined in the Y-axis and vibrates in the X-axis. Round kernels exit through a trough located at the lower edge of the table. Nonround kernels slide off the inclined edge. The tabler inclination, as well as the amplitude and speed of its vibration, can be varied.

Sintered kernels are stored in a hopper connected to a rotary feeding system. Round and nonround kernels exiting the tabler are collected in favorable geometry containers.

5.3. PROCESS PARAMETER CONTROL

During each step of the kernel manufacturing process, key processing parameters control the size and quality of the resulting kernels.

In the developmental line, process uniformity is obtained through the use of detailed written procedures that describe each unit operation. The written procedures describe the equipment that will be used; the manual procedures that the operator will have to perform (grease rotary joints, etc.); how to program the microprocessor, and the sequential checks operators must perform to ensure that both the equipment and the controller are functioning property. In addition, an operator qualification program ensures that only personnel familiar with radiation hazards and the individual processes are permitted to operate the equipment.

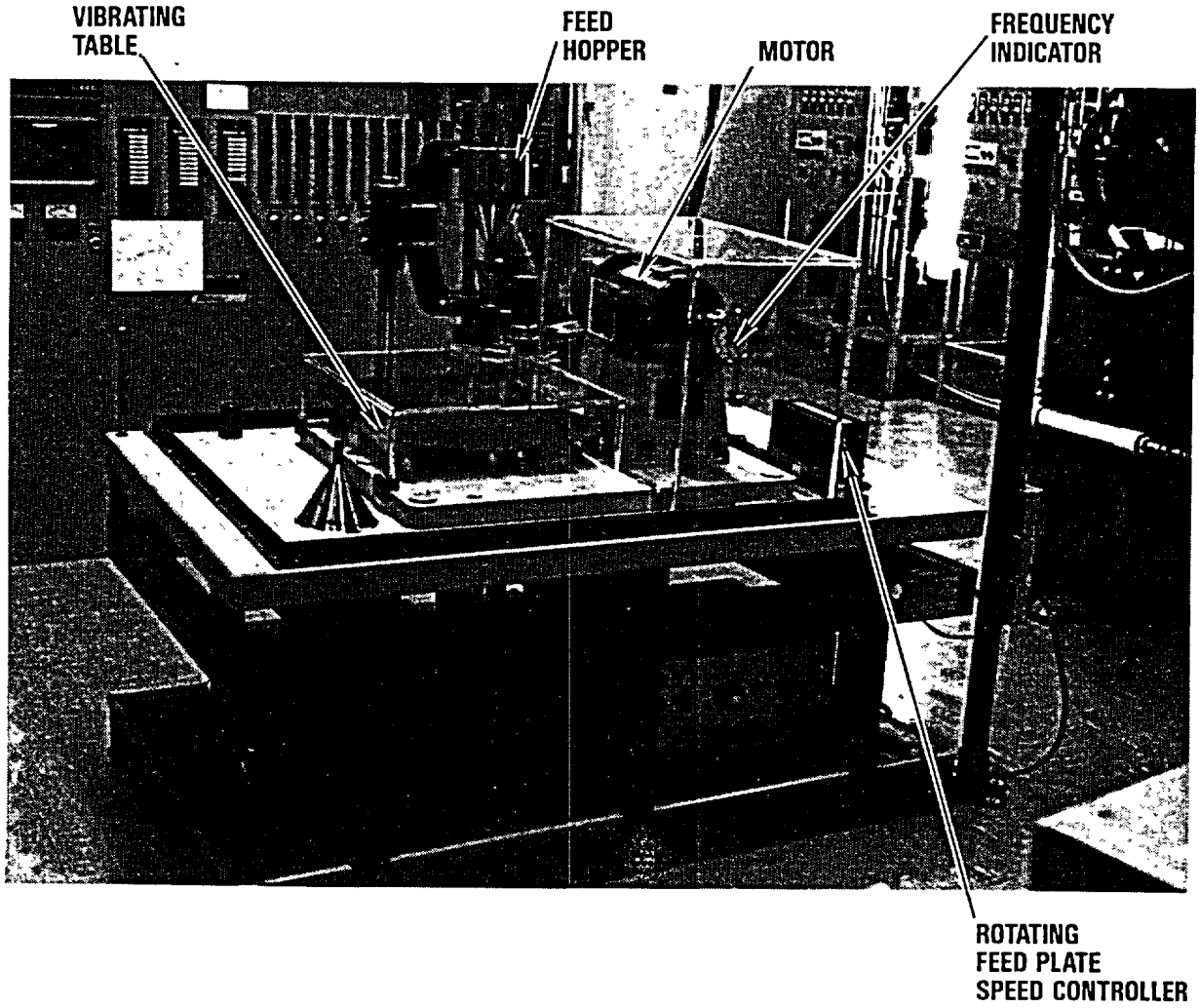

K-222(6)
9-9-91

Fig. 5-8. Tabler

A programmable microprocessor controls key process parameters such as temperature, pressure, and flow of gases. The process parameters as defined in Parameter Sheets are used to program the microprocessor. Process data obtained during manufacturing is continuously recorded in a programmable data recorder. As a manual check, operators also record the same information on Data Sheets at preselected intervals.

The Parameter and Data Sheets, as well as the data obtained by the Quality Control Department, are attached to a Traveler that contains all the information pertaining to each batch of kernels as it makes its way from raw material feed to tabled kernels.

On the developmental line, some processing parameters such as the ammonia feed and flow rate, are manually controlled by the operator. However, it is anticipated that the commercial manufacturing plant will be totally automated. It will have an integrated data system to store and manipulate data from quality control and manufacturing. Software will be developed to analyze this data and maintain a real-time SNM inventory.

5.3.1. Broth Fabrication Control

Excessive amounts of nitrates are deleterious to kernel formation. Therefore, the mol ratio of nitrate to uranium in the UNH is controlled to 1.5 to 1.8.

It is important that THFA forms a complex with uranium before it is mixed with PVA. Therefore, the UNH solution is mixed with THFA for an hour before it is mixed with PVA.

5.3.2. Drop Formation Control

The product specifications describe the kernel size (diameter) and density. From these two parameters, the theoretical amount of uranium is calculated for each generated droplet.

A key to obtaining uniform kernels within specifications is to generate droplets of the same size with the same uranium concentration. The critical parameters that are controlled to obtain uniform kernels with the desired properties are uranium concentration in the broth, broth flow rate, broth viscosity, orifice diameter, and orifice vibration.

Microsphere generation processes are based on Rayleigh's theory on the breakup of a laminar jet into droplets. Surface tension causes the droplets to form spheres. Rayleigh's instability theory predicts the behavior of disturbance on a liquid surface (Ref. 5-17).

Selection of an orifice diameter places several constraints on the usable range of broth flow rates. The flow rate must be sufficient to form a jet, the jet must be laminar, and the resultant spheres must not collide during free fall.

It has been shown (Ref. 5-17) that the minimum jet velocity is a function of the orifice diameter, density and surface tension of the liquid. If the flow rate is low, rather than form a jet, drops will grow and fall off one at a time.

For a particular broth, there is a range of useful orifice sizes. For a very small orifice, it will be difficult to form spheres below their terminal velocity and maintain a good production rate. For very large orifice diameters, reaching the minimum jet forming velocity is difficult. Each intermediate diameter will allow a usable range of flow

rates. Each orifice is individually characterized using the broth to be processed.

An operating window for a combination of these parameters produces droplets of such size and uranium concentration that, after calcining and sintering, they yield kernels within the product specifications.

Figure 5-9 shows the maximum and minimum acceptable broth flow rate per orifice as a function of orifice diameter (Ref. 5-17).

The gelling and washing operations are manually controlled in the developmental line. Temperature in the aqueous ammonia column is controlled to 30°C. The water and IPA washing columns are kept at room temperature.

The average kernel residence times in each column are 60, 45, and 45 min for the ammonia, water, and alcohol columns, respectively. The average kernel residence time is controlled by adjusting the column stages internal circulation flow rates.

Kernels are dried in batch mode in a rotary dryer. A controller regulates the temperature of the incoming nitrogen to 55°C. A pressure controller regulates the internal dryer pressure to 14.7 psig. After a batch cycle, the dryer is cooled to room temperature.

5.3.3. Calcining Control

During calcining, PVA is decomposed, ammonia and water are driven off, and uranium is reduced from UO_3 to UO_2. All of these reactions are temperature induced; therefore, the key parameter is arriving at a temperature of 700°C.

A programmable controller monitors the temperature in each of the three heating zones and adjusts the input power to maintain the desired heating profile. Cooling is provided by forced air circulation around the furnace retort.

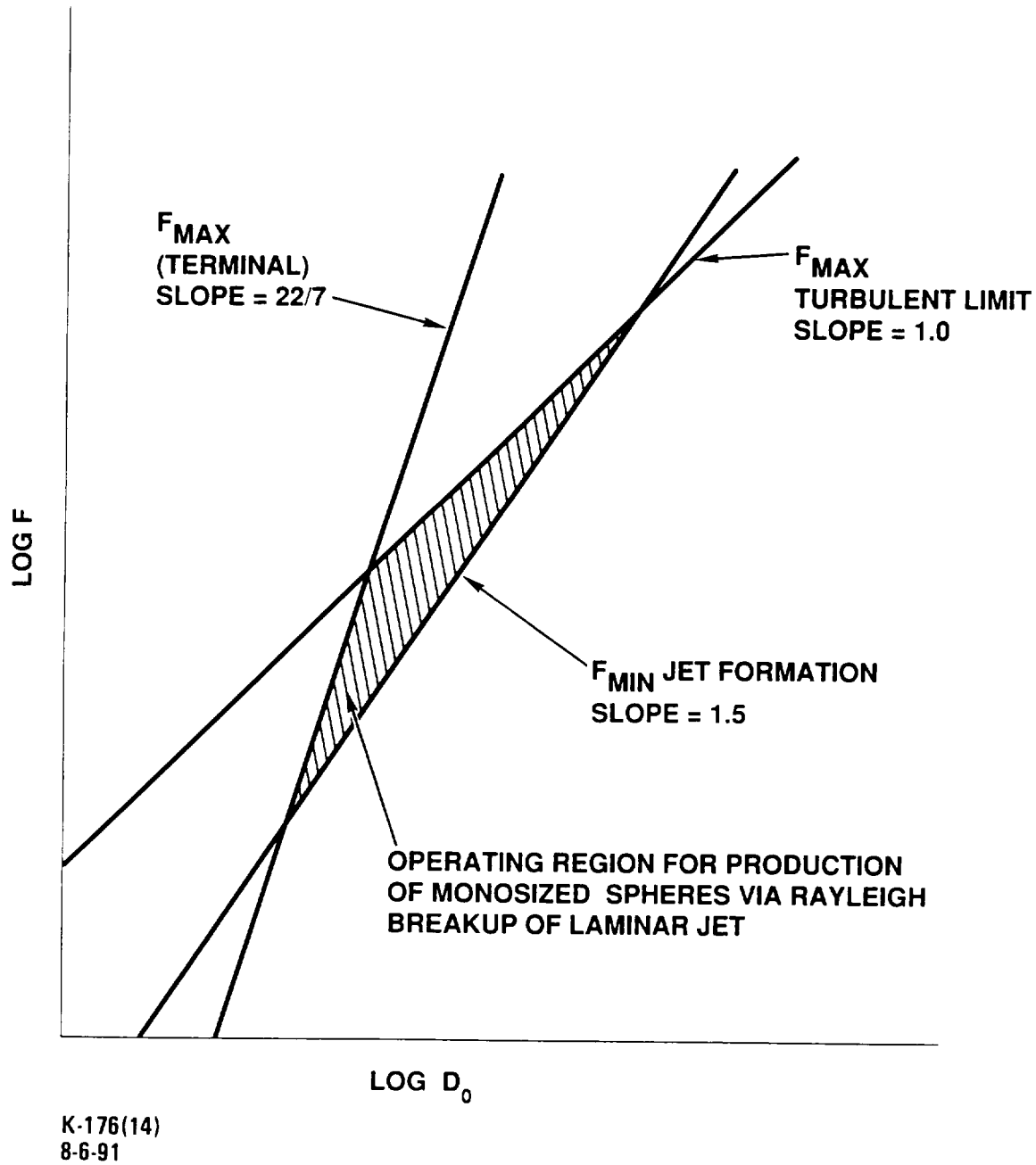

Fig. 5-9. Operating region for production of monosized spheres

The calciner atmosphere includes argon, nitrogen, and air. The programmable controller regulates the gas flows to the furnace. Adjustable flow meters control the amount of each gas flowing to the calciner. The calciner gas outlet is piped to the building filtering system.

A programmable alarm system monitors retort rotation, flow of cooling water, overtemperature, flow of gases, and other conditions.

5.3.4. Sintering

During sintering, the UO_2 is partially converted to UC_2 and the kernels are densified by solid phase diffusion across boundaries.

To obtain thermodynamics conditions that are favorable for densifying kernels to almost theoretical values, it is critical that the furnace reaches a temperature of 1800°C.

The required final kernel composition is a physical mixture of UO_2 and UC_2. A sintering temperature of 1800°C is required to achieve the desired chemical composition and density.

The rotary sintering furnace employs a programmable heater controller for a slow heat-up to 1600°C. The furnace then ramps to 1800°C. At 1800°C there is a 30 min soak, followed by cooldown to room temperature.

Two independent programmable controllers regulate the pressure inside the retort and heating box. A pressure relief valve is provided to avoid overpressurizing the heating box. The sintering furnace outlet gases are piped to the building filter system.

A safety system automatically stops the furnace and sounds an alarm in case of faulty rotation, high oxygen concentration in the retort,

high CO concentration outside the furnace, low pressure or flow of the different gases, or low cooling water flow.

5.4. FUEL KERNEL RAW MATERIALS

UO_3 is the reference uranium oxide feedstock material used in the manufacture of MHTGR fuel. Depending on availability, either U_3O_8 or UO_3 can be used. The requirements applicable to both forms of enriched uranium oxide powders are listed in two separate sections.

5.4.1. U_3O_8 Uranium Oxide

5.4.1.1. Material Requirements.

Impurities

The chemical impurities of the U_3O_8 powder shall not exceed the values, in ppm, listed below:

Al	100	Fe	150	Pb	100
Ag	0.5	Hf	50	S	50
B	1	In	5	Sb	10
Ba	100	K	20	Si	100
Be	1	La	50	Sn	100
Bi	2	Li	2	Sr	50
C	1000	Mg	100	Ta	50
Ca	100	Mn	100	Th	15
Cd	0.5	Mo	100	Ti	50
Ce	50	Na	40	V	50
Co	5	Nb	50	W	50
Cr	100	Ni	100	Zn	100
Cs	25	P	150	Zr	50
Cu	100				

Eu + Gd + Sm $<$ 0.6 (total)

Dy + Pr + Nd + Tb + Ho + Er + Tm + Yb + Lu $<$ 2.0 (total)

Boron Equivalents

For the above list of elements, the sum of individual boron equivalents shall not exceed 10 ppm.

Uranium

The minimum uranium content shall be 84.0 wt %.

Isotopic Composition

The isotopic composition shall be 19.80% ± 0.05% U-235.

Moisture Content

The moisture content of the powder shall be no greater than 0.5 wt %, dry basis.

5.4.1.2 Physical Properties.

Solubility

At least 99% of the material shall be dissolved after four hours at 85° to 95°C in dilute nitric acid with NO_3/U mole ratio in the final solution ≤ 1.8.

Surface Area

The surface area of the powder, as measured by a standard adsorption test, shall be at least 2.0 m^2/g.

Workmanship

The material shall be uniform in quality and, based on macroscopic examination, shall not contain tramp material or foreign particles in excess of 30 particles per gram of material.

5.4.2. UO_3 Uranium Oxide

5.4.2.1. Material Requirements.

Impurities. The chemical impurities of the UO_3 powder shall not exceed the values shown in Section 5.5.1.1 for U_3O_8.

Boron Equivalents

The sum of individual boron equivalents for all impurities shall not exceed 10 ppm in the UO_3 feed.

Uranium

The minimum uranium content shall be 80.0 wt %.

Isotopic Composition

The isotopic composition shall be 19.8% ± 0.05 wt % U-235.

5.4.2.2. Physical Properties.

Solubility

At least 99% of the material shall be dissolved after four hours at 85° to 95°C in dilute nitric acid with NO_3/U mole ratio in the final solution ≤ 1.8.

5.4.3. Process Chemicals

Table 5-1 lists the grade/purity requirements for other chemicals used in kernel fabrication.

5.5. KERNEL FABRICATION CHEMISTRY

The UCO kernel is a two-phase mixture of UC_2 and UO_2 in the desired proportions (typically 15% UC_2 and 85% UO_2). Following is a summary of the chemistry involved in UCO kernel manufacturing.

5.5.1. Uranyl Nitrate

Uranium oxide feed material is dissolved in nitric acid to form UNH. UO_3 is the preferred uranium source because it dissolves rapidly and does not produce any by-products. However, U_3O_8 can also be used as the uranium feed material.

Uranium in the form of UO_3 is dissolved in nitric acid by diprotonation of the oxide anion to yield water:

$$UO_3 + 2HNO_3 + 5\ H_2O \rightarrow UO_2(NO_3)_2 \cdot 6H_2O$$

5.5.1.1. Stability of UNH Solutions. The solubility and stability of UNH in water and in HNO_3 are important to broth preparation (Refs. 5-18 and 5-19). The equilibrium phase diagram (Ref. 5-18) for the $UO_2(NO_3)_2$ - HNO_3 - H_2O system indicates that four UNH solid phases are found to be in equilibrium in different regions of the phase diagram: hexahydrate, trihydrate, dihydrate, and a solute tentatively formulated as $UO_2(NO_3)_2 \cdot 3NHO_3$ existing in regions of high nitric acid.

During broth preparation, UO_3 is dissolved in nitric acid at ~80° to 90°C. The final solution has a density of ~1.66 which corresponds to ~52 wt % UNH. Very little nitric acid exists in the solution. In

TABLE 5-1
KERNEL PROCESS CHEMICALS

Material	Grade/Purity
Ammonium hydroxide	ACS analytical reagent grade
Anhydrous ammonia	≥99.99% NH_3
Argon	≥99.997% Ar
Carbon monoxide gas	≥99.5% CO
Isopropyl alcohol	ACS analytical reagent grade
Nitric acid	ACS analytical reagent grade
Nitrogen	≥99.95% N_2
Polyvinyl alcohol	Polyvinyl alcohol type American Hoechst Mowiol 56 to 98
Tetrahydrofurfuryl alcohol	≥98% purity, colorless (white-white), 100% volatile

a ternary phase diagram, the solution composition lies close to the $UO_2(NO_3)_2$ - H_2O line.

5.5.2. Broth

The dissolved uranium THFA and PVA form a feed solution called the broth: $UO_2(NO_3)_2 \cdot 6H_2O$ + THFA + PVA.

5.5.3. Polyvinyl Alcohol

The role of the polymer in the GSP process is to adjust the rheological properties of the broth so that spherical droplets can be formed, and to strengthen the gel spheres during the early stages of solidification.

The GSP process uses PVA as the polymeric matrix. PVA has a slow rate of solution in water at room temperature, yet passes into solution in water readily at temperatures above 70°C. The viscosities of freshly prepared concentrated aqueous PVA solutions increase over long periods of time.

Concentrated aqueous solutions of PVA, prepared above 70°C, will set to a gel when cooled to room temperature. The solution for uranium kernels contains 80 g/ℓ PVA. Temperatures $<$14°C are necessary to cause gelation.

5.5.4. Tetrahydrofurfuryl Alcohol

A modifier in the broth is needed to give good sphericity to the product and to slow the rate of rheological changes in the stored broth. THFA is used as the modifier.

THFA is a liquid reagent with the chemical structure

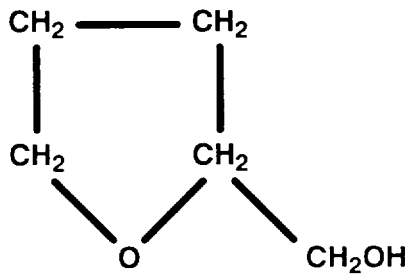

The chemical formula is C_4H_7O - CH_2OH.

The presence of THFA in the broth stabilizes the PVA by forming a complex with the uranyl nitrate, thus lowering the rate of photodepolymerization caused by the catalytic activity of the uranyl group (Ref. 5-20).

5.5.5. Gel Formation

The aqueous solution of UNH is acidic as a result of hydrolysis. The uranium can be precipitated from this solution by increasing the pH above a critical value. Droplets of broth free-fall in air to ensure spheroidizing, pass through gaseous NH_3 to harden the outer shell of the drop, and then are bathed in an aqueous ammonia solution to complete hardening of the kernel interior.

When a freshly formed droplet of broth is exposed to ammonia gas, the ionic strength of the droplet is increased by the formation of ammonium nitrate (NH_4NO_3) salt. This salt lowers the free water of the broth, causing precipitation of the PVA. As ammonia diffuses inward, a PVA gel lattice forms in the outer layer of the sphere, forming a hardened shell over the drop. Complete gelation occurs when the kernel is bathed in the aqueous ammonia.

At the same time the PVA is gelling, the uranyl ions react with the ammonia to form ammonium diuranate (ADU) precipitate. The chemical form is $UO_3 \cdot XNH_3 \cdot (2-X)H_2O + 2NH_4NO_3$, where X varies from 0.33 to 0.67.

5.5.6. Water Wash

During the washing process, excess ammonia, THFA, and nitrate diffuse out of the gelled kernel. In common with precipitation, washing of waste products and excess precipitants is diffusion controlled at a rate determined by transport of excess impurities through the gel structure.

5.5.7. Kernel Drying

Drying removes residual water and IPA. A rotary drier is used to dry the kernels in an inert atmosphere of N_2. The gel formed has the chemical form ($UO_3 \cdot xNH_3 \cdot yH_2O$ + PVA), where x and y vary depending upon the amount of water available.

Significant volume shrinkage occurs during drying. The volume of spheres is about 45% of the volume of the wet spheres. Capillary forces caused by the removal of water from the polymer/ADU matrix results in closer packing of both the aggregates and of the grains within the aggregates.

Replacement of water with alcohol reduces the volume of the gelled spheres, but the resulting structure better withstands the capillary forces. The reason for the increased rigidity is thought to be related to the absence of water in which the polymer is more soluble.

5.5.8. Calcining

The dry spherical gel consists of ADU crystallites held together by a PVA matrix. The calcining step is necessary to decompose the polymer,

drive off chemically bonded water and ammonia, and reduce UO_3 to UO_2. Calcining is accomplished by a slow heatup to 700°C.

Calcining proceeds in three different phases. The first phase is the decomposition of PVA and removal of ammonium hydrate:

$$(UO_3 \cdot xNH_3 \cdot yH_2O + PVA) \rightarrow UO_3 + rC + NH_3 + H_2O$$

The "r" denotes residual carbon left from heating. The ratio of uranium to carbon is approximately 1.73.

5.5.9. Decomposition of PVA

The thermal decomposition of PVA occurs in two stages. The first stage, which begins above 170°C, is mainly dehydration accompanied by the formation of some volatile products. Acetaldehyde, crotonaldehyde, benzaldehyde, and acetophenone have been reported among the decomposition products (Ref. 5-21). The distribution of oxygen compounds in the products based on 100 monomer units in the original polymer is: water, 86.4 mole; aldehydes, 1.9 mole; ketones, 0.5 mole; other, 0.7 mole (Ref. 5-22). In the second-stage decomposition of PVA, the macromolecules having polyene structure are degraded to produce carbon with the volatile products consisting mainly of hydrocarbons.

5.5.10. Decomposition of Ammonium Uranate

The thermal decomposition of ammonium uranate to give uranium dioxide occurs in several stages prior to the final reduction to UO_2. Between 20° and 200°C a two-stage dehydration occurs involving removal of coordinated water molecules and some dehydroxylation. Thermal decomposition of AU occurs between 200° and 350°C with loss of ammonia and water, but some ammonia remains within the structure of the uranate (Ref. 5-23). Between 350° and 450°C, ammonia retained in the solid

reduces UO_3 to the form U_3O_8 and U_4O_9. The proportions of U, C, and O are approximately 1/1.73/2.67.

The second phase of calcining consists of reducing U_3O_8 to UO_2 at temperatures above 500°C. In the final phase of calcining, excess carbon must be removed. Oxygen in the form of air is introduced to deplete carbon. At 700°C, all carbon is removed except for residual amounts at the core of the kernel. The proportions of U, C, and O at this point are approximately 1/0.6/2.0.

The ammonia and nitrate contents of the AU affect the stages of decomposition and also affect the surface area of the product during decomposition. The amount of self-reduction to U_3O_8 increases with increasing combined ammonia and the presence of nitrate impurity decreases the degree of reduction in inert atmospheres (Ref. 5-24).

Nitrate containing AU shows a significant increase in the surface area during decomposition in the 200° to 350°C range. There is also an increase in surface area with increasing ammonia content (Ref. 5-25). The loss of water and ammonia during decomposition promotes the formation of a network of internal porosity (Ref. 5-26).

5.5.11. Sintering

The final step in production of dense UCO fuel kernels is to convert the calcined microspheres containing UO_2 and C into a two phase UO_2 UC_2 mixture (Ref. 5-12).

Sintering is performed in two stages. In the first stage, the UO_2 is reduced in an inert argon atmosphere as the temperature is increased from 1100° to 1600°C. The chemical reaction can be expressed as:

$$UO_2 + 0.6C \rightarrow 0.8UO_2 + 0.2UC + 0.4CO$$

The proportions of U, C, and O atoms at this stage are approximately 1/0.2/1.6. This intermediate stage is necessary for the process to result in high density kernels.

The final sintering stage involves converting most of the UC xOy to UC_2 in a CO atmosphere at 1800°C. The reaction is:

$$UC + (1/2)CO \rightarrow (1/4)UO_2 + (3/4)UC_2$$

The overall reaction in sintering is:

$$0.8UO_2 + 0.2UC + 0.1CO \rightarrow 0.85UO_2 + 0.15UC_2$$

At this point, the proportions of U, C, and O atoms are at the desired values of 1/0.3/1.7.

5.6. FERTILE THORIUM OXIDE KERNELS

Thorium oxide kernels are made by gaseous and liquid ammonia gelation of a thorium oxide sol. The process is shown schematically in Fig. 5-10. The thoria sol is prepared by dispersing fine ThO_2 powder in dilute nitric acid. The ThO_2 powder is made by steam denitration of thorium nitrate solution. A gelling agent is added to the sol to increase the toughness of the spheres. The resulting mixture is the broth. Microspheres are generated by the breakup of a jet of the broth using an electromagnetic vibrator. After gelling, the kernels are washed and dried to remove volatiles before sintering the resulting ThO_2 to high density.

5.6.1. Thorium Broth Preparation

Broth preparation is essentially a batch process. The flow sheet is shown in Fig. 5-11. First, a 2.4 M $Th(NO_3)_4$ solution is made by mixing $Th(NO_3)_4 \cdot XH_2O$ ($x \sim 5$) crystals and hot deionized (DI) water in a nitrate prep tank. Density, the control parameter, is 1.8 g/cm^3.

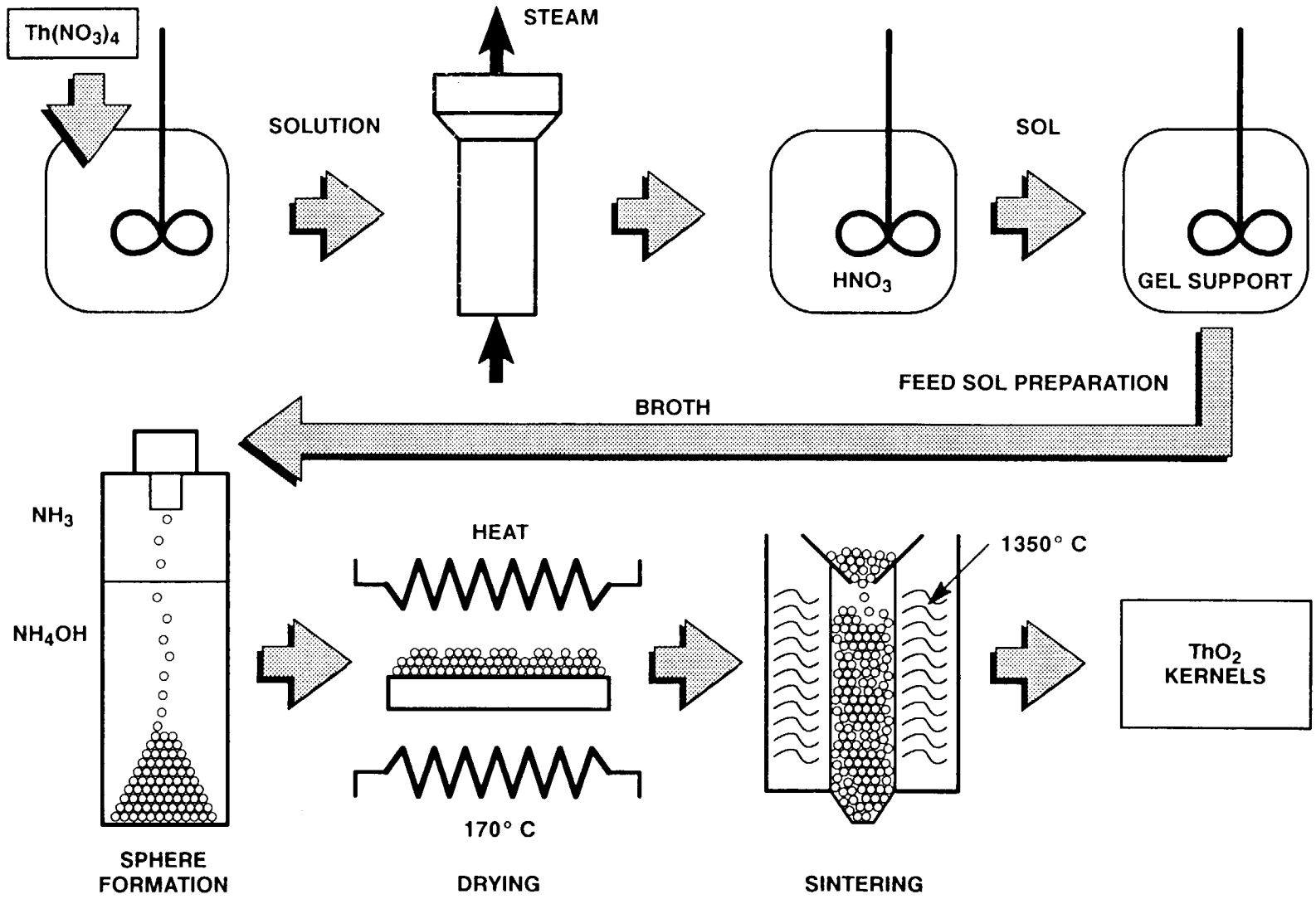

Fig. 5-10. ThO_2 kernel summary flowsheet

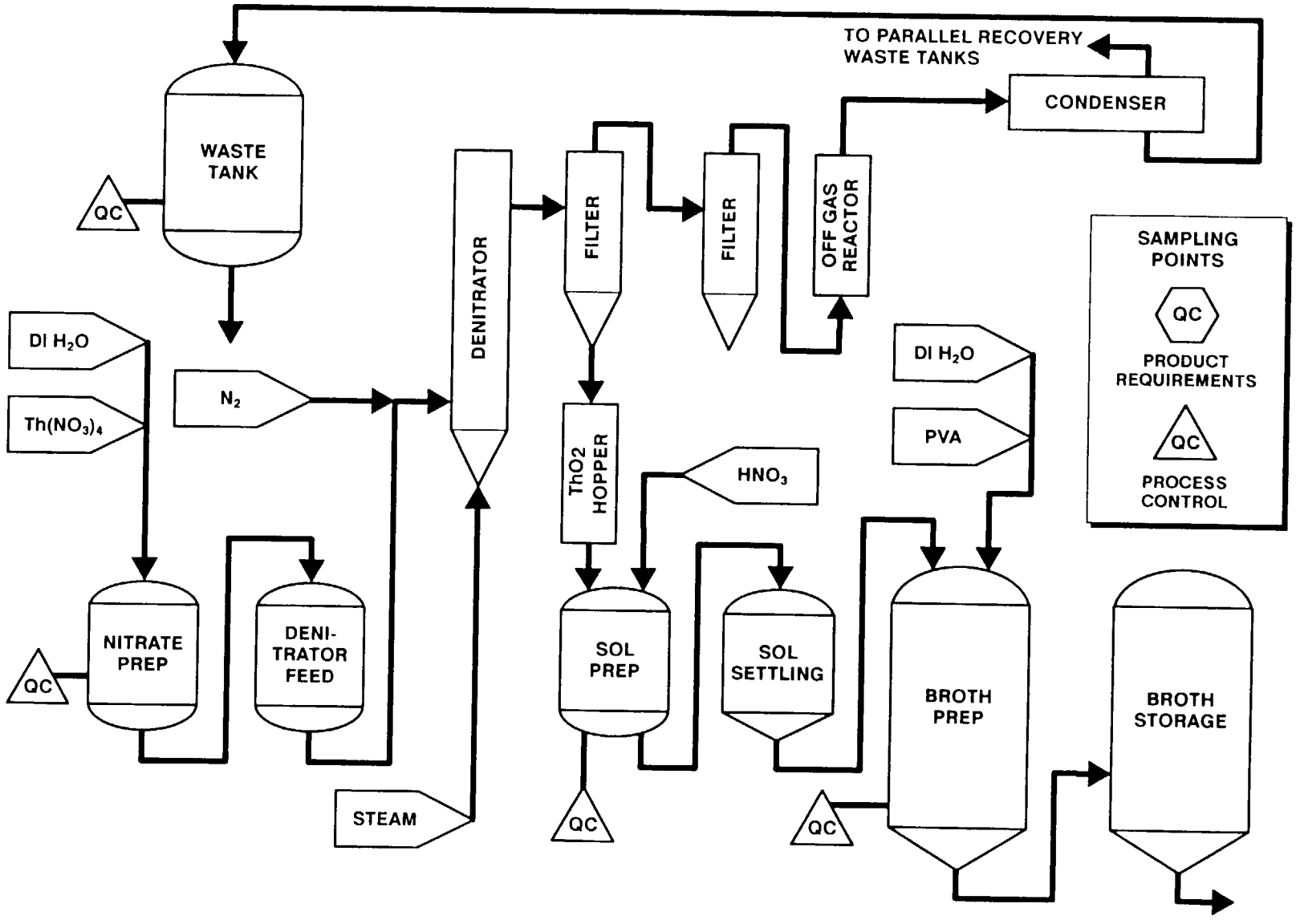

Fig. 5-11. ThO_2 broth preparation flowsheet

The solution is next transferred to a denitrator feed tank and injected at the bottom of the steam denitrator. This is a continuous fluid bed reactor utilizing 300 micron diameter ceramic beads to accelerate the reaction. The $Th(NO_3)_4$ solution is sprayed onto these beads while the bed is fluidized by superheated steam at the rate of 30 lbs/hr. At these conditions, $Th(NO_3)_4$ solution is thermally decomposed and reacts with the steam to form ThO_2 powder, water, nitric acid, and nitrogen oxides.

The powder product is transported from the denitrator by a fluidizing gas. The powder collects on sintered metal filters which are blown down every 20 sec by nitrogen jets. The powder falls into a ThO_2 hopper. The capacity of the denitrator unit is about 6.6 Kg ThO_2/hr (5.8 Kg Th/hr).

To eliminate excess liquid wastes, an off-gas reactor is used to decompose HNO_3 gas to N_2, O_2, and H_2O. The gases pass to a condenser, where water and unreacted nitric acid are removed as liquid waste. The remaining gases are pumped to fume scrubbers.

The thoria powder is dispersed at 70°C into the sol prep tank. Each addition of powder raises the pH of the mixture slightly. The pH is maintained at approximately three throughout sol preparation by adding a 12% nitric acid solution. These additions of powder and acid continue until the density of the sol is approximately 1.95 g/cm^3. Overall material additions are approximately 80 l H_2O, 10 l HNO_3, and 105 kg ThO_2 powder.

The sol is then transferred to the sol settling tank, where it is allowed to cooldown. It is then pumped to the broth prep tank and mixed with 18% PVA solution. The final PVA concentration is 12 g/l of broth. Now it is ready for sphere production and is pumped to the broth storage tank.

5.6.2. Microsphere Production

The thoria line from sphere-forming through drying is a continuous process. The flow sheet for these steps is given in Fig. 5-12. The sintering furnace also operates continuously. The thoria line has four droplet generators with three nozzles each. This portion of the process has a capacity of over 10 Kg Th/hr. The piston vibrator of the droplet generator is driven by a wave frequency generator through an audio frequency power amplifier. The frequency setting and nozzle diameter are dependent on the desired final product size. Spheres with a final diameter of 200 to 850 μm can be produced using these sphering heads.

The falling droplets react with ammonia for the microsphere gelling process. The gelling spheres drop directly into the top stage of the wash column. This three-stage column uses aqueous ammonia as a countercurrent wash solution. Each stage has its own fluid recirculation loop to agitate the kernels and control holdup time.

A total holdup time of 30 min is needed to completely gel the spheres and sufficiently lower the concentration of ammonium nitrate by-product in the kernels. The wash solution is added at a rate equal by volume to four times the sphere dropping rate. Fresh wash solution is added to the lower stage recirculation loop. The spent wash solution is removed from above the top stage and is sent to a recovery system.

In the recovery system the fluid is reacted in the wash evaporator with NaOH to remove the nitrate ion as $NaNO_3$. The aqueous ammonia is then boiled off and condensed before recycling through the column. This system removes about 99% of the nitrates from the wash solution and recovers about 95% of the ammonia for reuse.

From the wash column, the microspheres fall onto a distributor plate which channels them into the trays on a dryer conveyor belt. The thoria line dryer has infrared heating elements supplemented by an air

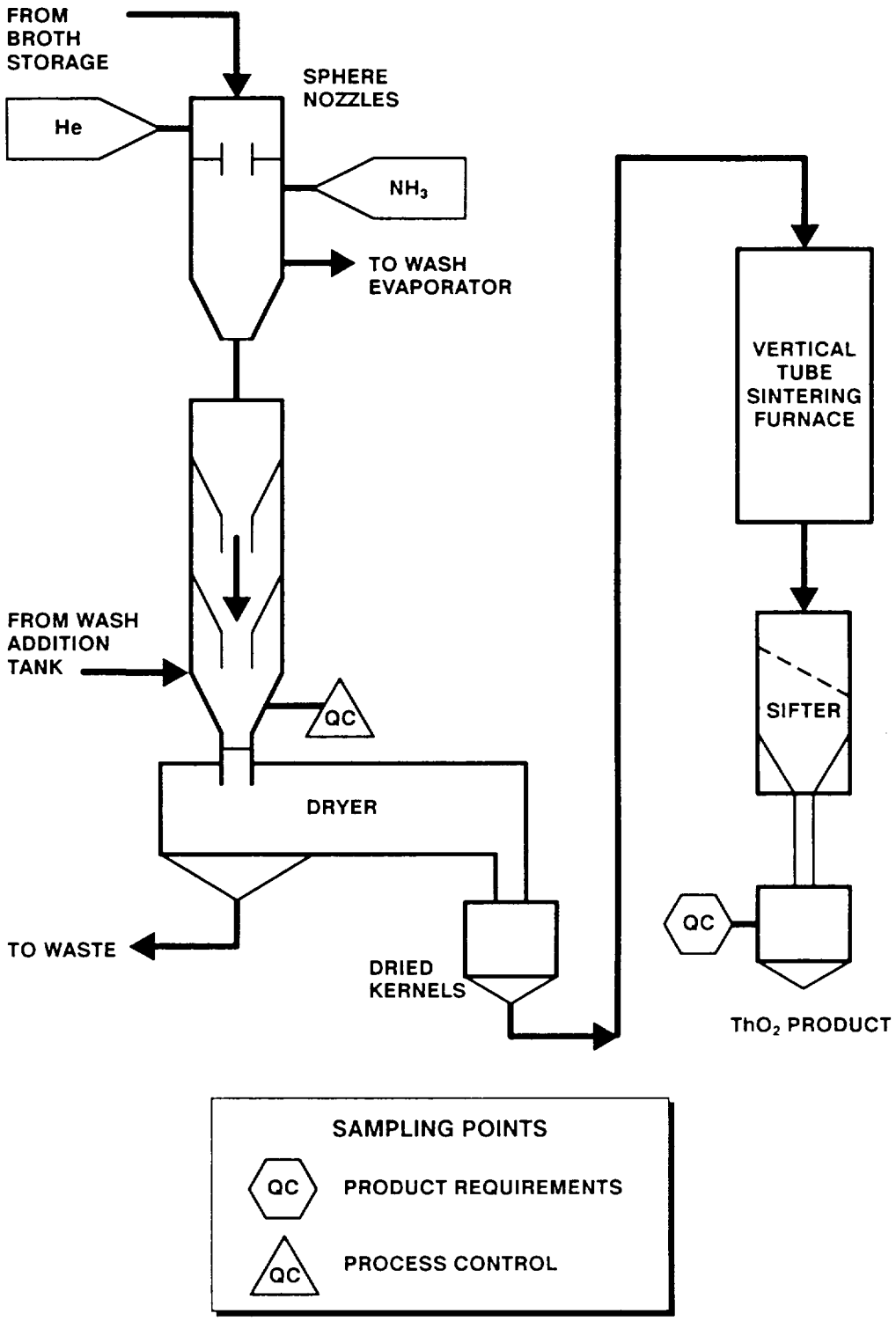

Fig. 5-12. ThO_2 microsphere production flowsheet

heater. Air is drawn through the dryer by a negative pressure supplied by the building filtered exhaust system. The kernels leave the dryer with a mean density of about 4 g/cm^3. The product is collected in a hopper and transferred by the operator to the sintering furnace feed.

The sintering furnace is a vertical unit with a silicon carbide glow-bar type alumina tube. The product is heated as a batch to 1300°C. After sintering and cooling, the kernels are unloaded and mechanically screened to isolate the product. The thorium oxide kernels are tabled in the same manner as UCO kernels (see Section 5.2.9).

5.6.3. Thoria Kernels Fabrication Chemistry

Fertile kernels are a one-phase system composed of almost theoretically dense ThO_2. This section summarizes the chemistry related to ThO_2 kernel fabrication.

5.6.3.1. Sol Preparation. The process begins with the dissolution of $Th(NO_3)\cdot 4H_2O$ crystals in water to form a concentrated solution of thorium nitrate feed.

Finely divided thoria powder is prepared by thermal decomposition of the thorium nitrate feed with superheated steam. Steam denitration of thorium nitrate solutions proceeds by the following reaction:

$$Th(NO_3)_4 \cdot x\ H_2O\ (l) + 2\ H_2O\ (g) \rightarrow ThO_2 \cdot zH_2O\ (s) + (x - z)\ H_2O + HNO_3\ (g)$$

where: $4 < x < 6$

$z \sim 0.05$

The degree of reaction completion depends on the residence time and reaction temperature. Since the residence time on a continuous feed

fluid bed reactor is an exponential distribution, a range of partially denitrated thorium salts occurs along with the $ThO_2 \cdot zH_2O$ crystals (Ref. 5-16).

This process produces a fine powder consisting of the ThO_2 crystals with some nitrate ions in place of the oxygen [$ThO(NO_3)_2$].

Thoria sols are obtained by dispersing the previously made powder in diluted nitric acid. The small (50 Å) thoria crystals have a high surface area to volume ratio, which allows much of the remaining NO_3^- ions to be displaced by OH^- when added to the diluted nitric acid solution, thus forming a concentrated, stable sol at a pH between 2.7 and 3.5.

5.6.3.2. Broth. The ThO_2 sol is mixed with a PVA dispersion to form broth.

$$ThO_2 + HNO_3 + H_2O + PVA$$

PVA changes the rheological properties of the broth to allow formation of droplets of uniform sizing and also forms a matrix that stabilizes those droplets during the early stages of gellation.

The chemistry of the PVA solution is described in Section 5.6.3 and will not be repeated here.

When a stable sol is formed, PVA is added as a gelling agent. PVA is a polymeric alcohol of varying molecular weights. When PVA is added to colloidal thoria, the PVA molecules cause an increase in broth viscosity due to bridging between the ThO_2 crystals and the PVA. The degree of bridging and viscosity is a function of the molecular weight of the polymer.

5.6.3.3. Drop Formation and Gellation. The theory of fertile drop formation is the same as the one described for UCO kernels in Section 5.4.

Gelation of the thoria sol is caused by the upset of a delicate ionic balance present in the sol. As ammonia diffuses into the sol droplet, H^+ ions are converted to NH_4^+, raising the pH of the broth. This causes the ThO_2 particles to polymerize, forming a gel. As the pH increases, PVA becomes insoluble in the broth, causing the PVA to gel also. This forms a very stable gel lattice to contain the agglomerated ThO_2 molecules. PVA and some nitrate ions as ammonium nitrate also are retained.

5.6.3.4. Heat Treatment. The gelled and washed kernels are dried at temperatures of up to 300°C. During this step, kernel volume is significantly reduced as water is thermally removed and the PVA matrix contracts.

Afterwards, impurities are thermally decomposed and the ThO_2 densifies as the kernels are sintered at temperatures of up to 1300°C.

At approximately 220°C, residual ammonium nitrate decomposes and exits the kernel by diffusion. The decomposition of ammonium nitrate occurs very rapidly and can create internal stresses and breaking of kernels. For that reason, the gelled kernels are washed in diluted ammonia to extract ammonium nitrate formed during gellation.

Washing in ammonia makes the gelled spheres even more stable by more completely displacing the remaining H^+ ions.

PVA decomposes in a two-step process. During the first step, PVA begins to dehydrate at 170°C. Dehydration is accompanied by formation of volatile products such as acetaldehyde, crotonaldehyde, benzaldehyde, and acetophenone. In the second step, the polymer macromolecules are

thermally decomposed in the presence of air to form CO and CO_2 according to the following formula:

$$-(CH_2 - COH)_2- + 2.5O_2 \rightarrow 4CO + 3H_2O$$

$$-(CH_2 - COH)_2- + 4.5O_2 \rightarrow 4CO_2 + 3H_2O$$

After all the impurities (H_2O, PVA, NH_4NO_3, NH_3) have been removed, sintering takes place between 1000° and 1300°C by solid phase diffusion across boundaries.

6. COATED FUEL PARTICLE FABRICATION

6.1. PARTICLE DESCRIPTION

6.1.1. Coating Technology

Both fissile (UCO) and fertile (ThO_2) kernels are coated with eight layers of PyC and SiC to make up the TRISO coating as described in Section 3.3. The combined coatings of IPyC and SiC on the fuel particles are the primary barrier to fission product release during irradiation in the MHTGR.

Each layer of coating is deposited onto the fuel particle by chemical vapor deposition (CVD). PyC coating is accomplished by the thermal decomposition of acetylene, propylene, or a mixture of those gases in a fluidized particle bed. Argon is used to maintain fluidization velocity in the coater gas to desired coating concentration. Methyltrichlorosilane (MTS) thermally decomposes at high temperature in the presence of hydrogen to form the SiC layer.

The type and quality of the coating deposited are determined by complex chemical kinetic and fluidization dynamic mechanisms related to high temperature pyrolysis reactions. LeFevre first described the mechanism for the thermal decomposition and deposition of PyC onto fuel particles (Ref. 6-1). First the heated coating gas molecules undergo dehydrogenation. The molecules nucleate, forming agglomerates in the gas phase. As the gas phase agglomerates pass through the fluidized particle bed, contact with the circulating particles causes some of the agglomerates to attach to the particles. The attached agglomerates lose the remaining bonded hydrogen and undergo a surface migration to form a solid coating.

Most of the gas phase agglomerates escape contact with the particles in the fluidized bed. The agglomerates bond together and dehydrogenate to form soot. LeFevre correlates the diameter of agglomerates to the deposition conditions. A large agglomerate diameter coupled with a short residence time in the coater give a coating with low density and high porosity. A small agglomerate diameter gives a high density coating with low porosity. Figure 6-1 shows a schematic of LeFevre's PyC coating mechanism for producing large and small diameter agglomerates. Figure 6-2 shows the generalized coating zones for a typical fluidized bed coater.

Shortly after the coating gas enters the coater, it dehydrogenates and forms agglomerates in Zone 1. In Zone 2, the decomposed agglomerates attach to the particles, forming a coating. In Zone 3, the agglomerates attach to each other to form soot.

Although LeFevre's mechanism was developed for PyC coatings, a similar mechanism defines the deposition of SiC onto the fuel particles.

To deposit coatings with the required physical properties (Ref. 6-1), the concentration of the gas phase agglomerates must be controlled in relation to the surface area of circulating particles in the active coating zone. Controlling the particle bed fluidization characteristics is more precise in small diameter coaters (<70 mm diameter) than large coaters (240 mm diameter). Most of the coating bed area in a small diameter coater is located in the active coating zone, where each particle has a greater chance of exposure to a similar coating environment during the total coating process.

As the coater diameter increases and the number of particles to be coated becomes greater, the nature of the coating environment changes. Because individual particles are exposed to slightly different local conditions during coating, the coatings may have very different physical properties from particle to particle in the batch. Coating defects such

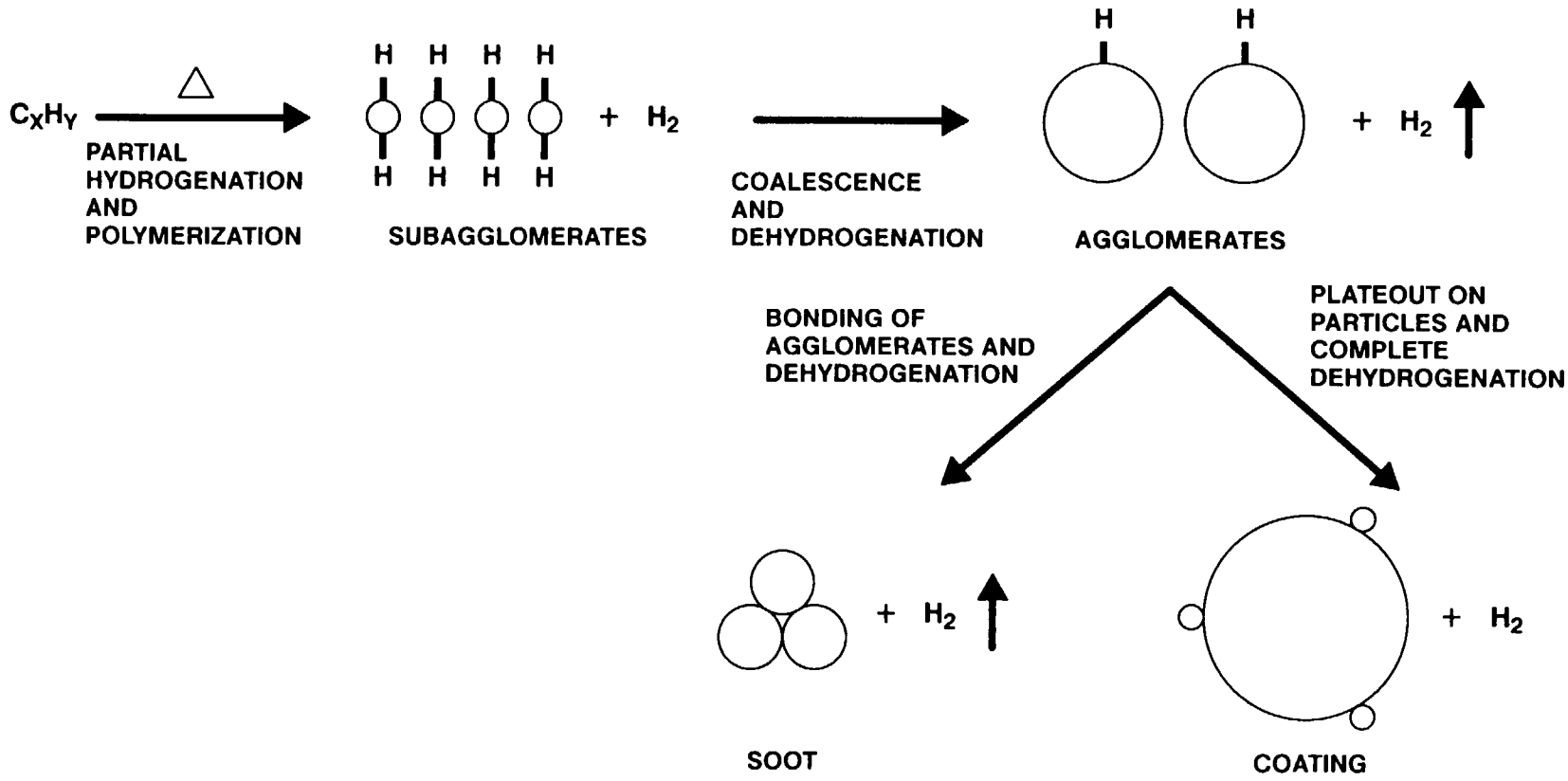

Fig. 6-1. Schematic of LeFevre's PyC coating mechanism

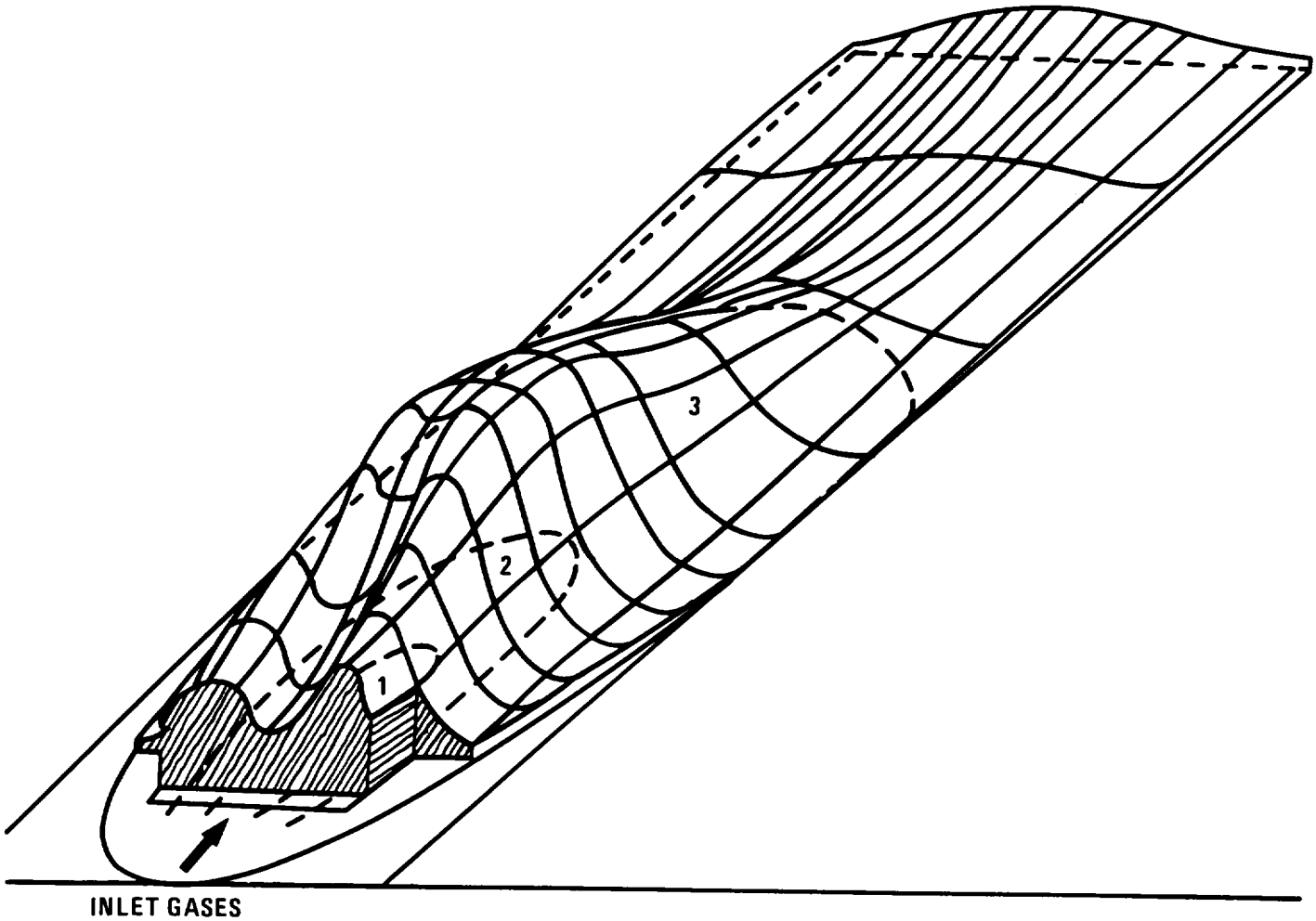

Fig. 6-2. Mapping of the coating zone in a fluidized bed coater

as density variation, faceting, voids in the SiC coatings (gold spots), and missing coating layers could result.

MHTGR coating process development has been performed in a 240 mm coater with batch sizes of 5 Kg for UCO fissile and 10 Kg for ThO_2 fertile. The number of particles in a typical coating run ranges from 18 million fertile to 24 million fissile particles per batch.

The quality of coated particles prepared with this technology is shown in Fig. 6-3, which illustrates the uniform particle size and coating thickness.

6.1.2. Coating Process Description

Coating process flow is diagrammed in Fig. 6-4. The coater furnace is maintained under a constant nitrogen purge when not in service. All process gases flow into the bottom of the coater column. At the start of operation, the coater is heated empty to approach the coating temperature. At approximately 1100°C, the control system switches from nitrogen purge to an argon purge. At high temperature, nitrogen reacts with the fuel particles to form nitrites. Once the coater loading temperature is reached, the fuel particles are loaded into the coater through the loading tube/funnel assembly. The gas velocity in the coater is high enough to completely fluidize the fuel particle bed. The gas flow into the coater is switched from argon to the coating gas by the gas regulation system at the time the coating commences.

PyC coating is accomplished by thermal decomposition of acetylene, propylene, or a mixture of those gases. The gas decomposes in the coater hot zone and deposits PyC on the fluidized particles. Argon and hydrogen are used as the diluent and fluidizing gases. SiC coating is accomplished by the thermal decomposition of MTS, which is carried into the coater as a vapor with a hydrogen stream.

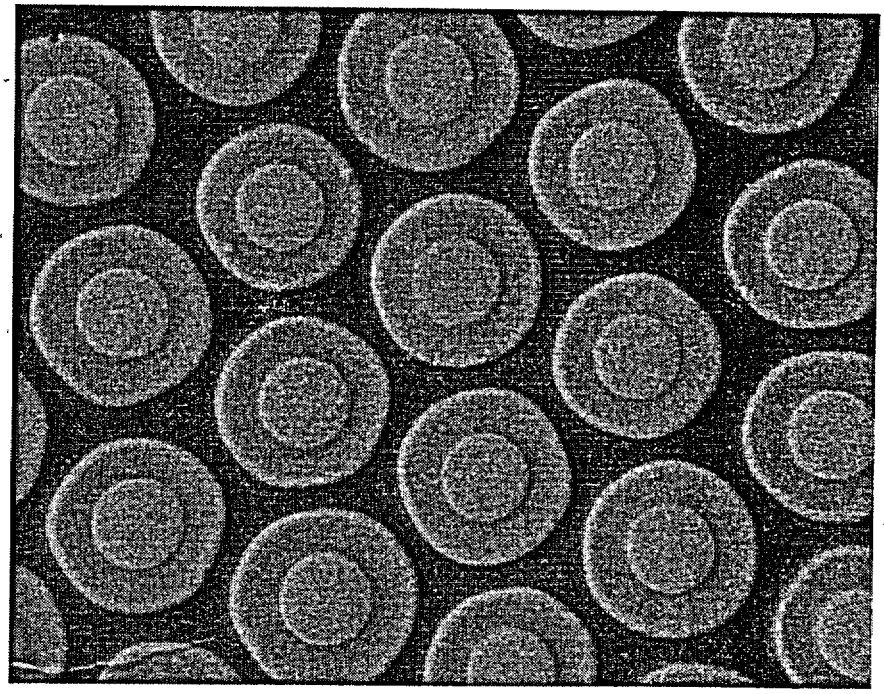

(A) X-RAY OF OPyC COATED UCO PARTICLES

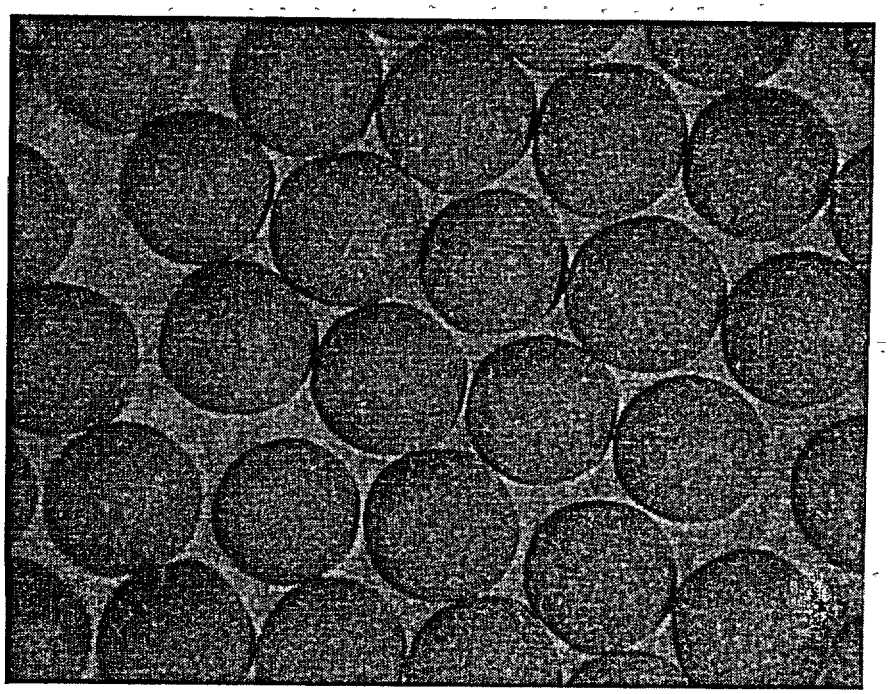

(B) PHOTOGRAPH OF OPyC COATED PARTICLES

K-232 (3)
9-13-91

Fig. 6-3. TRISO coated UCO particles prepared in the 240 cm coater (25X magnification)

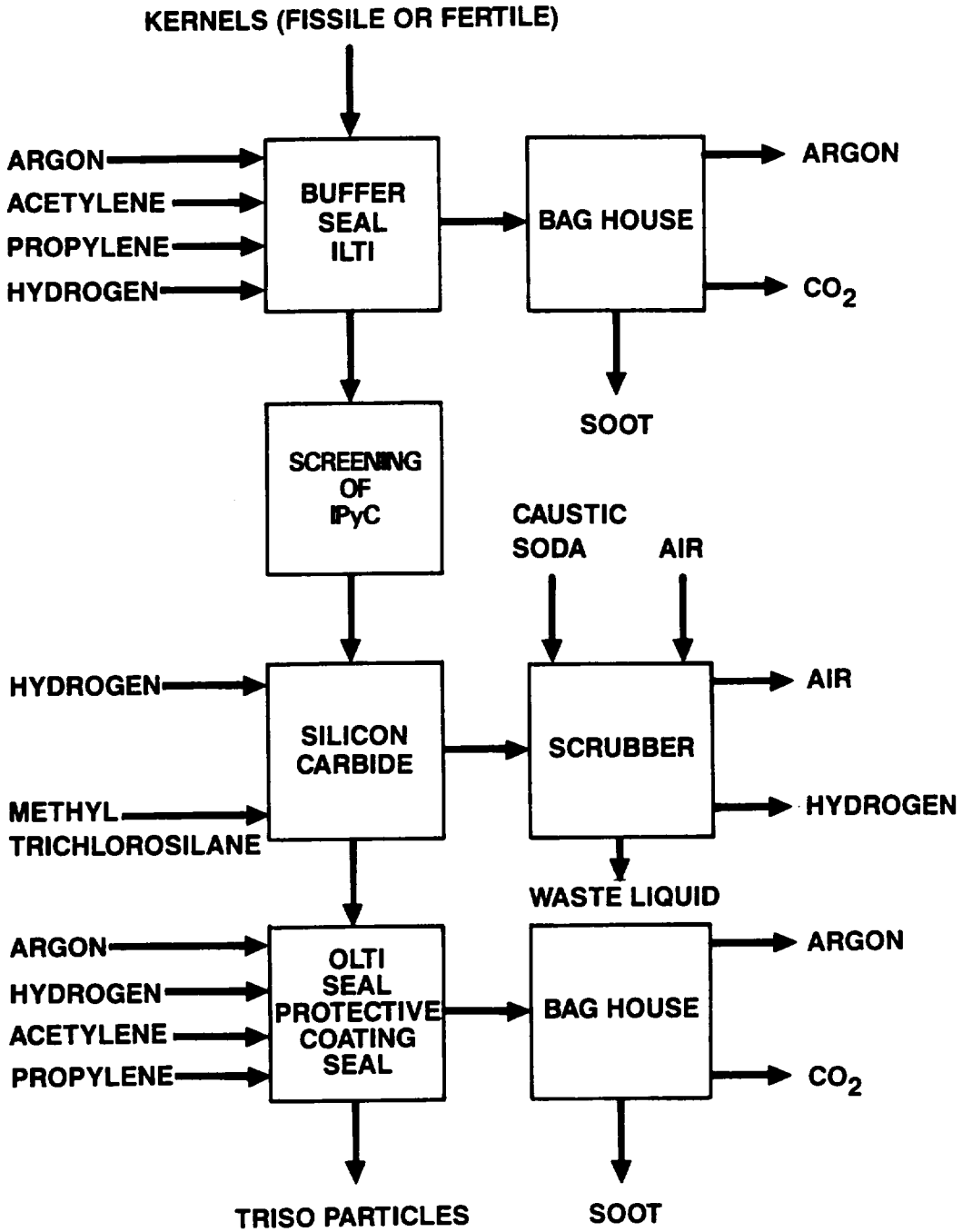

Fig. 6-4. TRISO particle coating process flow (sheet 1 of 2)

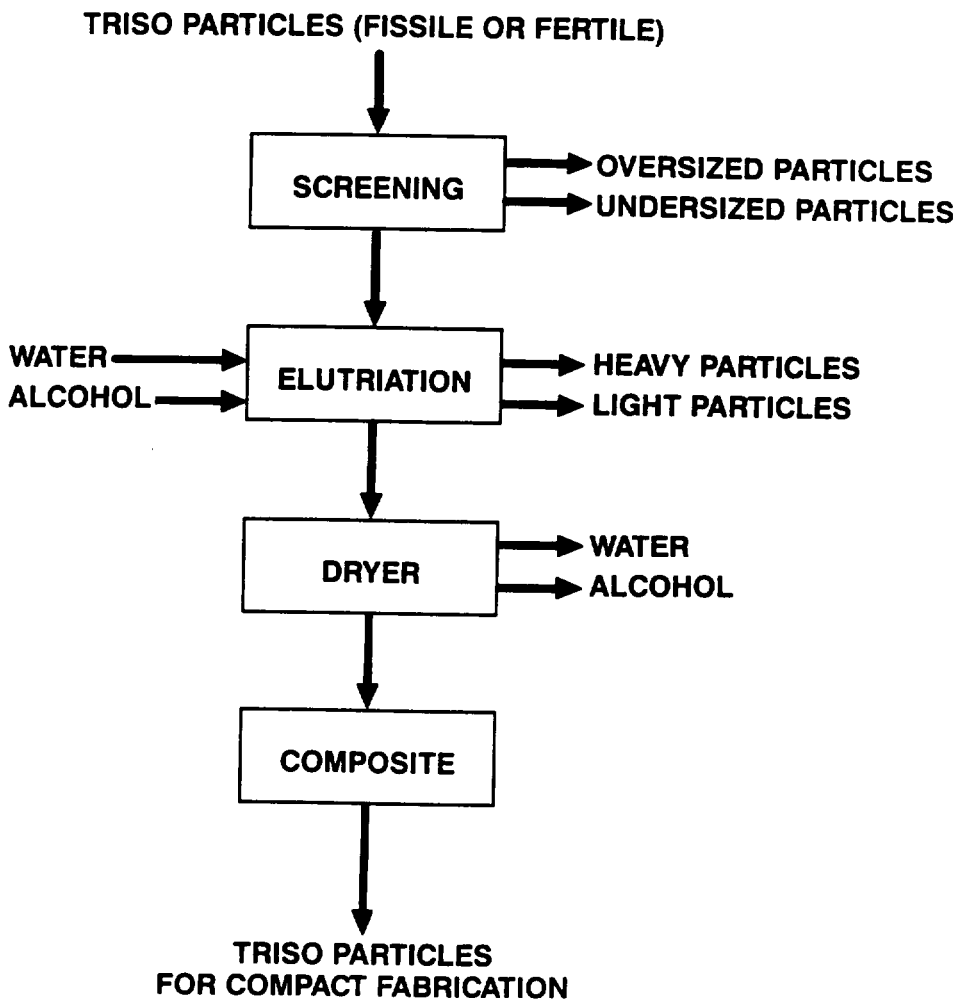

Fig. 6-4. TRISO particle coating process flow (sheet 2 of 2)

After the coating time has elapsed and coating for the particular layer is complete, levitation gas (argon) is turned on and coating gas turned off by the gas regulation system. If more than one coating layer will be deposited during the coating run, such as the change from buffer to IPyC layer, the coater is heated (or cooled) to the next required temperature and the gas regulation system is switched to the levitation gas until the new coating temperature is reached.

At the new coating temperature, the gas regulation system is switched to the new coating gas and the coating sequence resumes. After the coating run, the temperature controller is turned down as required to cool the furnace. The levitation gas aids the cooling process and maintains an inert atmosphere in the furnace. At 1125°C, the coated particles are unloaded through the discharge chute into the unload hoppers.

The harvested batch is sampled for quality control measurements. Once all coating layers have been applied and approved by quality control, the particles are tabled, screened, and elutriated before compositing for compact fabrication.

During PyC coating, exhaust gases are directed to the soot filter, where the soot is removed. Then gases pass through the absolute filters to remove radioactive particulates, then are exhausted to the atmosphere.

6.1.3. Coater Selection

Fuel particle coating development has focused on preparing larger batches of higher quality coated fuel particles. Initially, small diameter (25 to 75 mm) coaters with simple cone gas distributors were used for small coating batches. Later development on the 240 mm coater demonstrated large batch sizes of quality fissile (5.7 Kg of UCO) and fertile (10 Kg of ThO_2) materials.

A diagram of the 240 mm coater is shown in Fig. 6-5. The coater is licensed to deposit TRISO coatings on UCO fuel particles at a batch size of 5.0 Kg of 19.9% enriched uranium.

In a standard fluidized bed, the coating thickness variation depends on the rate of particle circulation relative to the coating deposition rate in the coater. The fluidized particle bed consists of a series of active zones with varying coating rates (Fig. 6-6). During coating, fuel particles entering the most active coating zone more frequently obtain the thicker coatings; the opposite is true for those dwelling longer in the less active coating zones. The PyC coatings require a relatively short time to apply (10 to 50 min); the SiC coating requires over 120 min to apply, which results in a low thickness variation.

The coating thickness variation from particle to particle in the batch can be reduced by controlling both the particle circulation rate through the active coating zones and the entry point of the particles to a fixed point in the active coating zone. The small diameter tube (draft tube) in the center of the coater (Fig. 6-5) is installed to control the bulk flow of solids through an active reaction zone. The draft tube isolates the active coating zone from the close-packed particle zone near the liner wall. (Excessive faceting occurs in coatings deposited in the close-packed particle zone of the coater.) The particles are transported up the draft tube by entrainment in the gas stream because of the density difference between the draft tube and the annulus. As the bulk gas velocity increases, the particle circulation rate increases. At a given bulk gas velocity, increasing the opening at the base of the draft tube increases the particle circulation rate. Particle bed circulation rates are on the order of 200 to 300 cycles per coating run. This assumes that the particle velocity in the draft tube is close to the bulk gas velocity in the draft tube and approximately one third of the particles are in the draft at any given time.

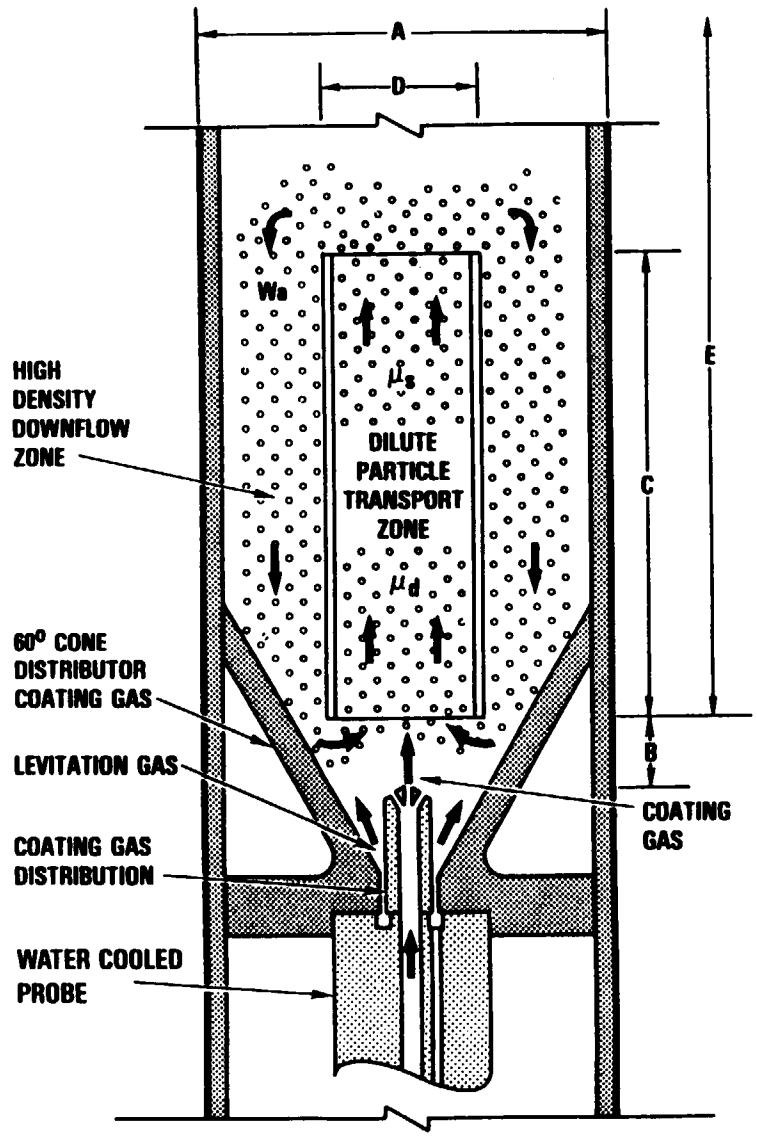

H-659(1)
5-12-86

KEY PROCESS VARIABLES

W_a = SOLIDS TRANSPORT RATE IN ANNULUS (kg/m^2 SEC)

μ_s = SOLID VELOCITY IN DRAFT TUBE (cm/sec)

μd = GAS VELOCITY AT BASE OF DRAFT TUBE (cm/sec)

A = COATER DIAMETER

B = DRAFT TUBE OPENING AT BASE

C = DRAFT TUBE LENGTH

D = DRAFT TUBE DIAMETER

E = COATER HEIGHT

Fig. 6-5. Fast fluid-bed coating apparatus

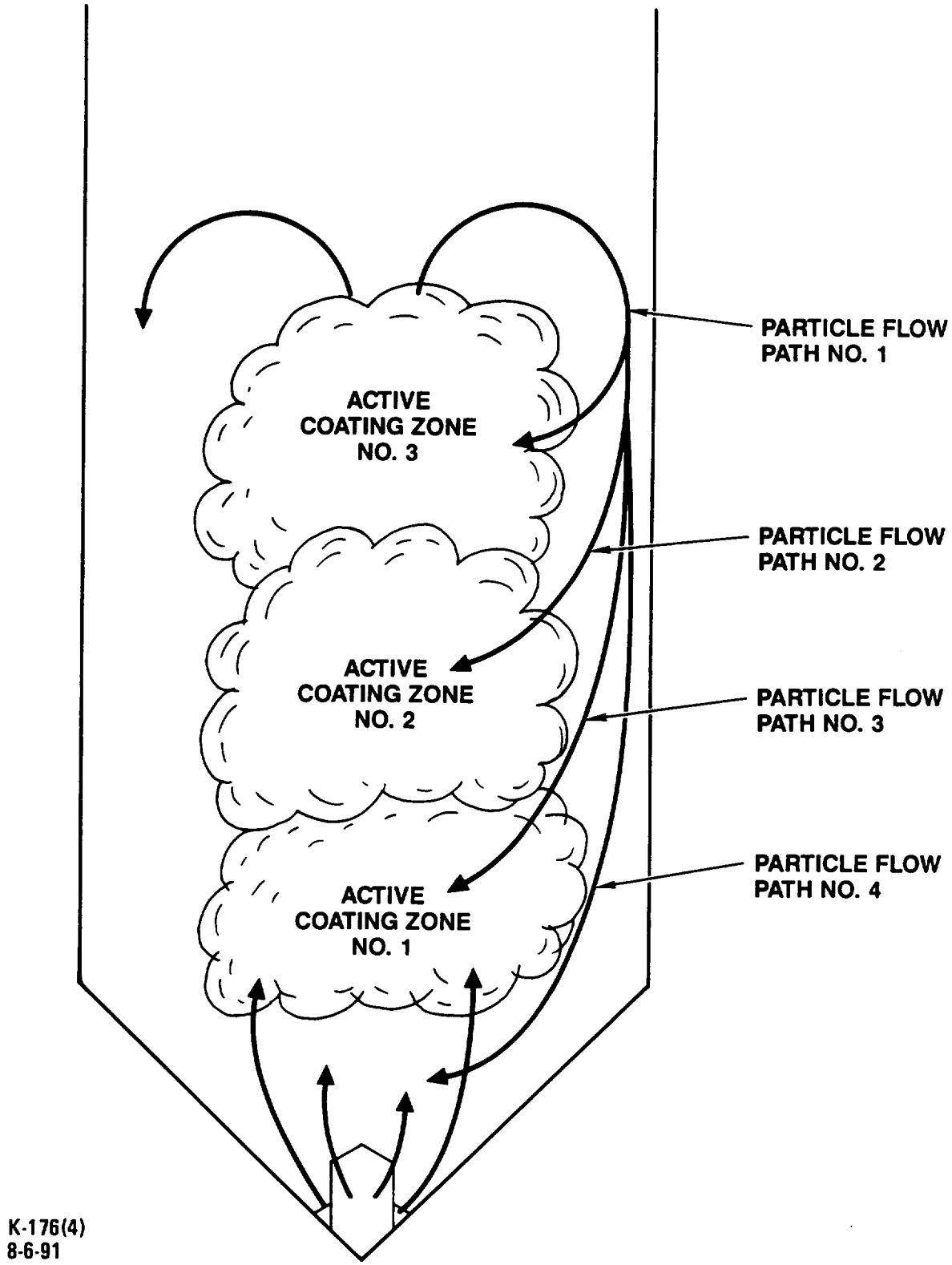

Fig. 6-6. Particle circulation paths during fluid-bed particle coating

Tests on a solid substrate suspended vertically in the draft tube have shown that the PyC coating rate increases vertically up the height of the draft tube. The PyC coatings deposited at the lower point of the draft tube near the gas inlet were of lower coating thickness, higher density, and higher anisotropy. Controlled particle circulation rates through all coating zones produce more uniformly coated fuel particles.

6.1.4. Coater Equipment

The 240-mm coater (Fig. 6-7) is composed of several subsystems, including a computer control unit, the coater body, the gas supply tanks, a gas control system, hot unloading, cooling, and off-gas system. The off-gas system includes a soot filter, off-gas filtration unit, and a caustic fume scrubber.

The control panel (Fig. 6-8) consists of the computer, the temperature controller, the gas controller, and all alarm/monitoring systems for the unit. The coater is operated in either an automatic or a manual mode. In the automatic mode, the controller is interactive with the operator, prompting the operator for input information as necessary.

The coater body (Fig. 6-9) contains a graphite cylinder, graphite liners, a draft tube, a gas probe assembly, and heater units. The stainless steel coater body is jacketed with channels to allow for cooing water to flow vertically up the column. A flow rate of ~30 gpm is required to cool the outside coater body. Inside the furnace are the upper and lower graphite liners, where the coating takes place. The draft tube is in the center of the lower liner. The probe assembly contains the gas distributor nozzle and the cone. The gas lines into the probe are water cooled to avoid any premature decomposition of the coating gases. The probe assembly mates to the lower liner when raised by the probe hydraulic system. A glove box is mounted around the probe assembly at the bottom of the coater. The glove box facilitates the removal of particles from the coaters without oxidizing.

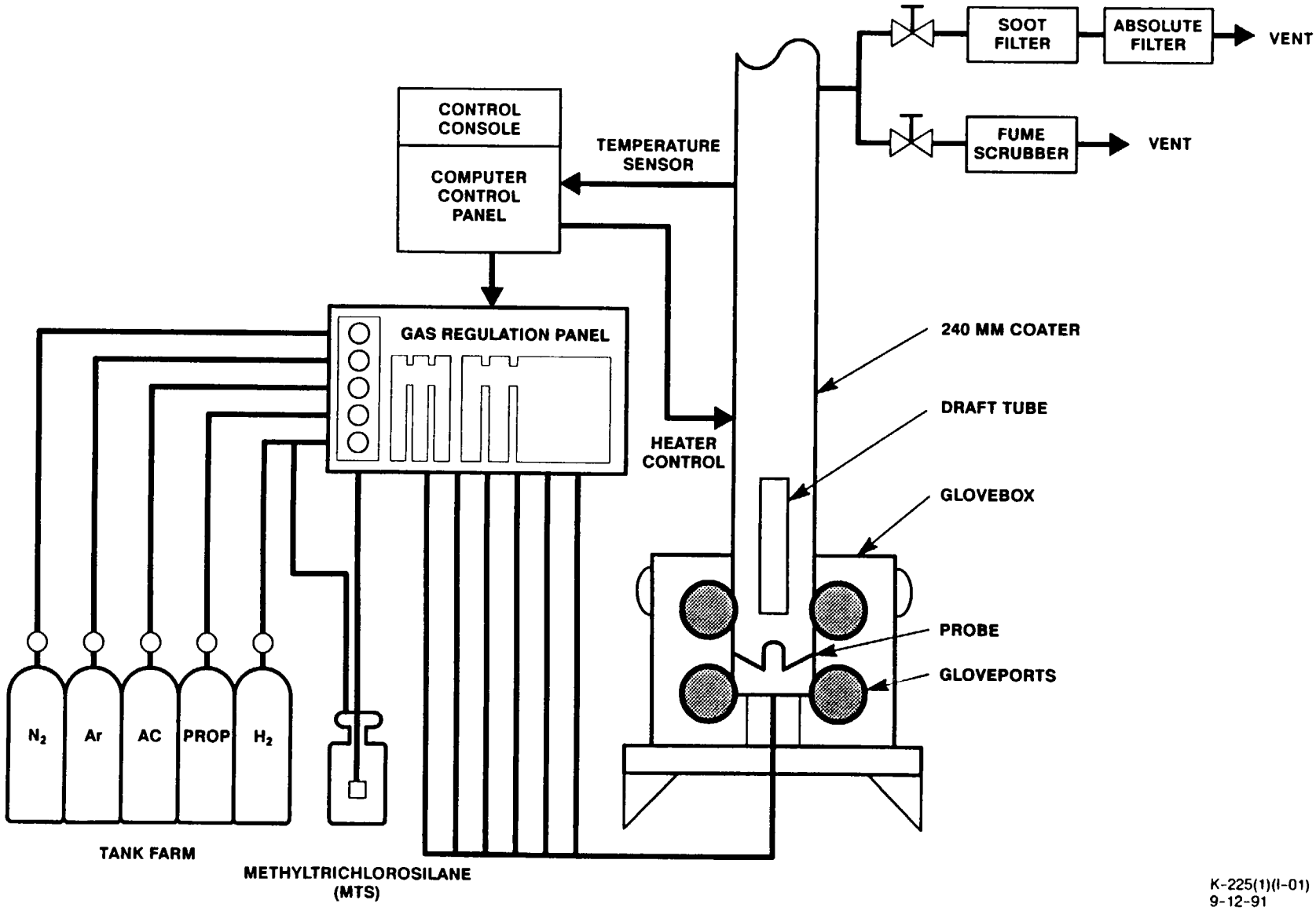

Fig. 6-7. 240 mm coater system

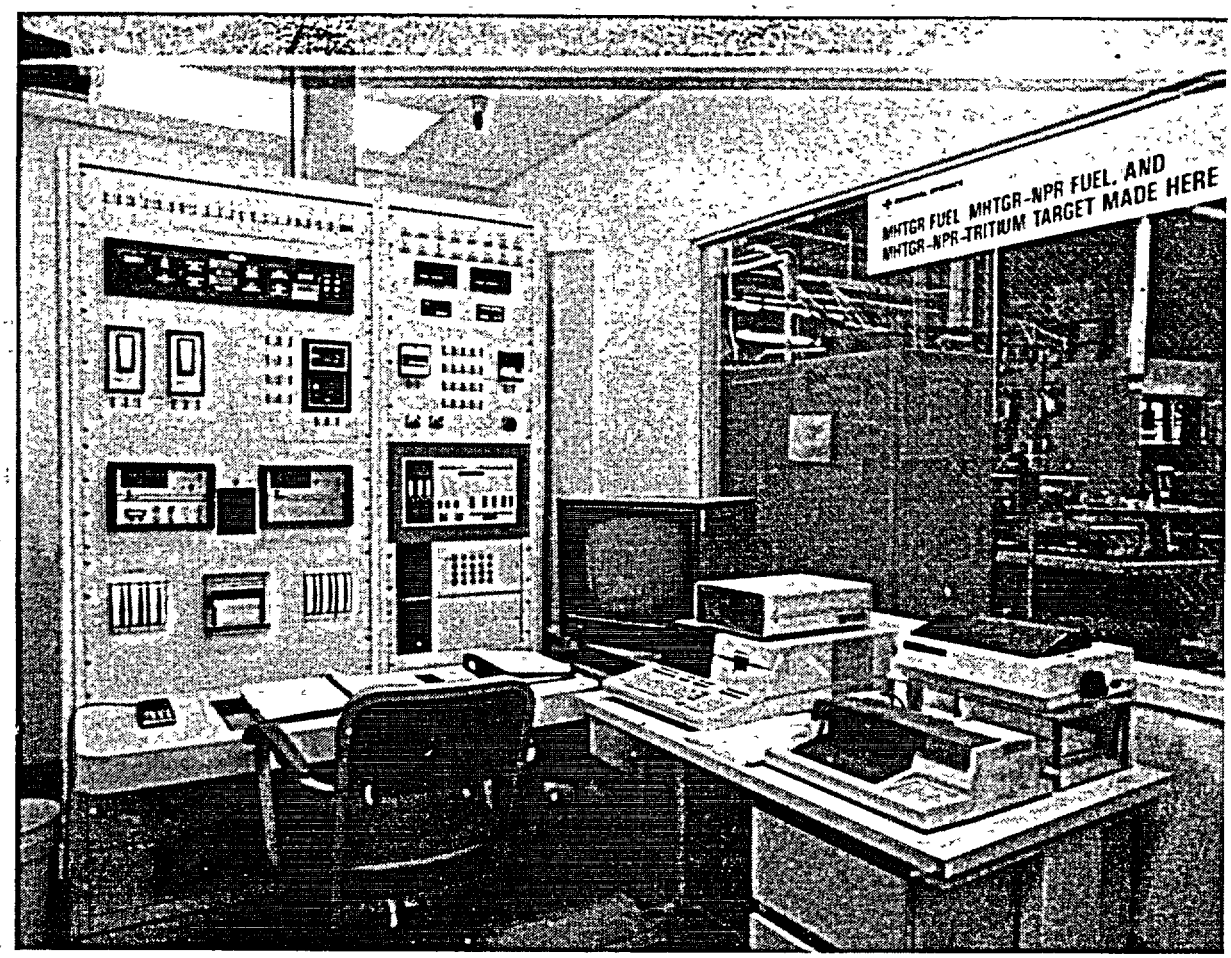

Fig. 6-8. Control panel

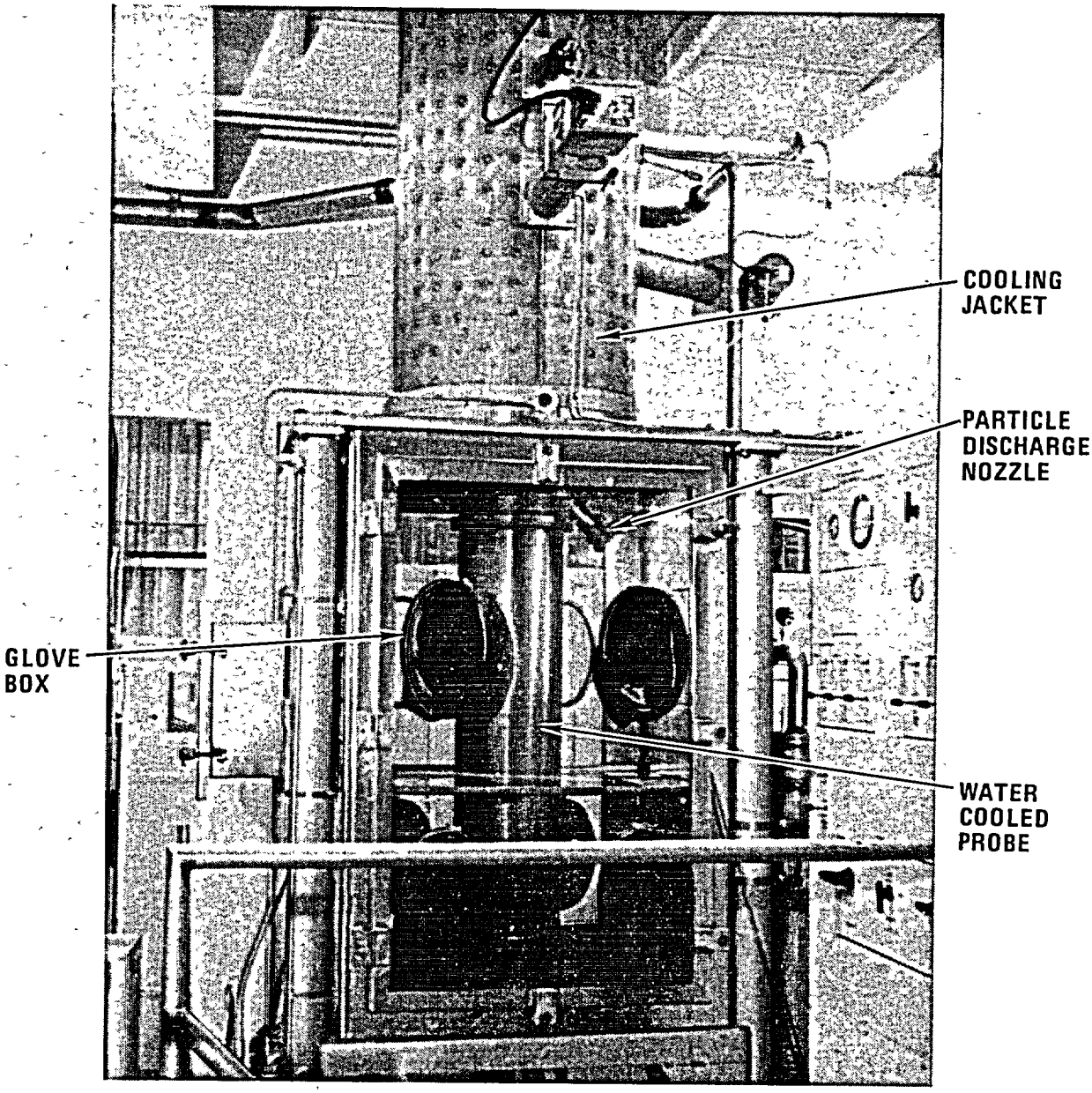

Fig. 6-9. 240 mm coater

Figure 6-10 shows the probe control panel. A 500 KV resistance furnace provides the heat required to raise the temperature inside the furnace to a maximum of 1700°C to apply the SiC layer on the fuel particles. An insulation layer limits heat losses from the furnace.

Substantial quantities of inert gases and coating gases are required during coating. Bulk storage of acetylene, propylene, nitrogen, hydrogen, and argon are provided onsite in a tank farm.

The gas control system controls gas flow to the coated particle bed during coating and noncoating. The system consists of panel-mounted calibrated rotometers and pressure regulators (Fig. 6-11). Included in the gas control system is the MTS tank. Hydrogen, initially brought from the tank farm, flows into the MTS tank from the gas regulation system. The hydrogen bubbled into the MTS tank carries the MTS vapor into the coater. The amount of hydrogen which flows into and out of the MTS tank determines the amount of MTS that flows into the coater.

The off-gas system consists of the soot filter, absolute filter, and fume scrubber. During PyC coating, the off-gas flows into the disentrainment chamber through the soot and absolute filters. The absolute filter removes potentially radioactive materials from the off-gas.

During SiC coating, HCl gas is produced from the decomposition of MTS. The off-gas from SiC coating is sent through a fume scrubber to remove gaseous HCl. The exit gas stream passes through the scrubber column, where the gas is mixed with water. HCl is stripped from the gas stream, forming aqueous hydrochloric acid. The off-gas and hydrochloric acid are pumped through a mixing tank containing NaOH. The hydrochloric acid is neutralized at this stage. The gas exits the mixing tank and flows through a demister column, stripping the gas stream of any water. Finally the gas flows through an absolute filter to remove any radioactive materials.

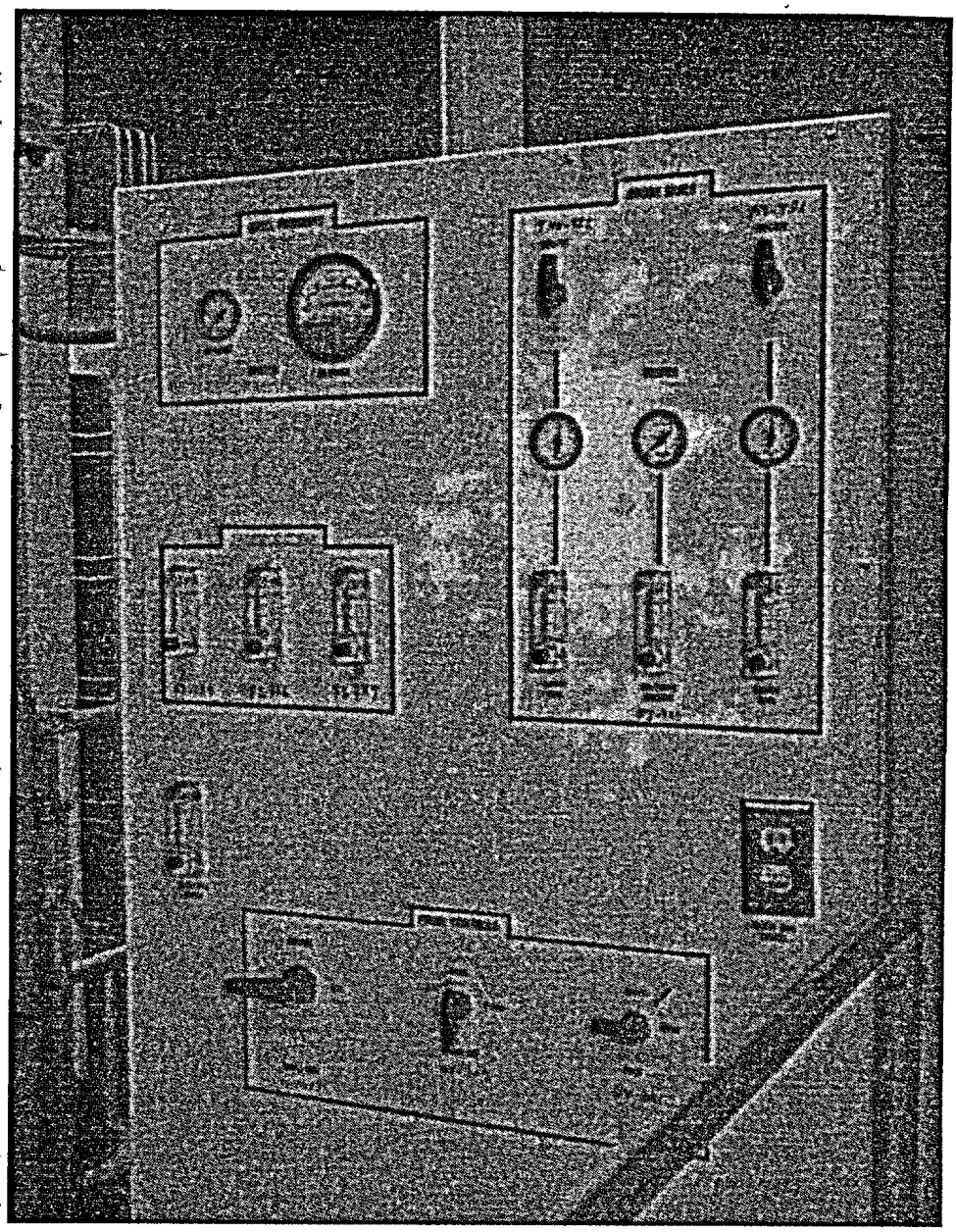

Fig. 6-10. Probe panel

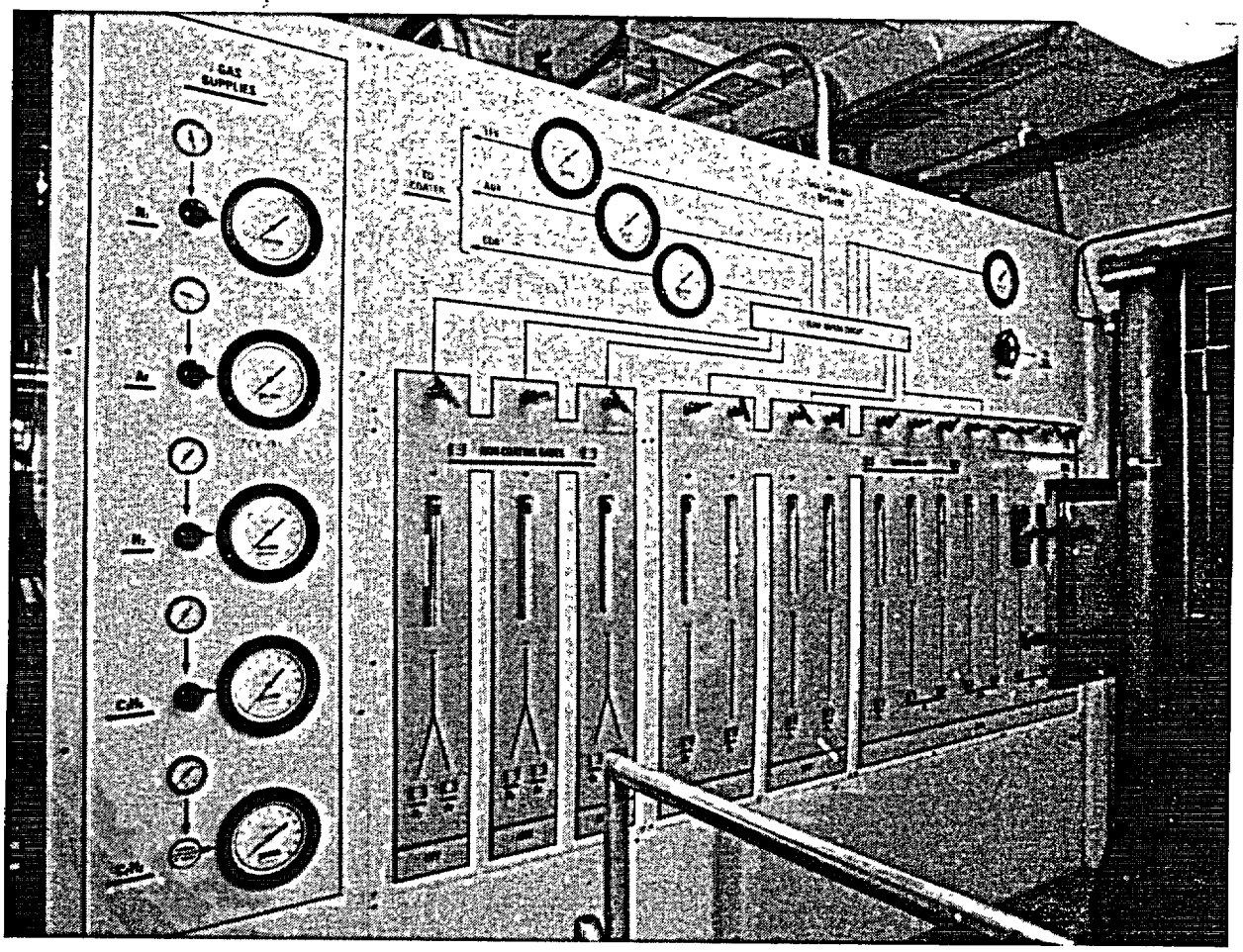

Fig. 6-11. Gas control system

Before exiting to the atmosphere, all gas streams feed into a blower system that dilutes hydrogen below its combustion level.

6.1.5. Safety

Stringent safety measures have been developed to prevent personnel injury or equipment damage. The coating operation uses combustible gases (hydrogen, acetylene, and propylene) in the presence of air and ignition sources. This combination creates a potential for explosion and fire if improperly controlled during coating operations. A combustible gas detector alarm system is included in the system to assure that no combustible gases are leaking. All coater systems exposed to the combustible gases are purged with argon or nitrogen to ensure that the gas atmosphere is free of combustible gases before exposure to air (levels below the LELs). The systems exposed to combustible gases are maintained at pressures above atmospheric pressure until completely purged so as to eliminate back diffusion of air (and a possible explosion).

Radiological safety procedures are required in handling radioactive source materials (i.e., enriched UCO kernels) and potentially contaminated components. Other safety considerations related to operating the coater are electrical safety, high pressure gas handling, and toxic chemical handling. Substantial chemical hazards are present in handling MTS and sodium hydroxide.

6.2. PROCESS MATERIALS AND CHEMICALS

All materials required for coating processes are listed in Table 6-1. The purity of all gases used in the coating process is certified by the supplier. These certifications include chemical analyses by the vendor's laboratory. Use of feed materials is controlled as specified in the MHTGR Fuel Product Specification (Ref. 6-2).

TABLE 6-1
REQUIRED MATERIALS FOR
COATING PROCESSES

Material	Purity (%)
Argon	99.997
Nitrogen	99.95
Hydrogen	99.98
Acetylene	99.6
Propylene	95.0
Methyltrichlorosilane	97.0

6.3. PROCESS PARAMETER CONTROL

Coated fuel particle properties such as density, coating thickness variability, faceting, anisotropy, and SiC coating defects are controlled by a number of coating process parameters (Fig. 6-12). The composition of the diluent and coating gases is highly important to the characteristics of the coating layers.

Coating rates are not specified as a requirement in the product specification. However, the coating rate is important in determining the quality of the coatings deposited. The coating rate is defined as the total coating thickness (microns) divided by the total coating time (minutes). Experience in the 240 mm diameter coater has shown that the best coating properties are obtained when coatings are deposited in the coating rate ranges shown in Table 6-2.

6.3.1. Buffer Coating

The buffer layer is deposited by CVD through the exothermic cracking of acetylene in a fluidized bed at a temperature between 1435° and 1565°C. Thermal effects of the exothermic cracking influence the temperatures in the coating zone. Key buffer coating process parameters for the 240 mm diameter coater are listed in Table 6-3.

Argon is the carrier gas for the buffer process. Nitrogen is not permitted because it may react with the carbide fuel kernel to form nitrides. The buffer coating gas is acetylene (C_2H_2).

Buffer coating porosity and thickness variability are the critical parameters in this layer. Porosity is controlled by a combination of bed temperature, coating rate, bed surface area, particle size, and acetylene gas flow rate and composition. A thin seal layer is deposited at the end of the buffer application by changing the coating temperature and gas composition.

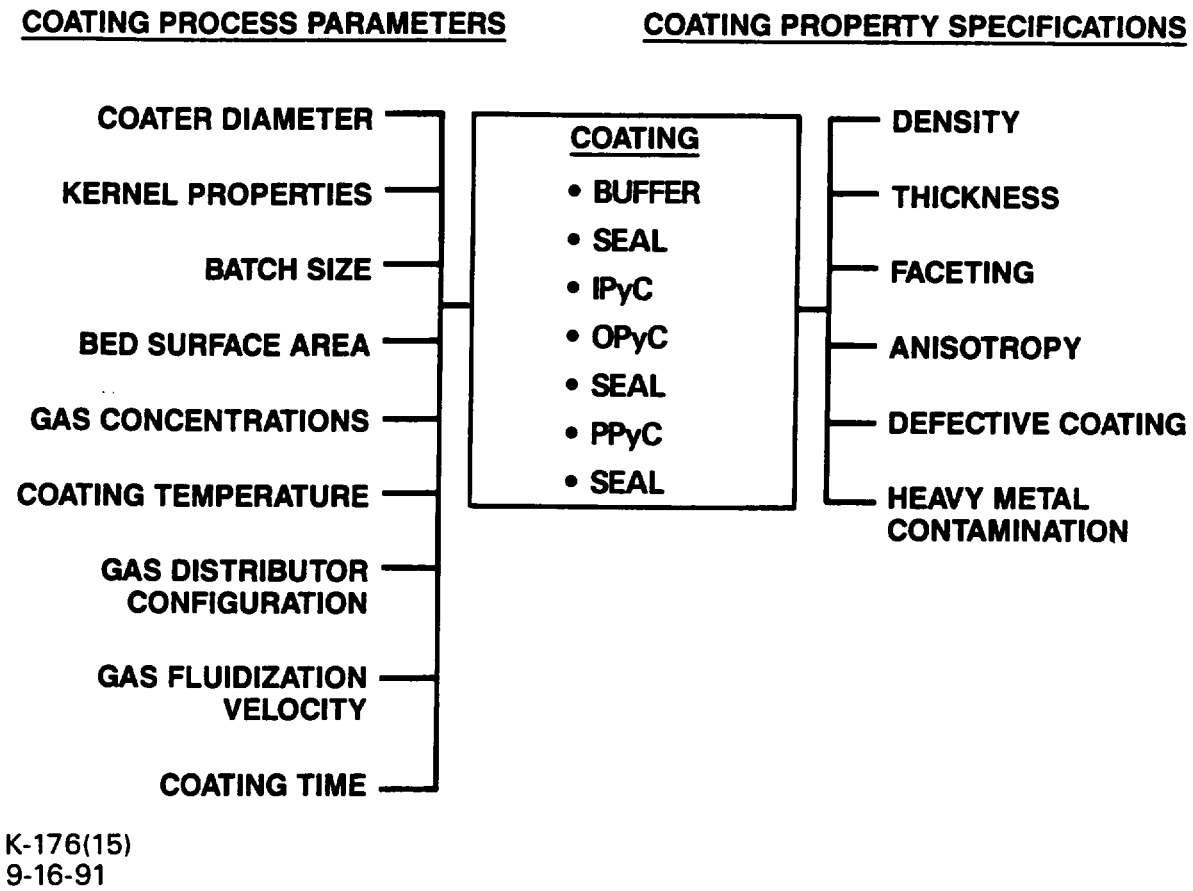

Fig. 6-12. Key coating process parameters and properties

TABLE 6-2
COATING RATES AND PROPERTIES

Coating Type	Coating Rate Range (microns/min)	Optimal Properties
IPyC and OPyC	1.0 to 2.5	1. Low porosity
		2. High density
		3. Low anisotropy
Buffer carbon	8.0 to 12.5	1. High porosity
		2. Low density
PPyC	4.0 to 6.0	1. High porosity
		2. Low density
Seal	0.1 to 0.5	1. High density
		2. High anisotropy
Silicon carbide	0.20 to 0.30	1. High density
		2. Low silicon
		3. low porosity

TABLE 6-3
BUFFER COATING PROCESS PARAMETERS

Process parameter	Range	
	Fissile	Fertile
Coating temperature (°C)	1450 ± 15	1550 ± 15
Aceylene to total gas (%)	40 to 50	45 to 55
Coating rate (micron/min)	9.5 to 12	8.5 to 10

6.3.2. IPyC Coating

High-density, isotropic PyC is added over a seal coat deposited on the buffer layer. The IPyC provides a high-density coating to protect the kernel from HCl attack during later SiC deposition. It also provides a secondary protective layer from fission recoils between the kernel and the SiC coating.

For the IPyC coating at a normal batch size of 5 Kg U, propylene is pyrolized to carbon and coats the seal surfaces with an isotropic pyrocarbon layer in an endothermic reaction at 1280°C.

This coating also may be applied with a combination of acetylene and propylene. The selection of a mixture depends upon the kernel size and the batch quantity. The coating gas mixture minimizes the temperature depression in the fluidized bed caused by the endothermic reaction and maintains a uniform bed temperature.

Key IPyC coating process parameters for the 240 mm diameter coater are listed in Table 6-4.

The anisotropy and aspect ratio (degree of sphericity) of the carbon layer are influenced by the coating rate and temperature. The coating quality depends on the batch size and configuration of the coater gas flow. The most isotropic material is obtained using a high coating rate and a high temperature. The high density required for the IPyC is obtained by reducing the reaction temperature, which tends to increase anisotropy.

6.3.3. SiC Coating

SiC, the primary load bearing member and fission product diffusion barrier in the fuel particle system, requires high strength to resist stresses imposed by the internal gas pressure generated during fission.

TABLE 6-4
IPyC COATING PROCESS PARAMETERS

Process Parameter	Range	
	Fissile	Fertile
Coating temperature (°C)	1280 ± 10	1280 ± 10
Coating gas to total gas (%)	>20	>20
Coating rate (micron/min)	1.5 to 2.0	1.5 to 2.0

High SiC strength is associated with high-density beta phase SiC. The presence of H_2 with MTS during processing suppresses the formation of volatile silicon chloride compounds.

Key SiC coating process parameters for the 240 mm diameter coater are listed in Table 6-5. The fluidized particles can be coated over a wide range of temperatures and coating rates, but the process parameters and the hydrogen/MTS ratio must be controlled to provide an optimum ceramic layer. The properties of interest in the SiC product are:

- Thickness
- Strength
- Density
- Grain size and orientation
- Crystal phase
- Surface morphology

Although surface morphology is not a direct property of the coating, it becomes important because of the notch sensitivity of SiC and the direct relationship between surface morphology and microcrystalline integrity. Generally, the crystallinity of the coating is optimum for coating temperatures between 1550° and 1620°C. Both below and above these temperatures, the structure appears more amorphous, globular, and disordered, thus reducing the density and increasing the microporosity. The crystallinity is most uniform when the lowest coating rates are used.

These property considerations indicate that an optimum process for coating has a reaction temperature of 1572°C and uses a relatively low coating rate (below 0.4 μm/min). Such a SiC coating process requires that fluidizing furnace parameters be maintained up to 2 hr, which is readily achieved by existing equipment.

TABLE 6-5
KEY SiC COATING PROCESS PARAMETERS

Process Parameter	Range	
	Fissile	Fertile
Coating temperature (°C)	1570 ± 30	1570 ± 30
Hydrogen to MTS ratio	>50	>60
Coating rate (micron/min)	0.25 to 0.30	0.25 to 0.30

6.3.4. OPyC Coatings

The OPyC coating provides a secondary barrier to the release of fission gases, protects the SiC from external gas reaction, and provides compressive prestressing of the SiC layer to improve its function as the primary pressure boundary. The OPyC coating also protects the SiC during compact formation. Key OPyC coating process parameters for the 240 mm diameter coater are listed in Table 6-6. Crystallographic isotropy is the most critical requirement of the OPyC coating. A fully isotropic coating allows uniform compressive prestressing of the SiC coating.

The OPyC layer must assure low permeability to fission gases while maintaining structural integrity during irradiation. A lower limit on the OPyC active coating gas ratio of 0.25 is directed at controlling the structural stability of the OPyC layer during irradiation.

Comparisons have been made between properties of coatings fabricated in large commercial coaters (approximately 240 mm in diameter) and those produced in smaller (<125 mm in diameter) equipment. Pyrocarbons from the 240 mm coater can be made identical to coatings from smaller coaters.

A mixture of acetylene and propylene is specified for the outer isotropic deposition gases. This combination of gases, the decomposition of which involve endo- and exothermic processes, is necessary to prevent excessive temperature changes during the deposition run in a 240 mm coater.

6.3.5. PPyC Coating

The outer PPyC provides an interface layer between the coated particle and the compact matrix to prevent damaging OPyC or SiC during compact formation. The protective outer coating is similar to the

TABLE 6-6
OPyC COATING PROCESS PARAMETERS

Process Parameter	Range	
	Fissile	Fertile
Coating temperature (°C)	1300 + 10	1300 + 10
Coating gas to total gas (%)	>25	>25
Coating rate (micron/min)	1.5 to 2.0	1.5 to 2.0

initial carbon buffer coating and is applied using a CVD reaction from acetylene gas.

Key PPyC coating process parameters for the 240 mm coater are listed in Table 6-7.

6.3.6. Seal Coatings

A seal coating is a thin (<5 μm), anisotropic pyrolytic carbon coating. Seal coatings are applied between the buffer and IPyC, between the outer pyrocarbon and the protective pyrocarbon, and on the exterior of the finished particle. The first seal coating separates the buffer and IPyC to facilitate measurement of the IPyC coating density. The second seal coating protects the OPyC from failure induced by shrinkage and failure of the PPyC. The third seal coating facilitates flow of the particles through metering and blending equipment during compact formation.

The active coating gas for the seal coating is propylene (C_3H_6). Argon is used as the diluent/carrier gas. The temperature is controlled so that a dense structure is applied to arrest crack propagation through the protective layer, and to provide a hardened and smooth outer surface.

TABLE 6-7
PPyC COATING PROCESS PARAMETERS

Process Parameter	Range	
	Fissile	Fertile
Coating temperature (°C)	1450 ± 15	1550 ± 15
Acetylene to total gas (%)	40 to 43	43 to 46
Coating rate (micron/min)	>4.5	>5.5

7. FUEL COMPACTS FABRICATION

7.1. PROCESS DESCRIPTION

Fuel compacts provide a method for distributing the coated particle fuel throughout the graphite core of the MHTGR. A typical fuel compact is shown in Fig. 7-1.

Fuel compacts are manufactured by the hot injection process depicted schematically in Fig. 7-2. The process is summarized in Fig. 7-3. The total process includes formulation of matrix material, particle weighing, particle blending, green compact formation, carbonization, final heat treatment, and quality control inspection. A complete process flow diagram is shown in Fig. 7-4. Following is a detailed description of each process step in compact manufacture.

7.1.1. Matrix Fabrication

The reference compact fabrication process requires a binding material to bond fuel and shim particles into a close-packed cylindrical rod having specific thermal and structural properties for successful in-reactor service. The binder material developed for the FSV reactor is a carbonaceous matrix mixture containing petroleum-based pitch, graphite filler, and selected additives. This mixture has proven to provide an acceptable combination of fabricability and irradiation performance.

Matrix ingredients are blended and processed to provide dry, thermoplastic granules for the compact injection equipment. The matrix processing equipment consists of a barrel heating station, a mixer/extruder, drying pans, a grinder, ventilation hoods, and materials transfer/support equipment.

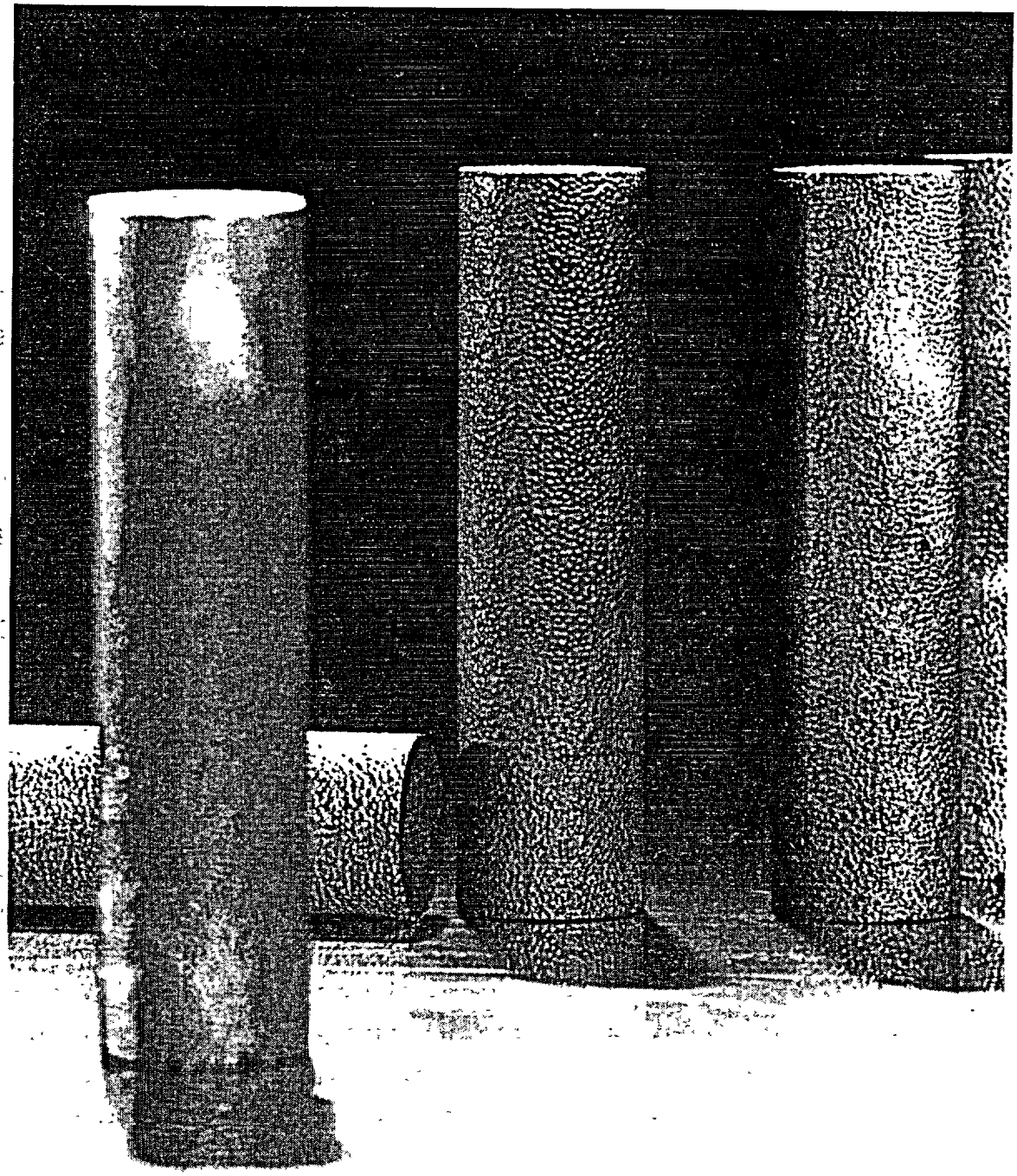

Fig. 7-1. Typical MHTGR fuel compact appearance (Scale = 2:1)

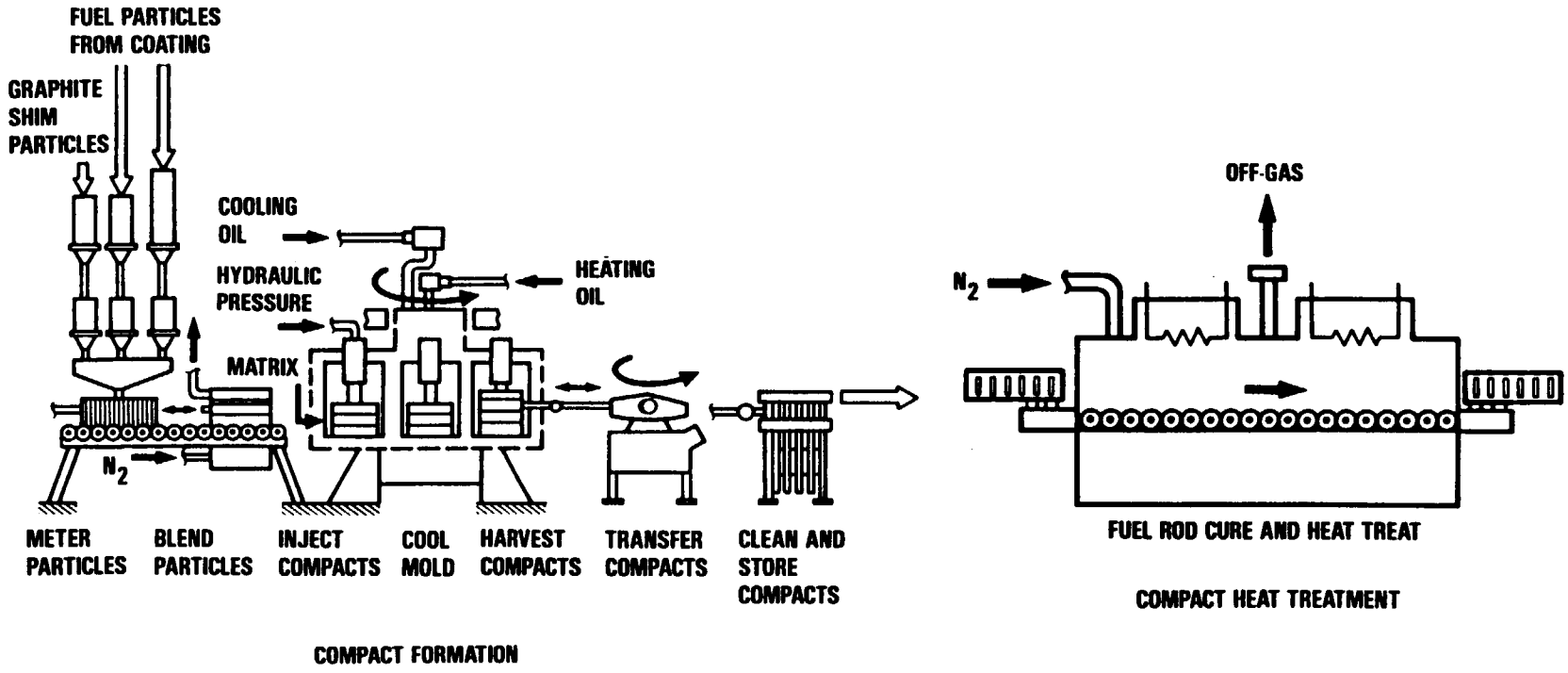

H-557(12)
8-6-91

Fig. 7-2. Fuel compact fabrication and heat treatment

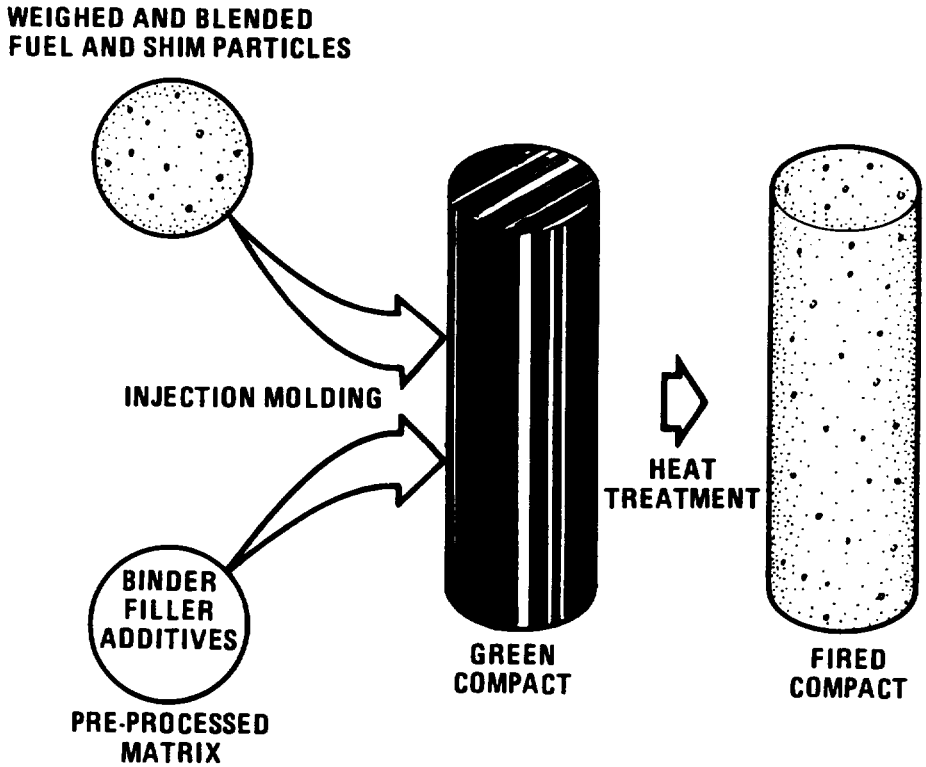

K-232 (1)
9-13-91

Fig. 7-3. Summary of compact fabrication

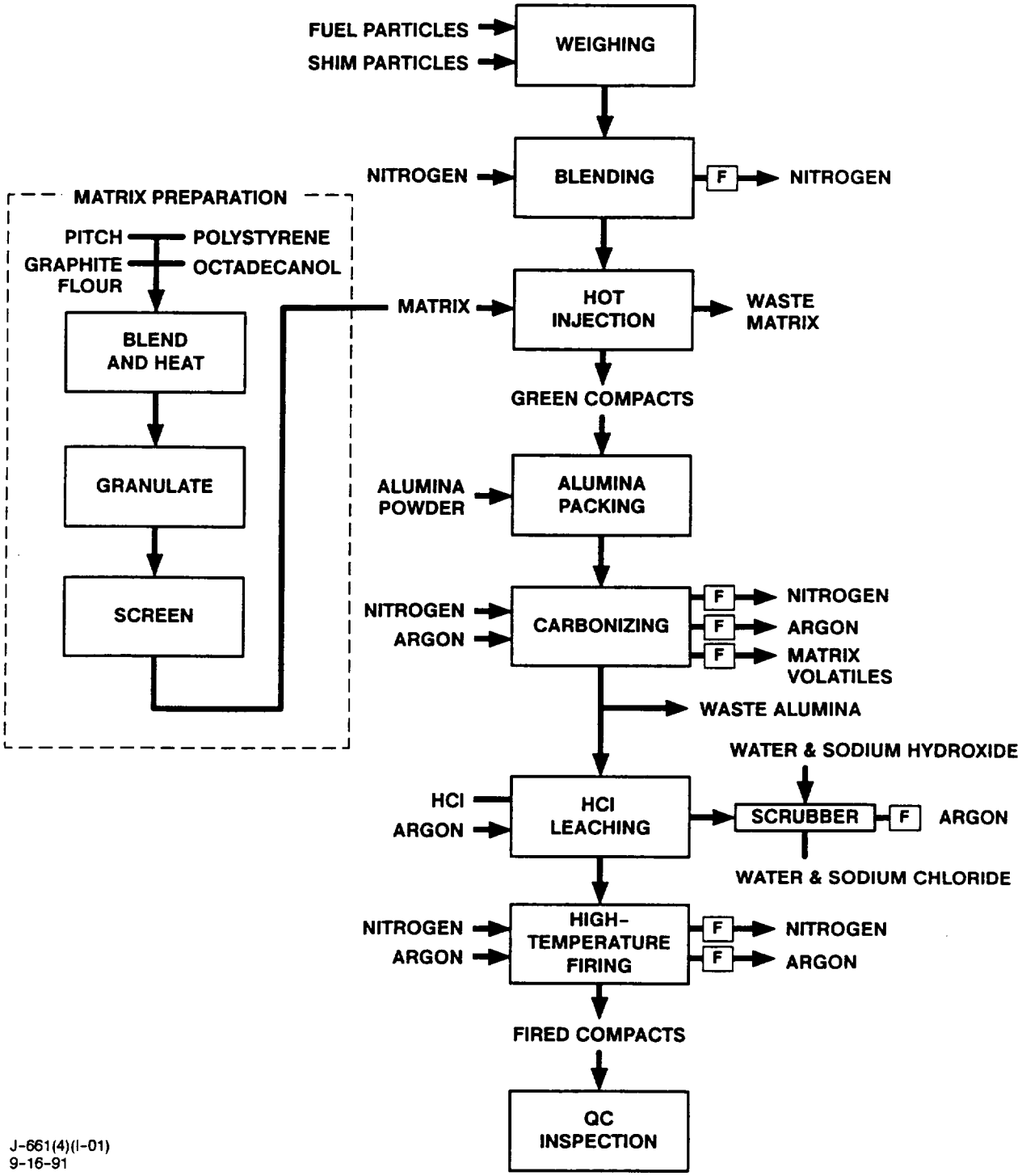

Fig. 7-4. Fuel compact manufacturing process flow

The pitch is passed through a magnetic separator before use to remove iron contamination. Because the pitch is solid at room temperature, it is heated in its shipping barrel to melting, then poured through a magnetized screen into a clean container and allowed to resolidify.

The required quantities of raw materials are then weighed to provide a mix of the following proportions:

Cleaned petroleum pitch	33 to 56 wt %
Graphite flour	32 to 42 wt %
Polystyrene	0 to 13 wt %
Octodecanol	3 to 12 wt %

These ingredients are placed into the mixer/kneader, which is heated throughout the mixing operation to soften the pitch. After thorough mixing, the molten matrix is extruded from the mixer into a receiving pan with grid separators that form 3-in. cakes when the mixture cools. The solidified cakes are removed from the pan and loaded into the grinder hopper for granulation. The ground matrix is screened as it leaves the grinder to provide granules of the proper size range.

7.1.2. Particle Charge Weighing

The mold cavities in which the compacts are formed must be completely filled with particles. This prevents rearrangement of the blended charges during matrix injection, which would result in fuel inhomogeneities. The theoretical volume fraction of perfect spheres within a cylindrical cavity (i.e., "packing fraction") is 0.64. Because of particle nonsphericity and shim particle shape, MHTGR fuel compacts achieve between 0.55 and 0.58 particle packing fraction.

The specified heavy metal loadings for the core and the fuel particle batch heavy metal content dictate the amounts of fuel particles

that must be loaded into each compact. Fuel particle volume packing fractions can vary from about 0.10 up to 0.50 depending on the fuel loading for the intended core location. Shim particles, which are granules of comminuted near-isotropic graphite, are used to make up the difference when the fuel particles do not completely fill the allowable particle volume within the mold. The fuel, shim, and any other particle types must be accurately metered to assure the mold cavities will be loaded completely.

On the process line, shim and fuel particles are bulk-loaded into separate hoppers atop the particle metering station, (Fig. 7-5). The metering system includes coarse and fine feed particle modules, valves, and slides which deliver particles to the scale assemblies.

The scales (Fig. 7-6), which are the heart of the system, are temperature-compensated nulling devices. Each uses differential capacitors to measure displacement; as a coil reduces the displacement to zero, the weight displaced is proportional to the current used by the coil.

The station sequentially fills each of the 40 cavities in a transfer tray with one charge of each particle type. When all cavities are filled, the charges are transferred by gravity drop through a slide gate into a carriage-mounted blender tray, which moves to the blending station.

7.1.3. Particle Blending

A fuel compact homogeneity specification places limits on the axial distribution of fissile material within a compact. This limits the magnitude of temperature differentials within compacts during irradiation as a result of inhomogeneous distributions of fissionable material. To meet this requirement, particle charges for compacts are combined before insertion in the mold cavities so that a uniform mixture of all phases

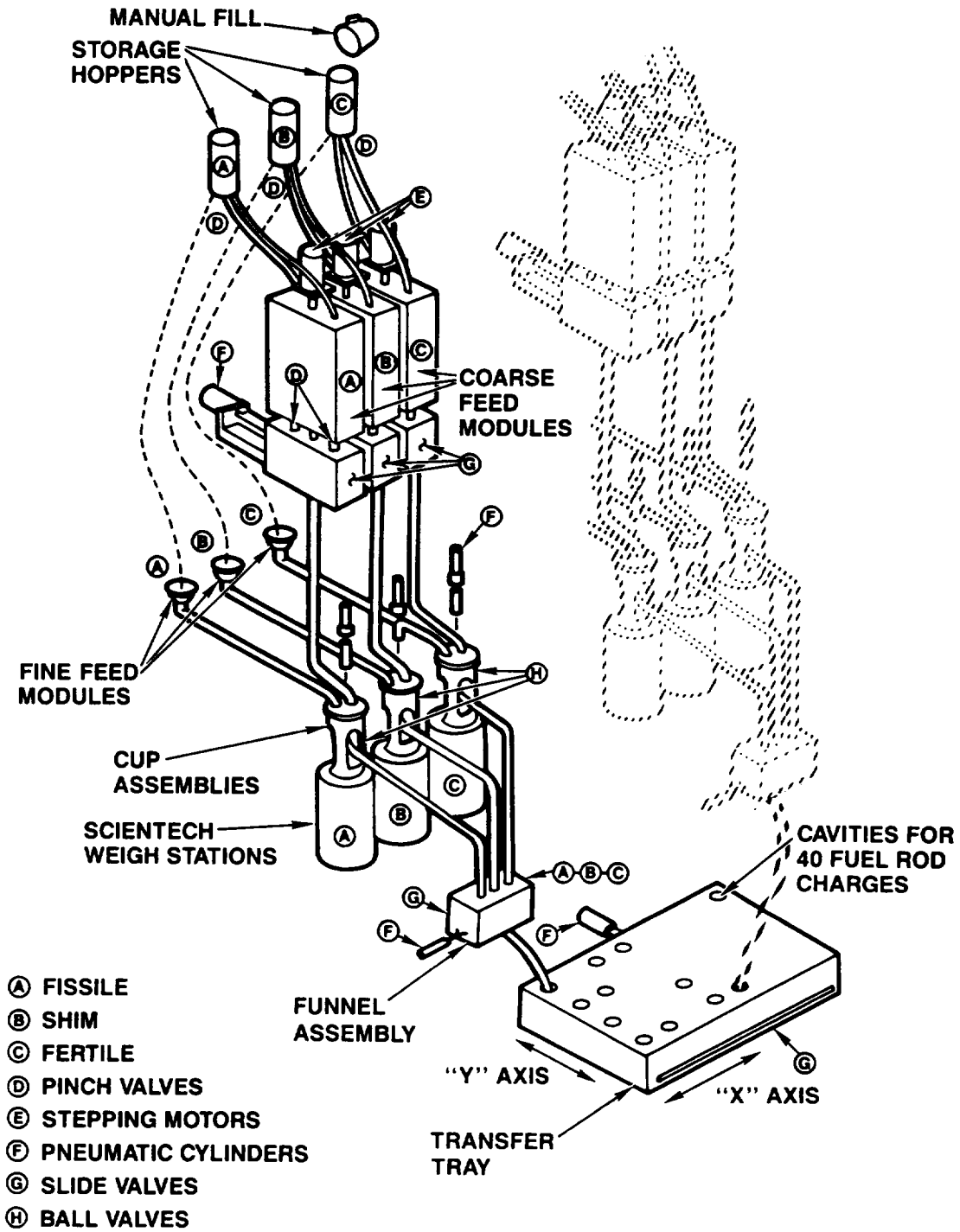

Fig. 7-5. Particle metering station

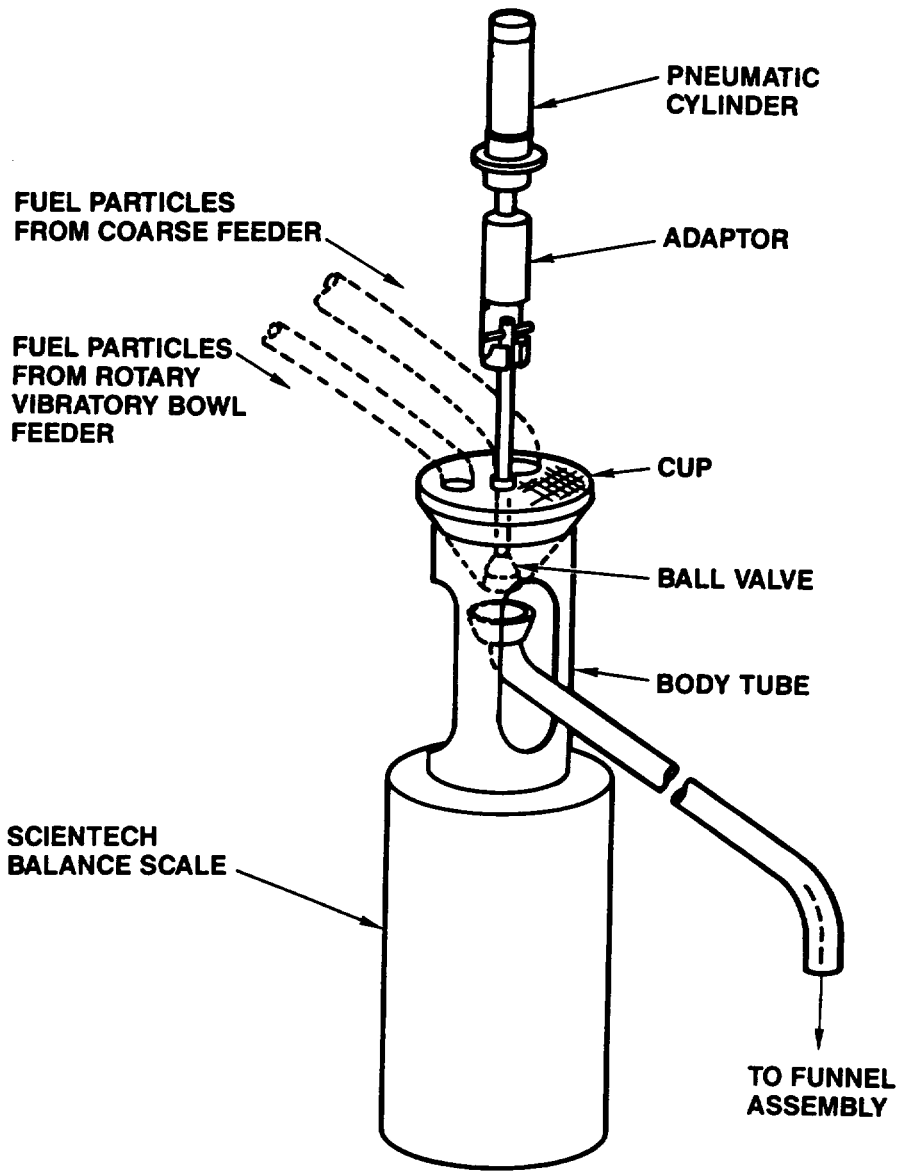

Fig. 7-6. Remote scale sensor

is obtained. Shim particle size, ranging from 590 to 1180 μm, and shape, an equiaxed particle morphology, are controlled to assure homogenous mixing with the fuel particles. Good mixing of the fuel and shim within the compact ensures uniform irradiation-induced dimensional change behavior (Ref. 7-1) and uniform thermal conductivity (Ref. 7-2).

The particle blending station (Fig. 7-7) accepts the preweighed particle charges within a blending tray. The tray contains mixing chambers slightly greater in volume than the compact mold cavities. The blender has 40 individual, adjustable gas nozzles mounted on two nitrogen manifolds. When the blending tray is indexed into position at the station, the manifolds are brought to bear against two sides of the tray that contain gas ports. Nitrogen gas is then admitted through specially designed inlets in the sides of the chambers in a rapid succession of several, short pulses. The particle charges in each chamber are levitated and randomly mixed with each gas pulse. A calibrated flowmeter is used to adjust the flow in each blending cavity at the start of a campaign.

Particle redistribution after blending is prevented by directly loading the blended charges into the mold cavities. The blending tray is moved from the blending station and indexed directly above a compact mold for the filling step, which is also gravity fed. Once the particles fall into the mold cavities and the mold pistons are raised, the particle charges completely fill the cavity volume, so relative movement of particles is minimized during matrix injection.

The metering and blending system contains automatic material accounting procedures that monitor the composition (by weight) of each charge dispensed while the system is running in its automatic mode. After each blender tray of 40 charges has been dispensed, the batch data is automatically recorded.

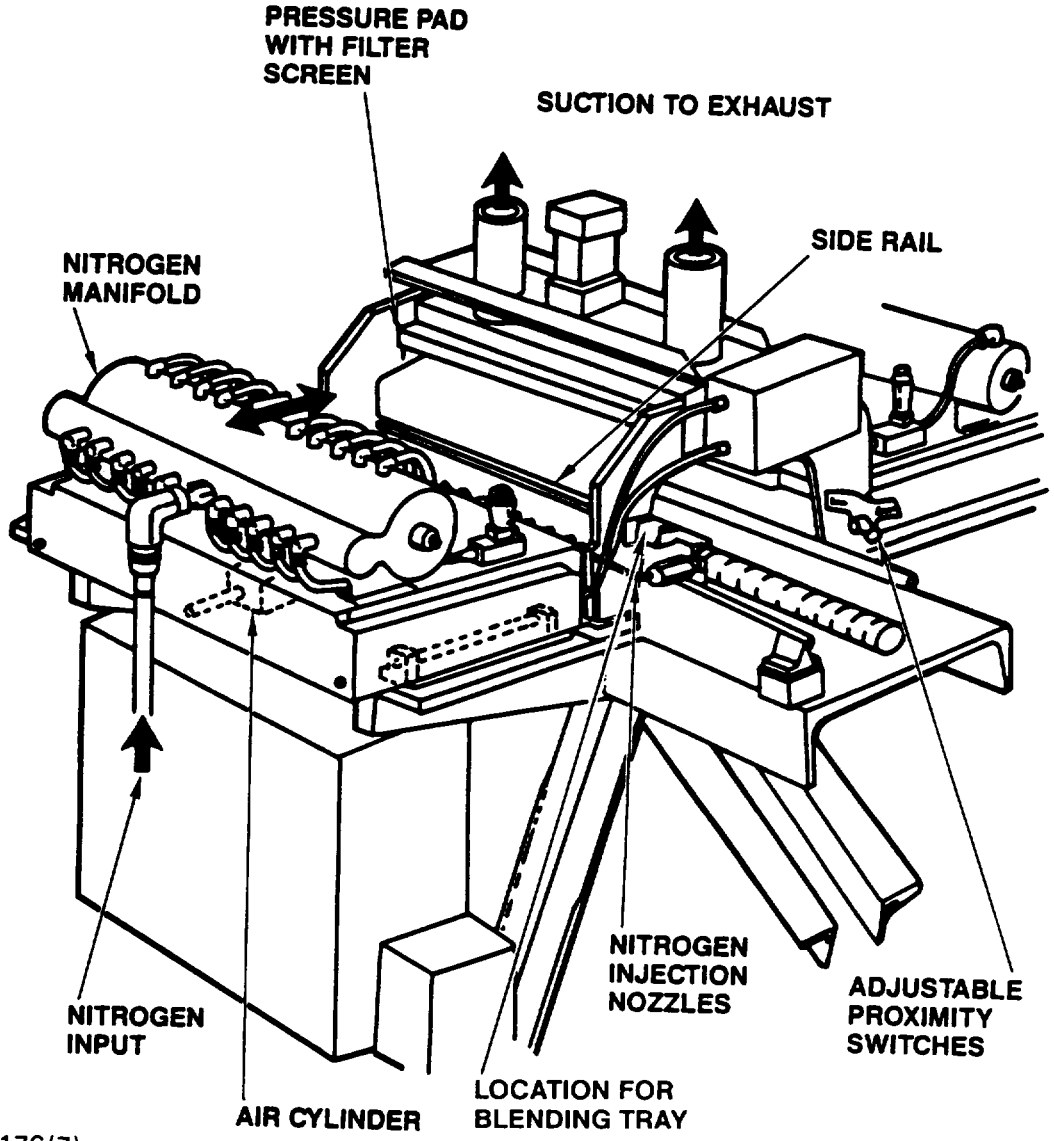

K-176(7)
9-17-91

Fig. 7-7. Particle blending station

7.1.4. Green Compact Formation

During the FSV compact manufacturing, two 40-hole molds were used in parallel, although the line could operate with a single mold.

Figure 7-8 shows a mold sequence from particle filling to ejection of the formed compact. The sequence of operations required to process one mold of compacts is as follows:

1. In the mold, the pistons are placed in the fully depressed position.

2. On receipt of a location signal, the 40-cavity blending tray indexes into position over the mold, self-aligning on dowel pins.

3. Travel over the blender drive forces the blender vertically down onto the mold upper face, actuating a microswitch to signal location interlocks.

4. The signal loop, self-contained within the blender assembly, triggers the slide, which discharges the blended particles into the mold. The blender carriage then moves back under the metering station to restart a metering/blending cycle.

5. The mold closes in preparation for the injection step.

6. While traveling to the injection station, the mold is heated to a preset temperature (range is 150° to 175°C) by heat transfer oil flowing through passages in the mold. Each mold is connected to the hot oil manifolds (pressure and return) as it indexes to the loading station.

7. The mold pistons move upward to a predetermined position which sets the green compact length.

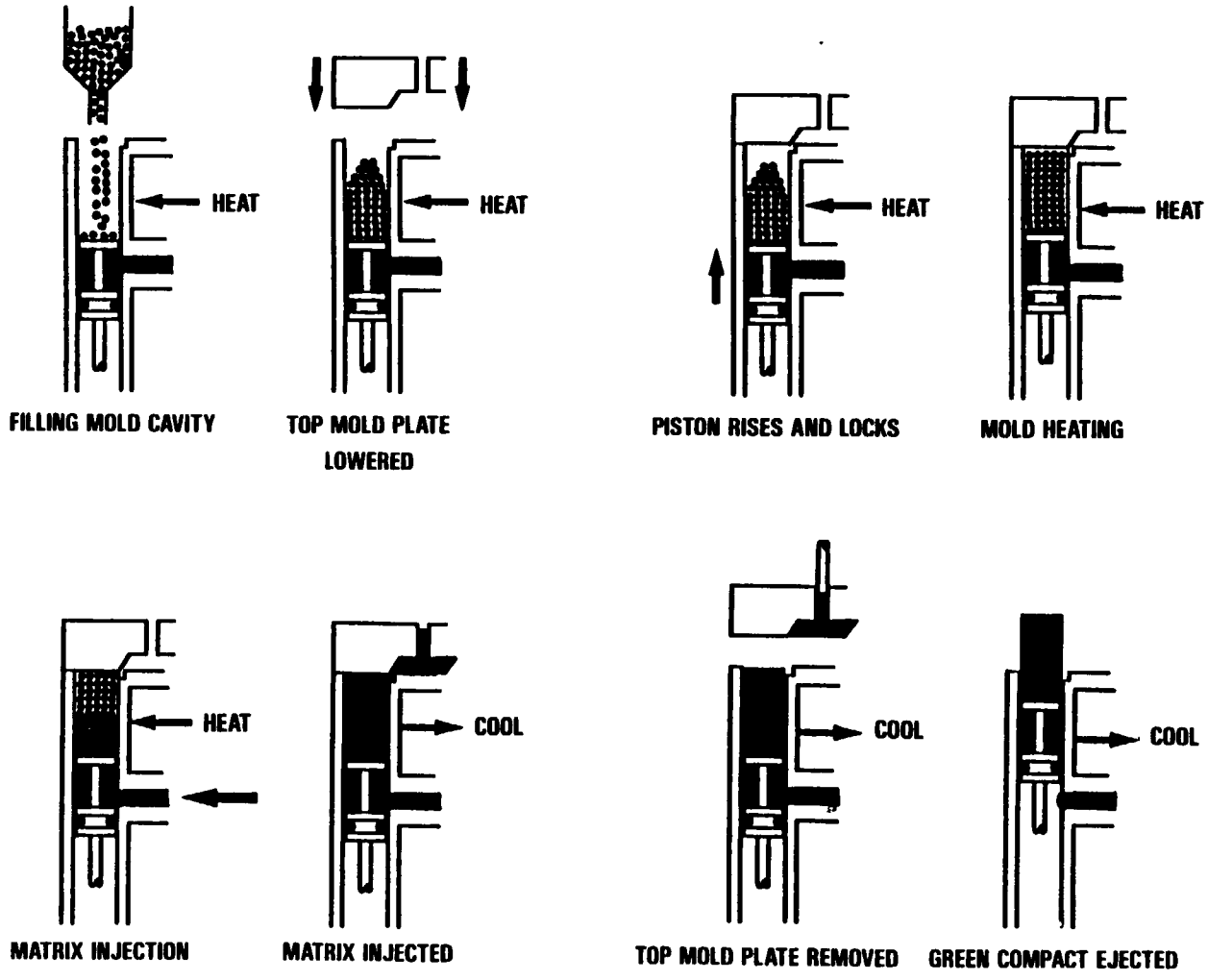

J-912(2)
2-5-91

Fig. 7-8. Green compact fabrication sequence

8. The matrix load is plasticized to a homogeneous molten mixture within the injector barrel.

9. While the mold is in the injection station, an infrared sensor continuously reads the mold temperature. Limits for high and low alarm are preset.

10. The injection nozzle is indexed into contact with the mold and a controller signals the start of matrix injection. The computer controls the matrix pressure and flow rate during injection.

11. The computer has pressure setpoints, flow rates, and volume-versus-time tables entered in its memory by a process engineer using a key lock control circuit and teletype. The computer reads the output from a pressure transducer in the injection nozzle at 1/2-sec intervals.

12. During the injection stroke, injection screw travel is continuously monitored by a linear potentiometer. The output from this is sampled at 1/2 sec intervals and differentiated with respect to time by the computer, thus providing a rate of injection signal.

    The pressure and injection rate signals sampled by the computer are compared with the tables of setpoints in the computer memory. Error signals thus produced are utilized to control the injection. The control mode can be either pressure- or rate-limited.

13. A normal injection cycle will result in an injection complete signal from a microswitch ahead of the machine process timer which terminates the cycle. If the injection stroke is not complete when the process timer contacts close, no action will

result because the microswitch is in series with the timer contacts. Thus, the injection time may be extended automatically to accommodate small excursions in the injection parameters. An increase in injection time of 5% constitutes an alarm situation requiring operator intervention.

14. At normal completion of an injection stroke, the process timer closes. The injection nozzle retracts from the mold and begins plasticizing a fresh charge of matrix. The pressure on the molded compacts is relieved.

15. Cooling oil is pumped into the mold to start the cooling cycle.

16. The mold will have reached room temperature by the time it indexes to a discharge station. The mold opens and a robot hand enters the mold to retrieve the compacts. Then the lower pistons move upward to eject the compacts into the robot hand.

17. The robot then moves to a transfer station, where the compacts are placed in 40 tubes assembled in an unload rack.

While the steps just described were completely satisfactory for FSV fuel, the MHTGR fuel compact specifications are much more stringent and have required some process improvements. For example, the required MHTGR combined heavy metal (HM) contamination and SiC coating defect fraction for U or Th is 6×10^{-5} gHM/gHM. Similar values produced for the FSV HTGR fuel were approximately 3×10^{-3} gHM/gHM. In addition, the MHTGR specification requires compliance using new and more discriminating testing procedures to satisfy NQA-1 standards.

The MHTGR specifications in effect demand that virtually no particles be damaged during green compact formation. The key to obtaining reduced defects was the addition of the 50 μm low density PyC overcoating. Five-layer TRISO coated particles have a crush strength of

~3 Kg per particle and are somewhat susceptible to damage during metering, blending, and injection molding. In contrast, eight-layer TRISO particles, with a crushing strength of ~6 kg, are significantly more resistant to damage during handling and injection molding. The improved particle strength makes the eight-layer TRISO the reference particle for MHTGR fuel.

Overcoated particles were made into fuel compacts using the process improvements derived from the development program. These compacts met the MHTGR quality goals.

The MHTGR Fuel Compact Process Specification (Ref. 7-4) was written to detail the process parameters required for laboratory-scale production of acceptable MHTGR fuel compacts.

Following process improvements, four blends of fuel compacts with varying quantities of uranium were made for confirmation in the laboratory four-hole press and tested in the HRB-21 capsule (Ref. 7-5). These fuel compacts were made using seven-layer TRISO coated particles with all layers except the outer seal coat.

The last step in the development process is scaleup from the laboratory equipment to the reference modular sized equipment. This must be accomplished with an improved 40-hole mold, piston, and hydraulic package. The new mold incorporates a central matrix channel running the length of the mold and sized to minimize the pressure differential between cavities. When the matrix channel reaches a row of cavities, it divides to feed each cavity.

A channel for heating and cooling oil surrounds each mold cavity. Oil is introduced on one side at the back of the bottom mold. It moves forward toward the matrix injection port, passes through an opening to the other size of the mold, returns to the back portion of the mold and exits.

The top part of the mold closes the mold cavities and permits air to escape when matrix is injected. This portion of the mold is identical to the one used to manufacture FSV fuel.

The new hydraulic actuators have dual-acting pistons to accurately control mold piston movements and positive stops to prevent compacting the bed of particles. An improved four-hole development press has been constructed for parametric tests of process variables.

7.1.5. Carbonization

Carbonization of green fuel compacts is the first step of the heat treatment process. In this operation, volatiles from the pitch binder are driven off as the component of the binder phase remaining in the compact (coke) is carbonized.

Controlling the coke yield of the pitch in the binder is important since it affects the irradiation-induced dimensional changes and integrity of the compact. This initial heat treatment must be performed with the compacts constrained. Otherwise, the thermoplastic pitch binder remelts during temperature ramp-up, allowing the compacts to lose their shape. Constraint is provided by packing the green compacts in fine alumina powder within graphite boats for the carbonization run. The powder is brushed off after carbonization.

Figure 7-9 shows the FSV production tube-type carbonization furnace with the outer insulation box removed. This resistance-heated furnace was capable of heating compacts to the 900° to 1000°C carbonization temperature in an inert gas atmosphere. A hot zone section approximately 16 ft long is followed by a cooling zone. Gas locks at both ends prevent intrusion of air as the graphite boats enter and exit. Volatiles released from the compacts during heating are carried away in the off gas, which undergoes building filtration.

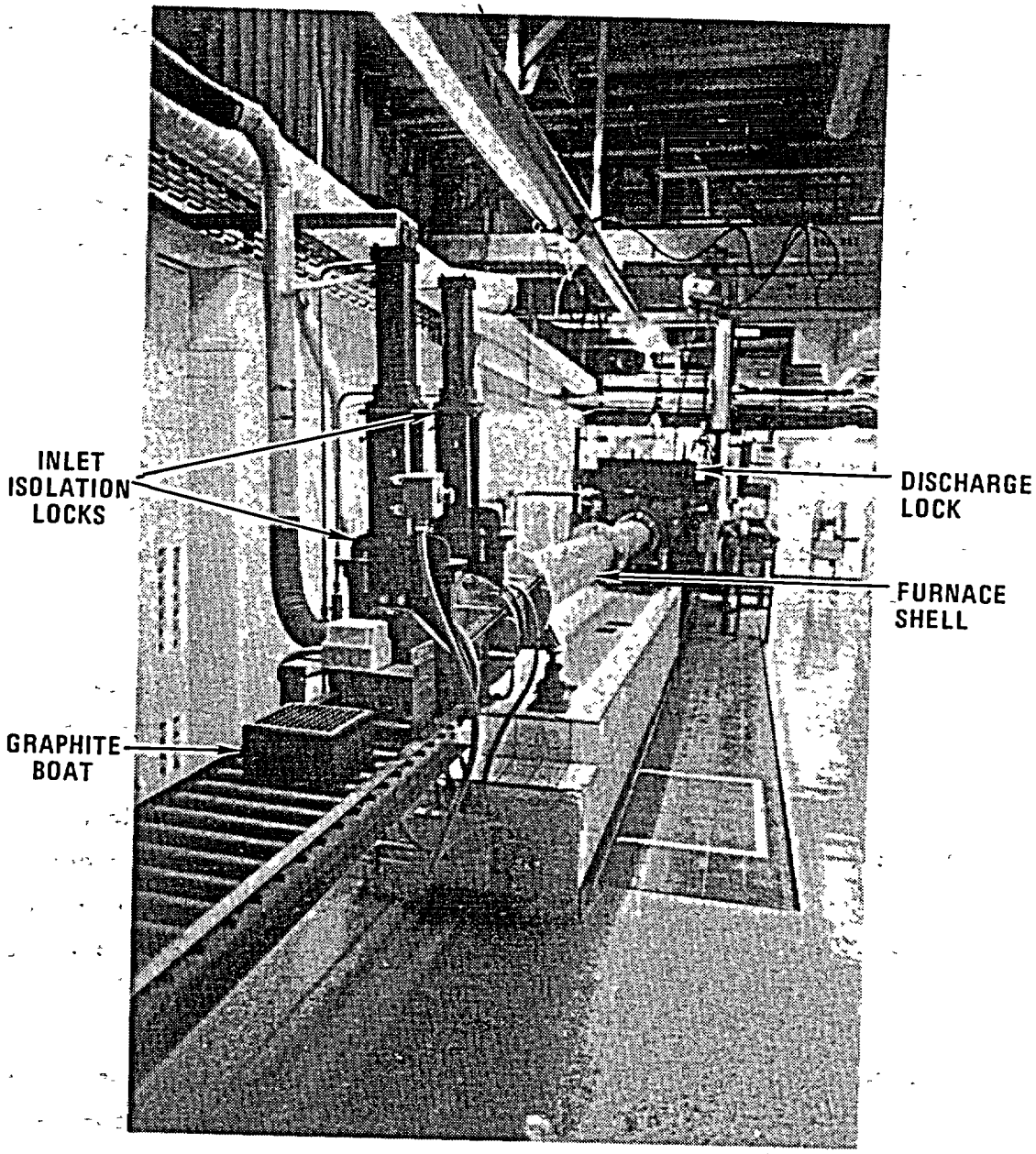

Fig. 7-9. Carbonization furnace

Graphite boats (Fig. 7-10) with 100 compact cavities each are first loaded with alumina powder until 10 to 20% of each cavity is filled. One green compact is then loaded into each cavity and more alumina is added until the holes are completely filled. The boat is then tamped several times to settle and pack the alumina surrounding each compact.

The loaded boats are placed at the furnace entry port (see Fig. 7-11) and automatically loaded into the gas lock and then the furnace tube on either a four or eight minute cycle. As each new boat is introduced into the furnace, it pushes the previous boat ahead so that fully heated and cooled boats are simultaneously pushed out the exit port and gas lock.

In the furnace, the compacts are heated at ~5°C/min up to ~1000°C in an argon atmosphere, then cooled to ~200°C before leaving the furnace. Fifty loaded boats can be accommodated within the heating and cooling sections. The total transit time through the furnace is a minimum of three hours.

After exiting the furnace and further cooling to room temperature, the boats are inverted to remove the carbonized compacts and alumina. Most of the alumina falls through a fine mesh screen; any remaining alumina adhering to the compacts is removed with rotating, nonmetallic brushes.

7.1.6. HCl Leaching

Gaseous HCl leaching of carbonized fuel compacts has been employed to remove heavy metal contamination and impurity elements before final heat treatment. This operation has been performed in a vertical push-through type, inductively heated furnace. This step is an alternative which is available for use as necessary to lower impurities or contamination.

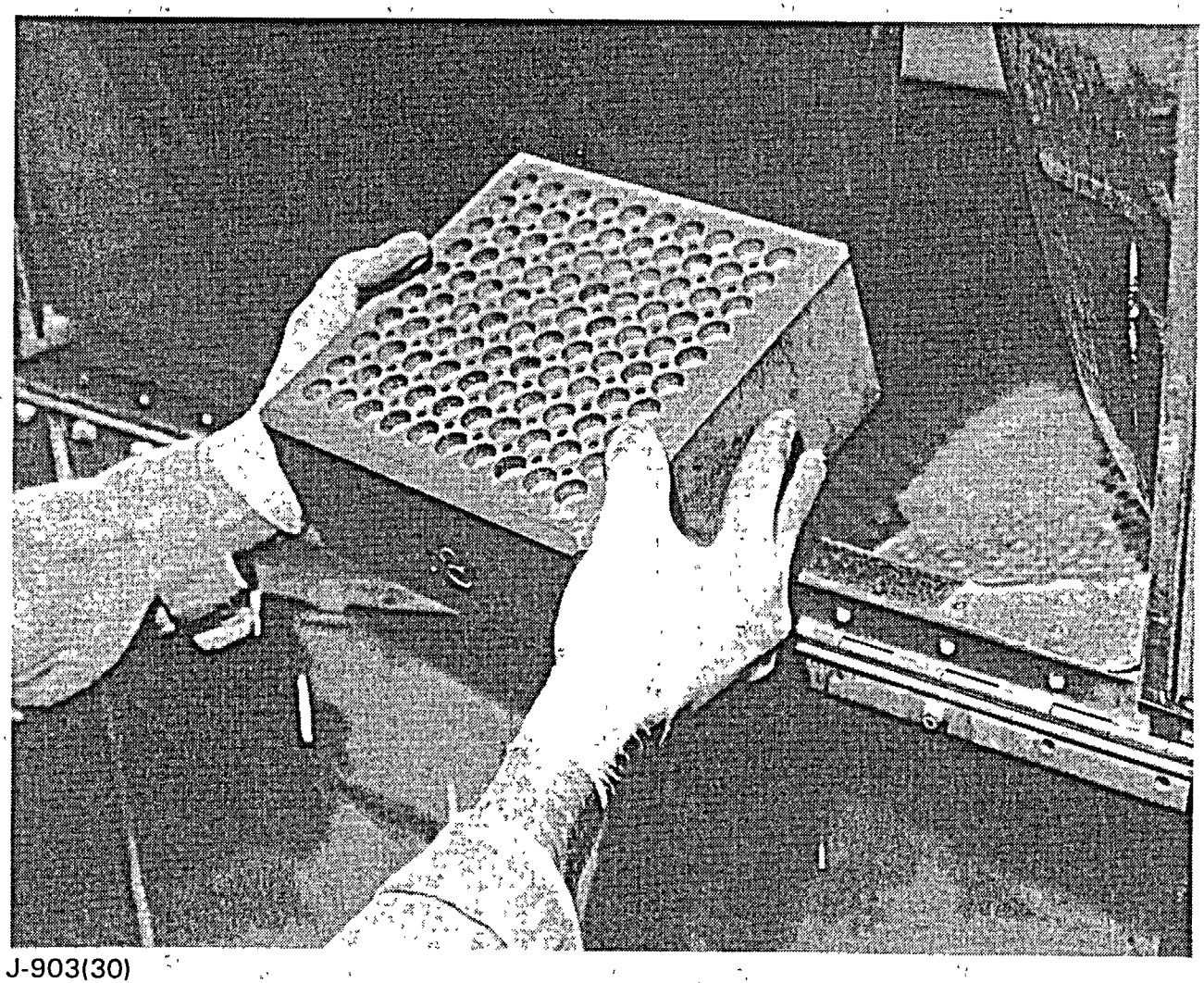

J-903(30)
1-28-91

Fig. 7-10. Graphite boats used for compact carbonization and final heat treatment

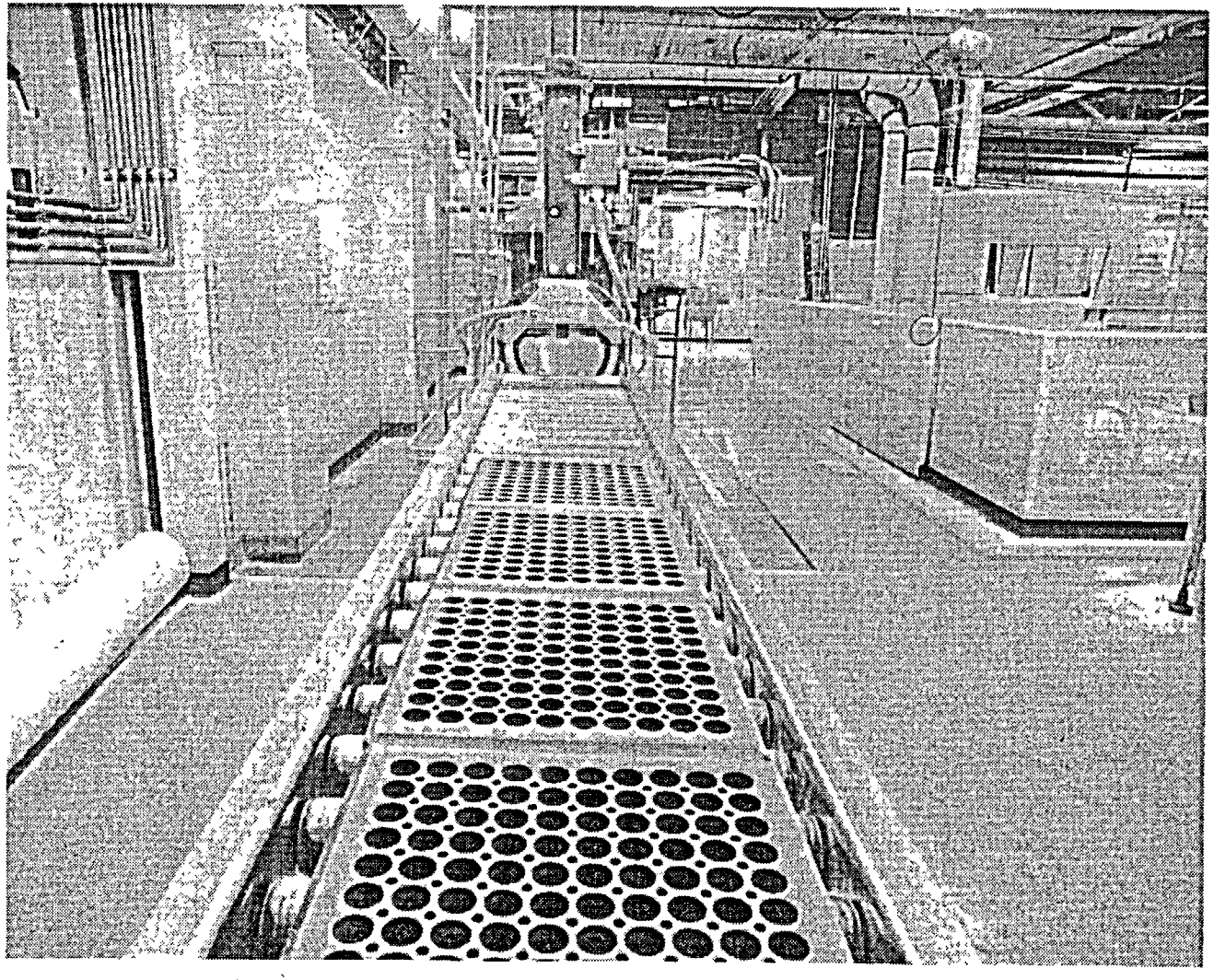

J-903(33)
1-28-91

Fig. 7-11. Graphite boats ready to be loaded into carbonization furnace

Compacts are loaded into individual holes in graphite crucibles and heated in a mixed gas atmosphere of argon and HCl. During heatup to 1800°C, contaminants leach from the compacts and form gaseous chlorides. The total time at temperature is limited to 90 min to prevent possible reaction of the chlorine with the fuel particle coatings. Compacts are removed from the graphite crucibles after cooldown.

7.1.7. Final Heat Treatment

The final step in fuel compact production is high-firing or final heat treatment (FHT). At the temperatures employed in this step (1600° to 1850°C), residual chlorine gas from the HCl cleaning step and any remaining impurities are removed. At the same time, remaining hydrocarbons in the binder are decomposed and limited graphitization of the binder coke takes place. Lastly, the high-firing step conditions the compacts by subjecting them to higher temperatures than will be encountered in normal reactor service or licensing basis events.

The FHT furnace is the same in configuration and operation as the carbonization furnace, but is inductively heated. Again, the compacts are loaded into individual holes in graphite boats. (Alumina powder constraint is not required for FHT.) The loaded boats are fed through the horizontal furnace in sequence, with an in-furnace residence time of 5 to 6 hr. Heatup rate in the hot zone is ~10°C/min. There is a 30 to 90 min hold time at the peak temperature. Compacts are unloaded from the firing boats at room temperature.

7.2. PROCESS MATERIALS AND CHEMICALS

All raw materials used as feed material for fuel compact processes must meet the procurement and inspection requirements specified in the MHTGR Fuel Specification (Ref. 7-6). Table 7-1 lists all input and output materials for the seven processes involved in compact manufacture. These are also shown on the process flow diagram, Fig. 7-3.

TABLE 7-1
COMPACT INPUT AND OUTPUT MATERIALS

Process	Input	Output
1. Matrix fabrication	• Petroleum pitch • Graphite flour • Polystyrene • Octadecanol	• Carbonaceous particulates from grinding operation (to waste filters) • Granulated matrix to compact pressing
2. Particle weighing	• Coated fuel particles • Graphite shim particles	• Weighed particle charges to particle blending
3. Particle blending	• Weighed particle charges • Nitrogen	• Nitrogen (to filtration) • Blended particles to compact pressing
4. Compact pressing	• Matrix • Blended particles • Mold release	• Waste matrix (to scrap) • Green fuel compacts to carbonization
5. Carbonization	• Green fuel compacts • Calcined alumina • Nitrogen and/or argon	• Waste alumina (to scrap) • Nitrogen/argon (to filtration) • Matrix volatiles (to filtration) • Carbonized compacts to HCl cleaning
6. HCl cleaning (optional)	• Carbonized compacts • Mixed argon plus HCl • $FeCl_2$ (deposits to scrap)	• Argon/HCl (to scrubber, then filtration) • Cleaned compacts to final heat treatment
7. Final heat treatment	• Carbonized/HCl cleaned compacts • Nitrogen and/or argon	• Nitrogen/argon (to filtration) • Sulphur (deposits to scrap) • Fully-processed compacts

Table 7-2 lists the throughput materials for each process on an 8-hr shift basis.

7.3. PROCESS PARAMETER CONTROL

Each part of the compact manufacturing process has parameters crucial to the quality of the fully-processed fuel compact. This section discusses the key process parameters in compact manufacture.

Control of process parameters is exercised during manufacture through the use of process specifications, procedures, and travelers. All parameters requiring control are specified on Parameter Sheets that are maintained under formal document control. These list actual values used or achieved for all specified process parameters. Data Sheets become part of the manufacturing traveler that documents the progress of a production lot of compacts from the start of processing to completion. The values used are those developed for unit operations. The final manufacturing plant would require a total process control system.

7.3.1. Matrix Fabrication

The weight proportions of the four matrix ingredients are controlled to obtain a consistently uniform material. The nominal mixture contains 47 wt % pitch, 38 wt % filler, 10 wt % octadecanol, and 5 wt % polystyrene. A minimum mixing time of 40 min is specified to ensure complete blending of the components.

The temperature of the matrix is controlled during processing to avoid boiling off the octadecanol, which has a 210°C boiling point. The mix temperature is thus monitored with a temperature probe and limited to 175°C during processing.

TABLE 7-2
COMPACT PROCESS MATERIAL THROUGHPUTS

Compact Operation	Input		Output	
	Material	Throughput[a]	Material	Throughput[a]
1. Matrix fabrication	Petroleum pitch Graphite flour Polystyrene Octadecanol	18.8 kg 15.2 kg 2.0 kg 4.0 kg	To compacts	
2. Particle weighing	Fuel particles Shim particles	20 kg 4 kg	To compacts	
3. Particle blending	Fuel, shim particles Nitrogen	Same as above	To compacts	
4. Compact pressing[b]	Fuel, shim particles Matrix	Same as above 14 kg	Green compacts	4000/mold
5. Carbonization[c]	Alumina powder Argon	171.6 kg 1.6×10^3 l	Carbonized compacts	12,000
6. HCl cleaning[d] (optional)	Argon HCl (gas)	1.2×10^4 l 65 l	Cleaned compacts	12,000
7. Final heat treatment[e]	Argon	1.3×10^3 l	Fired compacts	12,000

[a]All throughputs are daily quantities based on a single 8-hr shift per day.

[b]Assumes nominal compact would contain 5 g fuel particles, 1 g shim particles, and 3.5 g matrix.

[c]Assumes furnace capacity is 50 boats, 100 compacts per boat, 4 min cycle time.

[d]Assumes furnace capacity is 18 boats, 200 compacts per boat, 8 min cycle time.

[e]Assumes furnace capacity is 25 boats, 200 compacts per boat, 8 min cycle time.

7.3.2. Particle Weighing

Particle charges must be weighed accurately to ensure that the required core heavy metal loading is met (fuel particles), and that the compact mold cavities are completely filled during matrix injection (shim particles). The precision required for weighing fuel particles is dictated by the tolerance specified in the fuel product specifications.

7.3.3. Particle Blending

Particle charges must be properly blended to achieve a uniform distribution of heavy metal throughout the fuel compact. This is done by levitating the combined fuel and shim particle charges within pulsed streams of flowing nitrogen. The nitrogen pressure, flow rate, and the number and duration of pulses are specified as follows:

Nitrogen pressure	20 to 40 psig
Nitrogen flow rate	30 to 50 l/min
Pulse duration	0.1 to 0.5 sec
Number of pulses	3 to 5

These parameters achieve satisfactory mixing of the particles without damage due to collisions with each other or with the mixing chamber walls. The volume of the mixing chamber, which is set by equipment design, is slightly larger than the mold cavities used to form the compacts.

7.3.4. Compact Formation

This step of compact manufacture incorporates the weighed and blended particles into a cylindrical compact without damaging them. Particle damage during injection of the matrix into the particle-filled mold cavities can occur through mechanical and/or fluid interactions. Limiting the matrix injection pressure and controlling the time of injection ensure that the particles do not receive shock or impact loads

due to too rapid intrusion of the fluidized matrix into the particle bed. Control of the matrix injection and mold temperatures assure that the matrix viscosity will be the same from cycle to cycle. This is an important parameter in minimizing fluid pressure on the fuel particles during matrix injection. The ranges for the above parameters are listed below. These conditions have been characteristic of the four-hole press used for FSV process development. More precise control conditions will be optimized in tests on an improved four-hole press.

Matrix injection pressure	Increases as a ramp from 50 to 1000 psig
Matrix injection temperature	145° to 155°C
Mold temperature	125° to 175°C

After the green compacts are formed, they must be ejected from the mold cavities using hydraulic pressure. Studies on GA's developmental four-hole compact press show increasing defective particle fractions as the ejection pressure rises, so the lower this parameter can be, the better. Compacts have been ejected at pressures from 500 to 1200 psig, but a limit of 1000 psig has been set for the process. The matrix contains a mold release agent (octadecanol), which can be supplemented with sprays applied directly to the mold cavity walls if excessive sticking is encountered. The current process uses a constant-volume mold design that exerts no mechanical forces on the particles before or during matrix injection.

7.3.5. Carbonization

In the carbonization step, the compact is constrained in packed alumina powder and the volatile components of the matrix binder (petroleum pitch), are driven off. Thus the key process parameters relate to the alumina packing and furnace heating rates. Control of furnace atmosphere is also important to prevent oxidation of the graphitic matrix, particle coatings, and furnace internals. Temperature control is achieved with a thermocouple attached to the exterior of the furnace retort. Figure 7-12 shows a typical heatup and cooldown cycle for a

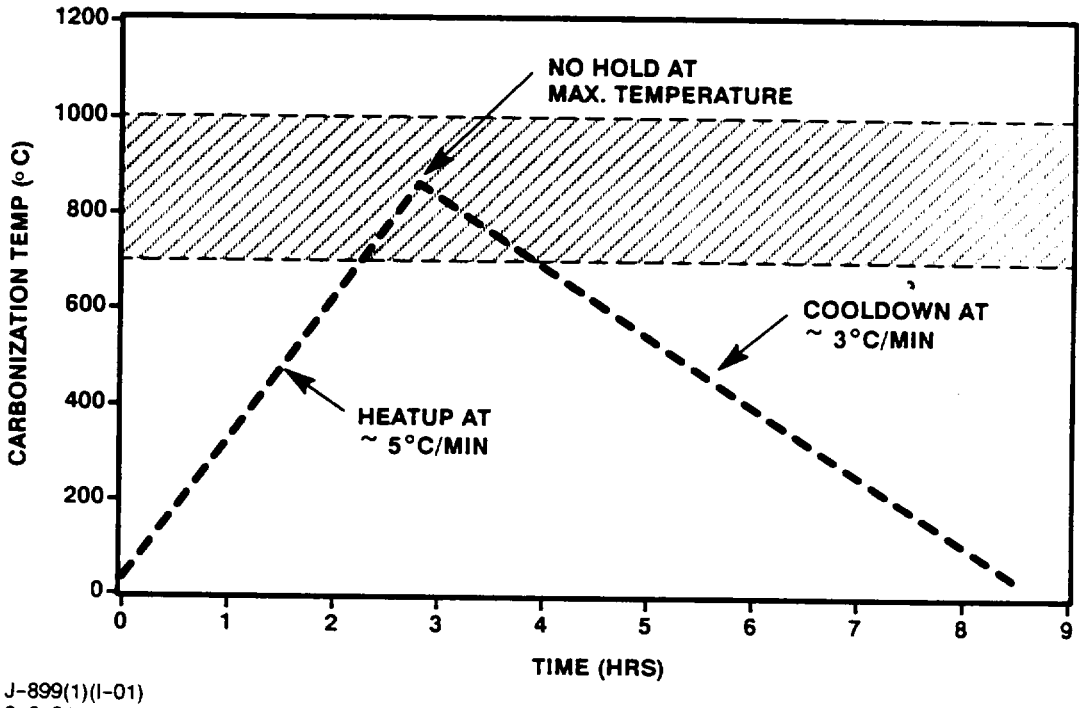

J-899(1)(I-01)
9-6-91

Fig. 7-12. Typical temperature profile for fuel compact carbonization

single carbonization furnace run. Following are ranges and values for key carbonization parameters:

Minimum depth of alumina above and below compact in graphite boats	1/2 in.
Packing time (Syntron vibrator or equivalent at medium setting)	15 to 30 sec
Process gases	Nitrogen and argon*
Process gas pressure	10 to 30 psig
Process gas flow rates	2 to 10 l/min
Furnace heatup rate	3° to 11°C/min
Furnace cooldown rate	1° to 3°C/min
Carbonization temperature	700° to 1000°C
Furnace unload temperature	200°C

7.3.6. HCl Leaching

Carbonized fuel compacts may be leached with gaseous HCl to remove impurity elements (notably iron) or reduce heavy metal contamination levels. This is an optional step that is incorporated only if impurities would otherwise exceed specifications. The key parameters are the concentration of HCl gas in the furnace, the time at temperature and the range of acceptable temperatures. The flow rate of the HCl/argon gas is not as critical as the other parameters. The temperature is lower for this process than for carbonization or final heat treatment. This avoids possible degradation of the SiC layers due to reaction with the HCl.

*Typically, nitrogen is used for purging and cooldown only; argon is always used during the run.

Key parameter ranges here are:

Furnace temperature	950° to 1150°C
Time at temperature	6 to 12 hr
Gas mix*	10% to 20% HCl in argon
Gas flow rate	2 to 10 l/min

7.3.7. Final Heat Treatment

This final compact processing step drives off any chlorine remaining from the HCl cleaning step, lowers the level of impurity elements not affected at the lower carbonization temperature, and achieves a degree of graphitization in the binder phase of the compact. Final heat treatment of FSV compacts was influenced by two requirements:

1. The heat treatment temperature was as high as possible to drive off volatile hydrocarbons and impurities, and to graphitize the binder-coke in the matrix to increase its irradiation stability.

2. The temperature was not so high as to cause excessive fuel dispersion (diffusion) within the coated particles.

Crystallite growth of the binder phase is a measure of the degree of graphitization; the major amount of crystal growth occurs at temperatures greater than 2200°C for binder phase materials. However, a limit of 1850°C was established for the final firing temperature to avoid diffusion of U and Th.

Final firing temperatures of 1650° ± 50°C have been investigated because of the incentive to lower furnace operating temperatures and to further reduce the effect of high-temperature heat treatment on fuel

*Pure argon is used for heatup and cooldown.

particles. The only discernible difference between compacts fired at 1650°C and those fired at 1800°C was the sulfur content after the heat treatment. Compacts fired at 1800°C had a substantially lower sulfur content. Thus, the allowable fuel compact firing temperature ranges between 1600° and 1850°C. This range is consistent with irradiation experience (Ref. 7-8).

As in the carbonization step, control of the furnace heatup and cooldown rates and maintenance of an inert processing atmosphere are important factors. Temperatures are monitored with either an optical measuring device or a high-temperature thermocouple attached to the graphite susceptor. A hold time at the maximum temperature is specified. Figure 7-13 shows a typical heatup, hold, and cooldown cycle for a single final heat treatment furnace run. The following are the key process parameters for compact final heat treatment:

Process gas types	Nitrogen and argon*
Process gas pressure	10 to 30 psig
Process gas flow rates	2 to 10 l/min
Furnace heatup rate	3° to 11°C/min
Furnace cooldown rate	1° to 3°C/min
Firing temperature	1600° to 1850°C
Hold time at maximum temperature	30 to 90 min
Furnace unload temperature	200°C

*Nitrogen used for purging and cooldown only.

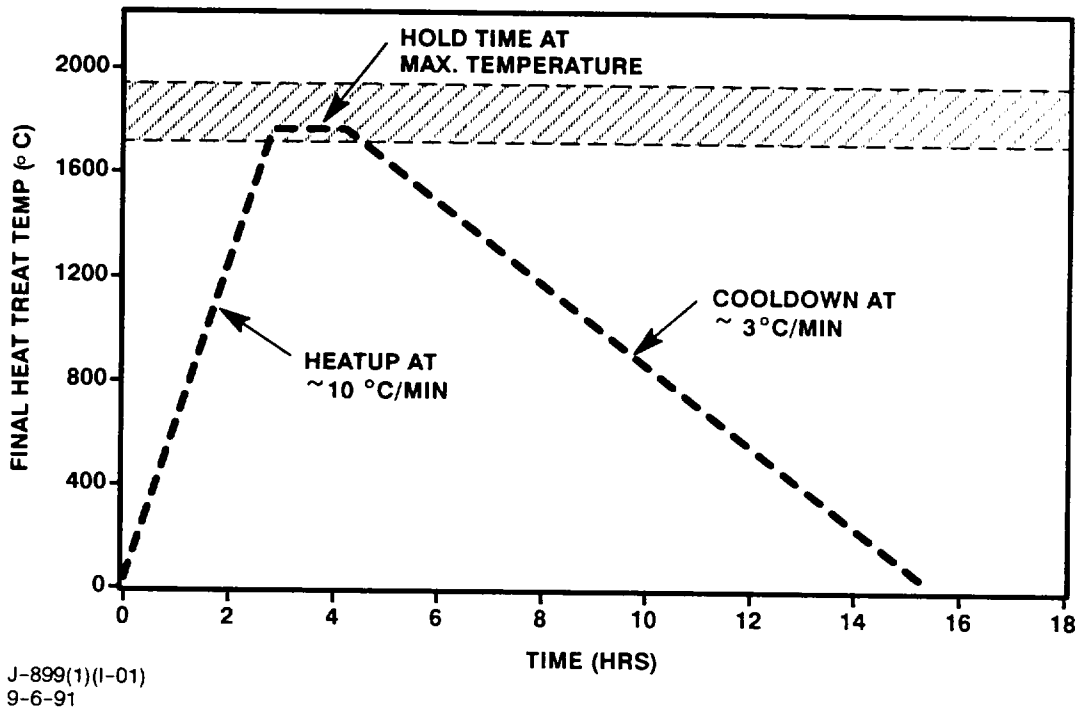

Fig. 7-13. Typical temperature profile for fuel compact final heat treatment

8. FUEL BLOCK ASSEMBLY

This last step in the fuel manufacturing process has two purposes:

1. To load the fuel blocks with the required type and number of fuel and poison compacts.

2. To identify and package the completed fuel element for shipment.

Traceable records are maintained for each fuel assembly to document inspections performed and the identification assigned for all components. To achieve this, written procedures specify quality control inspection points, parameter and data sheets, and qualified operators for all assembly/packaging operations. Process flow for the block assembly operation is shown in Fig. 8-1.

8.1. PROCESS DESCRIPTION

In preparation for final assembly, the manufactured fuel compacts are placed on a loading table which contains three grooves that hold sets of components. The grooves are each marked at a specific length corresponding to the projected height of a stack of fuel compacts in a fuel element. A Fuel Element Loading Sheet specifies the compact lot and blend type for each element, based on the previously determined heavy metal loadings for each compact lot. The loading sheet also specifies stack height limits for the different fuel compact stacks within each block. These limits prevent mechanical interference between compacts and fuel hole plugs.

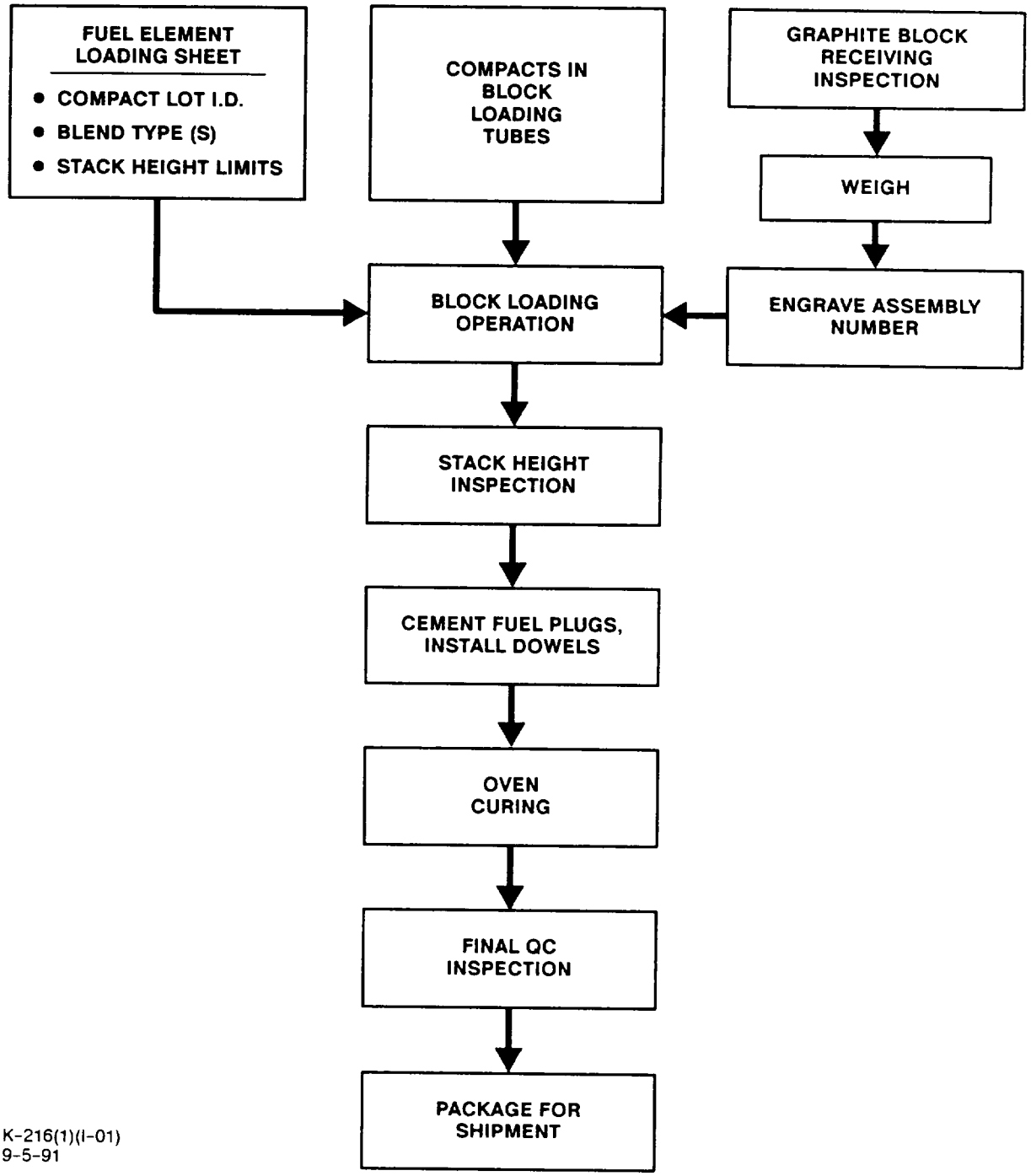

Fig. 8-1. Fuel element loading process flow

Fuel compacts are placed horizontally into the grooves on the loading table. The number of compacts per groove is determined by the marks on the groove. The compacts are placed in the grooves so that there is no space separating the compacts. After all the grooves on the table have been filled, the fuel compacts are loaded horizontally into open-ended, hollow aluminum tubes. The aluminum tubes are then transported to an adjacent location for loading into the fuel block.

Hexagonal graphite blocks are received fully machined and uniquely identified with an engraved serial number from the graphite vendor. The empty blocks are fully inspected for damage prior to loading. Each block is wiped clean and placed in a curing oven for approximately 1 hr to remove any absorbed moisture. After cooling, the blocks are transported to the fuel element loading area. An element assembly number, specified on the Fuel Element Loading Sheet, is engraved on the side of the block and the empty weight is measured and recorded.

A loading template is placed on the top of the graphite block. A vacuum fixture is placed over the fuel hole to be loaded. This fixture is a ring structure with an attached vacuum hose. It captures any loose fuel or graphite particles that may rub off during fuel loading.

Once the graphite block is ready for loading, an operator selects an aluminum tube containing a fuel compact stack and closes off the bottom end of the aluminum tube. The tube is uprighted and placed over the fuel hole to be loaded. The operator then allows the compacts to slide by gravity into the fuel hole. The column of air trapped beneath the stack of compacts and the small annular clearance between compact and fuel hole allow the compacts to descend at a controlled rate. This prevents impact loads to compacts when the stack bottoms out in the block. This process is repeated until all the fuel holes in the block have been filled.

The procedure for loading burnable poison compacts into the fuel blocks is similar. The Fuel Element Loading Sheet specifies which holes receive the poison rods, as well as the type and number of poison rods. The use of numbered templates further ensures that the poison goes only into the intended locations. The poison compacts are color coded to identify variations in boron density. The poison content varies for different core locations. Graphite spacers also are used in the poison stacks to allow a wider range of block poison content.

A quality control inspection is performed after each block is fully loaded to verify that stack heights are within specified tolerances. A specified void area is maintained at the top of each fuel compact stack to accommodate changes in length due to thermal expansion/contraction and neutron exposure.

Cylindrical graphite plugs are prepared as caps for the fuel holes. Graphite cement is applied to the edges of the fuel hole plugs. The cemented plugs are placed flush into the fuel holes. Any excess cement is removed from the top of the fuel block. After all the fuel plugs have been placed in the block, a seating tool is used to position the plugs within 0.030 in. of the top of the fuel holes. The locating dowels in the top of each block are installed. Then the top of the block is cleaned with solvent and the block is transported to the plug curing oven for curing.

The curing oven is heated to ~135°C and held for 40 min. The block is then removed from the furnace and allowed to air cool. Once the block surface temperature reaches ambient (room temperature), the block is removed for packaging.

Before the loaded elements are packaged, all parameter and run sheets are assembled and reviewed to ensure that block serial and assembly numbers are correct, legible and consistent on all documentation and on the blocks themselves.

The shipping containers for each fuel element consist of two steel drums approved by the Department of Transportation for nuclear fuel transport. After quality control inspection, the empty drums are stenciled on top and sides with the element assembly number, block serial number, and core layer identification. Only one fuel element at a time is permitted in the packaging area.

Packing material (vermiculite) is placed in the bottom of the outer drum and tamped firmly. Next the inner drum is placed inside the outer and the annulus between the two is filled with vermiculite. More vermiculite is placed in the bottom of the inner drum and tamped into place.

The fuel element is lifted with a lifting fixture and receives a final visual inspection. The element is double-bagged with plastic and the bags are evacuated and sealed. The element is then lowered into the inner drum. Additional vermiculite is added to fill all void spaces. The inner drum lid is clamped on, then the outer drum is filled with packing and also sealed. The outer drum receives a tamper-safe seal and is ready for shipment to the reactor site.

The typical throughput rate for the assembly/packaging process is six to eight fully loaded and packaged blocks per 8 hr shift.

8.2. PROCESS MATERIALS AND CHEMICALS

All materials required for fuel element assembly processes are listed in Table 8-1. Each is required to meet the equipment/inspection requirements and acceptance criteria specified in the FSV Fuel Specification (Ref. 8-1).

8.3. PROCESS PARAMETER CONTROL

Because the goal of this process is to place the required number and type of fuel compacts into correctly identified fuel elements, the

TABLE 8-1
FUEL ELEMENT ASSEMBLY MATERIALS

FUEL ELEMENT ASSEMBLY COMPONENTS
Graphite blocks
Fuel compacts
Burnable poison rods
Graphite spacers
Graphite plugs
Graphite dowels
RAW MATERIALS
Cement primer
Carbon cement
Acetone
TOOLS/FIXTURES
Block engraving tool
Loading templates
Vacuum loading fixture
Fuel element loading sheets
PACKAGING/SHIPPING MATERIALS
Plastic bags - loaded element
Vermiculite packing
Shipping drum - inner
Shipping drum - outer

most important control device is the completed Fuel Element Loading Sheet. This specifies all necessary loading and identification data for each fuel element.

Process controls specified in written procedures assure that the correct amount of graphite cement is applied to the fuel hole plugs, that excess cement is cleared from the exterior block surfaces, and that the plugs are positioned properly in the holes.

Loading templates are used to ensure that fuel compacts and burnable poison rods are placed only in the intended locations during loading operations. Block curing temperature and time at temperatures for curing the graphite cement are controlled to avoid any oxidation of the block or fuel compacts, since this step is not performed in an inert atmosphere.

9. PRODUCTION QUALITY CONTROL

Nearly all MHTGR fuel product specifications and the quality control methods employed to determine conformance of MHTGR fuel with these specifications are based on statistical sampling and analyses. This approach is dictated by the large size of the fuel product populations (e.g., kernels, coated particles, and compacts), and by the use of destructive test methods to measure many of the specified properties.

The quality control approach employed to determine the acceptability of the fuel with respect to a particular product specification (except for those few for which 100% inspection is performed), is to (1) collect a sample representative of the population, (2) perform a quality control test to measure the property of interest, and (3) apply a statistical test to determine the acceptability of the population based on the test results for the sample.

When using statistical acceptance testing, there is always a chance of making a wrong decision concerning the acceptability of a population. Two types of wrong decisions can be made. The first is when a population which does not meet the specifications is accepted (false acceptance). The second is when a population which meets the specifications is rejected (false rejection). The risk of false acceptance (i.e., the consumer's risk) is limited to 5% by the Fuel Product Specification, which imposes a 95% confidence requirement on virtually all statistical specifications. The risk of false rejection (i.e., the manufacturer's risk) is not fixed; it is dependent on the sample size and the quality of the fuel relative to the specification limits.

Larger sample sizes and higher fuel quality decrease the manufacturer's risk of rejecting good product. Conversely, if the actual product quality approaches specification limits, the risk of rejecting good product increases dramatically, even with relatively large sample sizes, and the manufacturer suffers a severe economic penalty due to low yields and/or high quality control costs. For this reason, the MHTGR fuel manufacturer must target a product quality level which significantly exceeds specification requirements, develop a process capable of meeting these quality goals, and implement statistical process control (SPC) as part of the manufacturing process to maintain average product quality at the desired level. This approach emphasizes real-time feedback of process and product quality information (i.e., SPC) to ensure product consistency and statistical acceptance testing for continuous verification of high product quality.

9.1. QUALITY CONTROL INSPECTION POINTS

Figure 9-1 is a fuel fabrication process flow diagram that shows the quality control acceptance testing performed on kernels, coated particles, compacts, and fuel assemblies. The methods used to sample the kernels, coated particles, and compacts are described in Section 9.2. The quality control test methods used to characterize the fuel are listed in Tables 9-1 and 9-2 and described in Section 9.3.

Individual batches of kernels or coated particles are blended to make up homogeneous composites. A composite is defined as a homogeneous blend of two or more batches of kernels or coated particles. Practically, the definition of a composite is related to the largest unit that can be conveniently blended with existing production equipment and within the restrictions imposed by nuclear safety considerations. For most specified properties, the samples for acceptance testing are obtained from these composites. Each compact lot is randomly sampled and tested. All fuel elements are inspected.

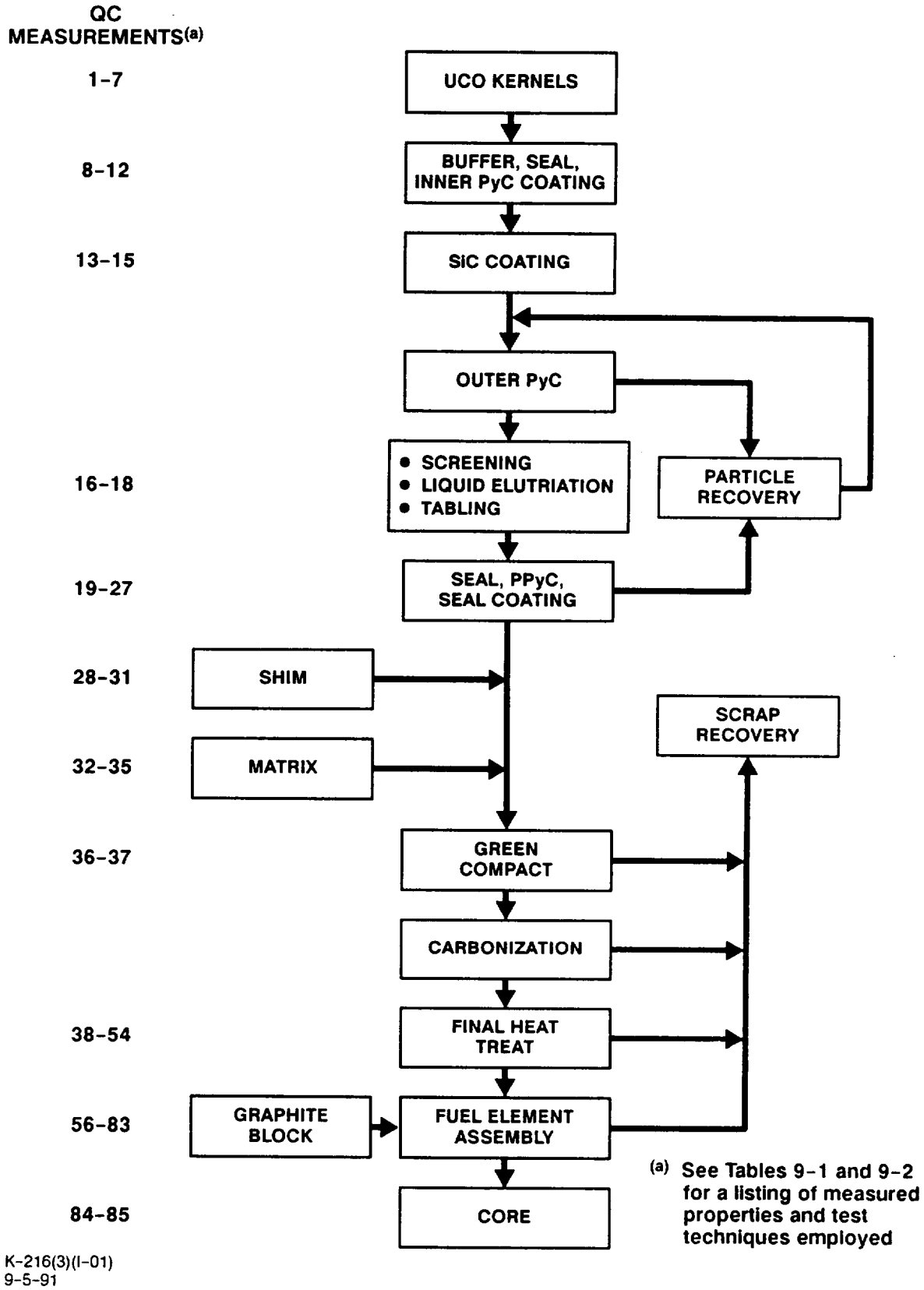

Fig. 9-1. Quality control measurements for MHTGR fuel manufacturing processes

TABLE 9-1
QUALITY CONTROL TESTING TECHNIQUES ASSOCIATED WITH PROPERTIES OF MHTGR FUEL PARTICLES AND COMPACTS

Measurement Number Per Fig 9-1	Property	Test Techniques
UCO and ThO_2 Kernels		
1	Impurities, ppm-wt (Fe, Ni, Cr, Mn, Al, P, Ca, Na)	Emission spectrography, atomic absorption spectrophotometry
2	Density, Mg/m^3	Mercury pycnometry
3	Diameter, μm	Radiography, particle size analyzer
4	Uranium wt %	Wet chemistry
UCO Kernels		
5	U isotopic composition, wt %	Mass spectrometry
6a	Carbon, wt %	LECO combustion analysis
7a	Oxygen, wt %	LECO fusion analysis
6b	C/U ratio	Calculation
7b	O/U ratio	Calculation
Buffer, Seal, IPyC Coated Particles		
8	Buffer thickness, μm	Radiography
9	Buffer density, Mg/m^3	Calculation
10	Coating rate, IPyC	Calculation
11	IPyC thickness, μm	Radiography
12	IPyC density, Mg/m^3	Gradient column

TABLE 9-1 (Continued)

Measurement Number Per Fig 9-1	Property	Test Techniques
SiC Coated Particles		
13	Coating rate, SiC	Calculation
14	SiC thickness, μm	Radiography
15	SiC density, Mg/m^3	Gradient column
OPyC Coated Particles		
16	OPyC thickness, μm	Radiography
17	OPyC density, Mg/m^3	Calculation
18	OPyC microporosity, Ml/m^2	Hg intrusion
Seal, PPyC, Seal Coated Particles		
19	Seal coat thickness, μm	Metallography
20	PPyC thickness, μm	Radiography
21	PPyC density, Mg/m^3	Calculation
22	OPyC oriented porosity	Metallography
23	IPyC coating anisotropy (BAF_o units)	Seidersdorf unit
24	OPyC coating anisotropy (BAF_o units)	Seidersdorf unit
25	Faceting, total particle	Radiography
26	Missing or incomplete buffer fraction	Radiography

TABLE 9-1 (Continued)

Measurement Number Per Fig 9-1	Property	Test Techniques
27	Missing or incomplete OPyC fraction	Radiography
Shim		
28	Grade	Vendor certs.
29	Particle size distribution, wt %	ASTM Tyler screen
30	Particle shape	Radiography
31	Reduction in surface porosity	Impregnation with polymerized furfuryl alcohol
Matrix		
32	Pitch and filler grades	Vendor certs. of PO requirements
33	Matrix additives	Vendor cert. of PO requirements
34	Filler crystallite size, Å	X-ray diffraction
35	Filler particle size, wt %	Coulter counter or Sartorius sedimentation balance
Green Compacts		
36	Matrix filler content	Pitch dissolution in quinolin
37	Fuel homogeneity	Gamma spectrometry
Fired Compacts		
38	U loading	Wet chemistry
39	Th loading	Wet chemistry
40	Integrity	Visual standards
41	Diameter (mm)	Ring gauge and air gauge

TABLE 9-1 (Continued)

Measurement Number Per Fig 9-1	Property	Test Techniques
42	Length	Mechanical
43	Coke content (g coke/ g coke plus filler)	Calculated from weights of green and fired compacts
44	Macroporosity	Metallography/grid intercept
45	Mean heavy metal contamination fraction	Gaseous HCl leach or wet acid leach
46	Mean defective SiC coatings plus heavy metal contamination	Burn-leach
47	Mean defective SiC coating fraction	Calculation
48	Mean defective IPyC coating fraction	Burnback/radiography
49	Burnable impurities	Spectrography and/or wet chemistry
50	Nonburnable impurities	Spectrography and/or wet chemistry
51	Iron content outside SiC	Burn/colorimetry
52	Transition metal content	Spectrography
53	Hydrogen	Spectrography and/or chemical
54	Chlorine outside SiC	Pyrohydrolysis/ spectrophotometry
55	Sulfur outside SiC	Combustion/iodometric titration

TABLE 9-1 (Continued)

Measurement Number Per Fig 9-1	Property	Test Techniques
Fuel Element Assemblies		
56-83	See Table 9-2	
Core Segments		
84	Total uranium mass in fuel blend	Calculation
85	Total thorium mass in fuel blend	Calculation

TABLE 9-2
QUALITY CONTROL INSPECTION TECHNIQUES ASSOCIATED
WITH FUEL ELEMENT ASSEMBLIES

	Property	Method
56	Block identification	Visual and record
57	Coolant holes (clear of obstruction)	Visual and record
58	Surface damage	Visual and record
59	Socket position and width	Gauge/check plate
60	Engraving depth and width	Dial depth gauge and scale
61	Empty block weight	Metric scale, ±0.5 kg
62	Compact lot	Visual and record
63	Template	Visual
64a	Stack height	Load makeup fixture
64b	Stack height	Fuel compact stack height gauge
65	Heavy metal loadings	Fuel loading verification
66	Proper loading technique	Visual
67	Correct holes loaded	Visual
68	Axial clearance	Depth gauge
69	Plug depth	Visual and gauge
70	Dowel height	Height gauge
71	Dowel location	Position gauge
72	Sample joints	Shear test
73	Plug joints	Load test
74	Dowel joints	Torque test, hand test
75	Excess cement	Visual and straight edge
76	Curing time and temperature	Temperature recorder chart
77	Misplaced plugs	Visual
78	Surface damage	Visual and recorded
79	Engraved verification	Visual
80	Weight	Metric scale ±0.5 kg
81	Surface contamination	Alpha count on exterior surface
82	Total U loading	Calculations
83	Total Th loading	Calculations

Figure 9-2 illustrates how fissile and fertile fuel particle batches are combined to form composites and how these composites are then used to make fuel compact lots. The particle batches are thoroughly blended to ensure homogeneity within a composite so that characterization of a composite or compact lot applies to all the localized regions in the MHTGR core where that composite or compact lot is used. In this way, MHTGR product specifications and quality control procedures are structured to assure fuel performance at the core level and in localized regions, i.e., at the compact lot and particle composite level. This approach provides considerable flexibility by controlling local fuel quality to meet core average requirements.

A product specification at the local level is stated such that the allowable fraction of defects is greater than or equal to the fraction of defects allowed at the core segment level. This is accomplished by limits at the local level that meet performance requirements, but are wider and less restrictive than the core segment average limits. The manufacturer must satisfy both specifications jointly, but he has the latitude to take advantage of a less restrictive local specification on selective composites or lots and still satisfy the core segment average specification.

9.2. SAMPLING TECHNIQUES

Quality control samples are obtained using several devices to mix and divide sets of particles. These devices include riffle, rotary, and 10-way splitters. The manner in which these devices are collectively used to obtain samples for quality control testing is illustrated in Fig. 9-3. Each of these devices is described below. Fuel compacts are randomly selected for testing using a random number table (or other means of generating random numbers).

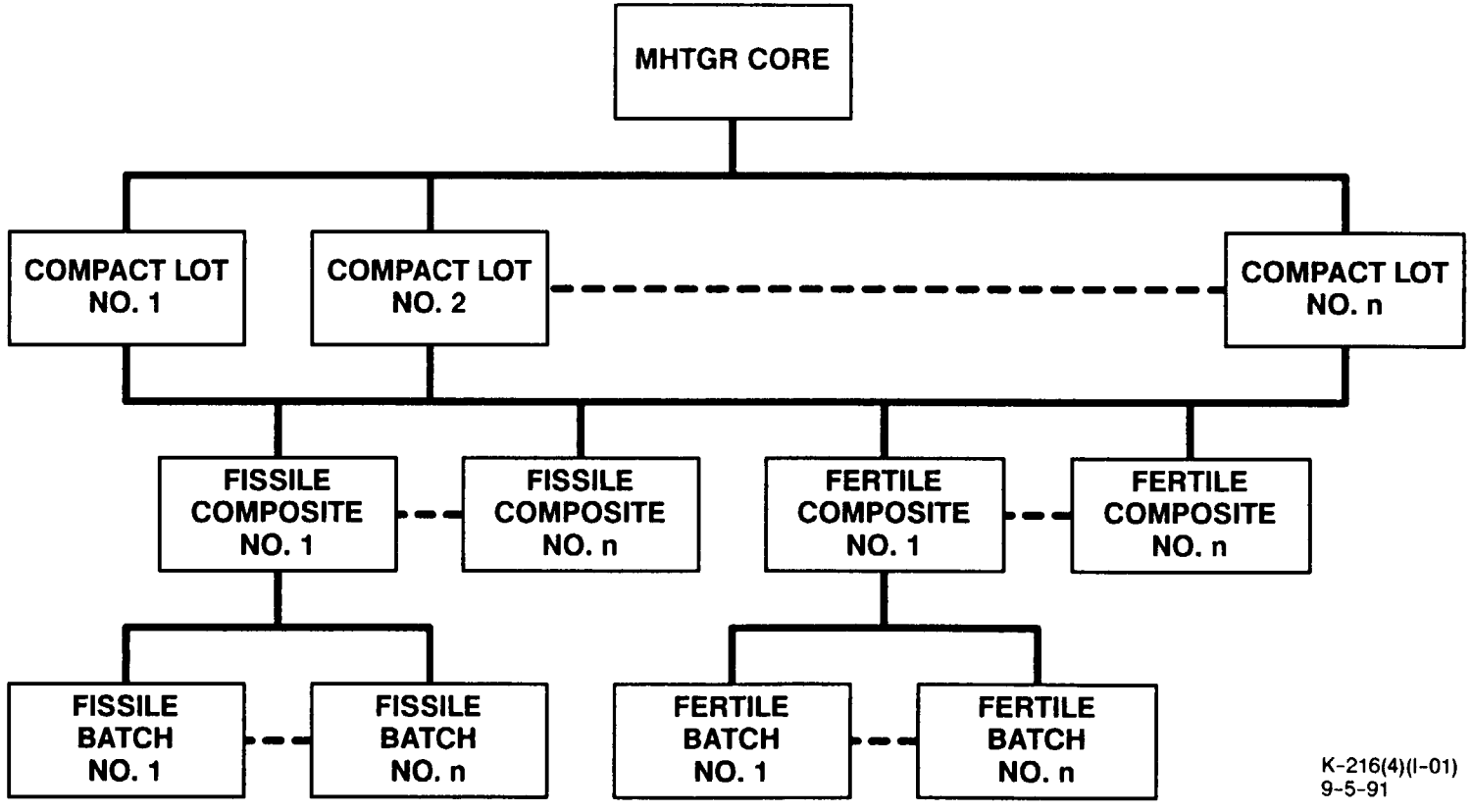

Fig. 9-2. Many separate fuel particle composites and compact lots comprise the MHTGR core

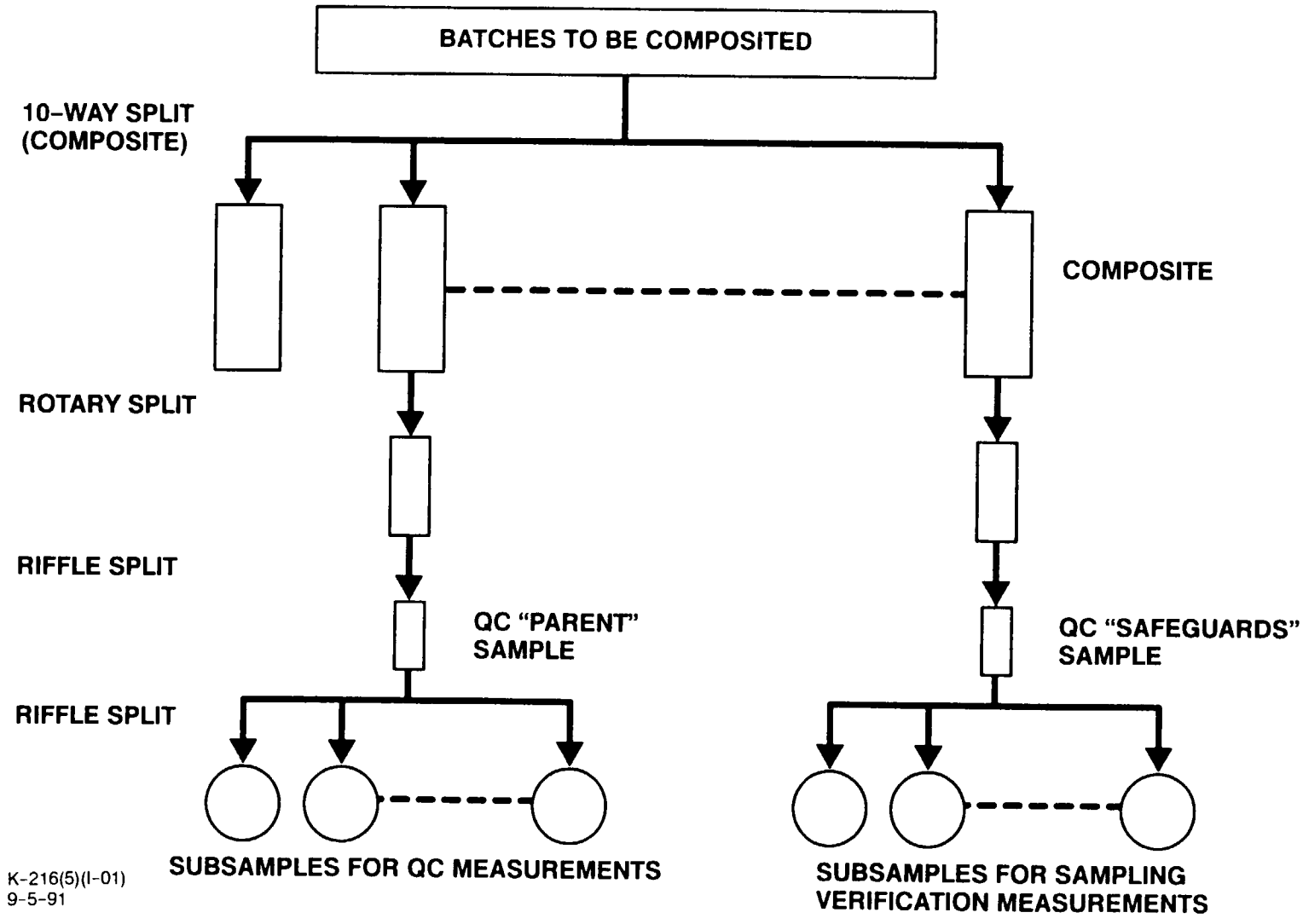

Fig. 9-3. Compositing and sampling kernel/coated particle batches

9.2.1. Riffle Splitter

Riffle splitters are widely used sampling devices. They are intended for finely divided free-flowing material such as kernels and coated particles. They are usually designed and built so that delimitation errors are nonexistent; however, bad maintenance and poor designs may greatly alter their delimitation correctness. The riffle splitters used by GA are commercially available from the Humboldt Manufacturing Company.

A typical riffle splitter (Fig. 9-4) contains a hopper that tapers down to a slot about 2 in. long and 1/4 in. wide. For purposes of this description, consider the length of the slot as running from north to south. Below the slot are 14 chutes, alternately tilted toward the east and west. The width of the chutes should be at least three times the diameter of the largest particle in the feed material. Particles are poured into the hopper from a pan that is equal in width to the total combined widths of the chutes (such that the feed material is evenly distributed to all of the chutes). When the particles fall through the slot they land in a chute and, depending on which chute they hit, are sent either to the east pan or the west pan. If a smaller sample is needed, the contents of one of the pans are poured into the hopper and split again. When the process is repeated in this way, the pans are selected alternately (first east, then west, then east, etc.) to avoid a possible bias.

9.2.2. Ten-Way Splitter

A 10-way splitter (Fig. 9-5) has a hopper with a chute at the bottom. The entire assembly of the hopper plus chute rotates, feeding into 10 ports, and these into 10 hoses to 10 bottles. Both the rotation speed and the hopper orifice are adjustable so that the assembly rotates many times as these particles pass through. The 10-way splitter is occasionally used for sampling large quantities of particles, but is more frequently used for making kernel and coated particle composites.

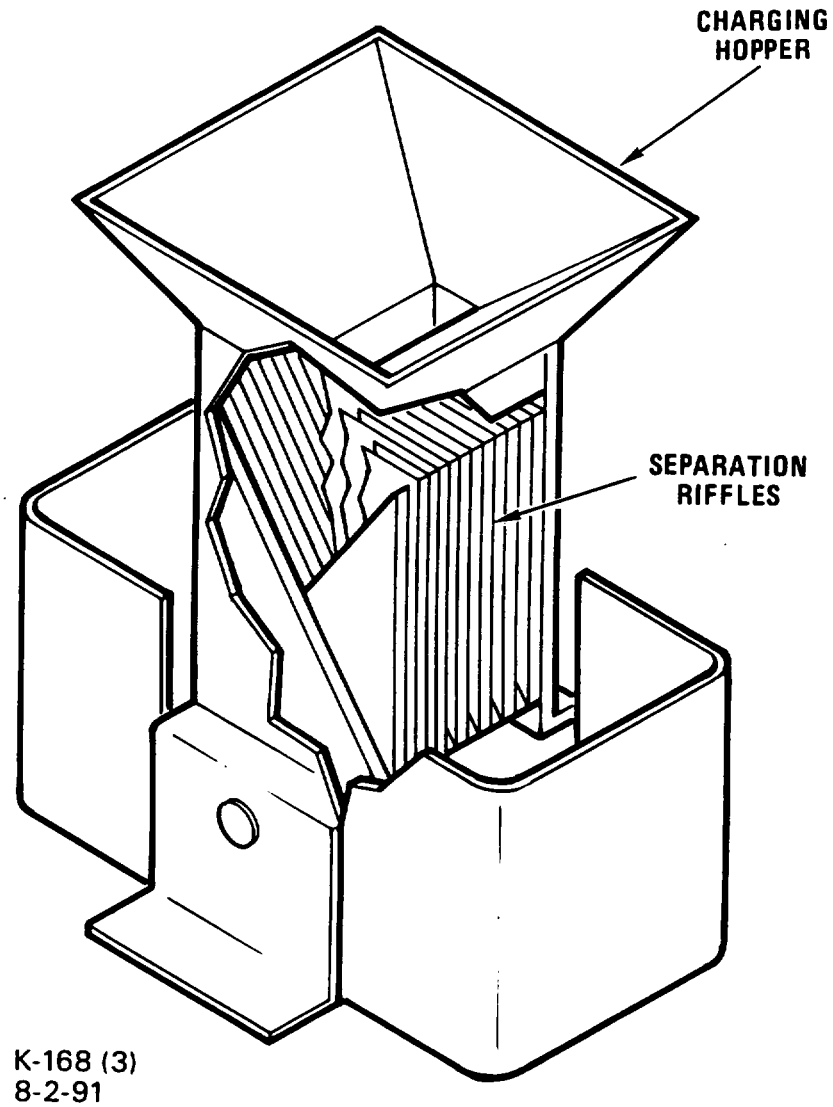

Fig. 9-4. Riffle splitter

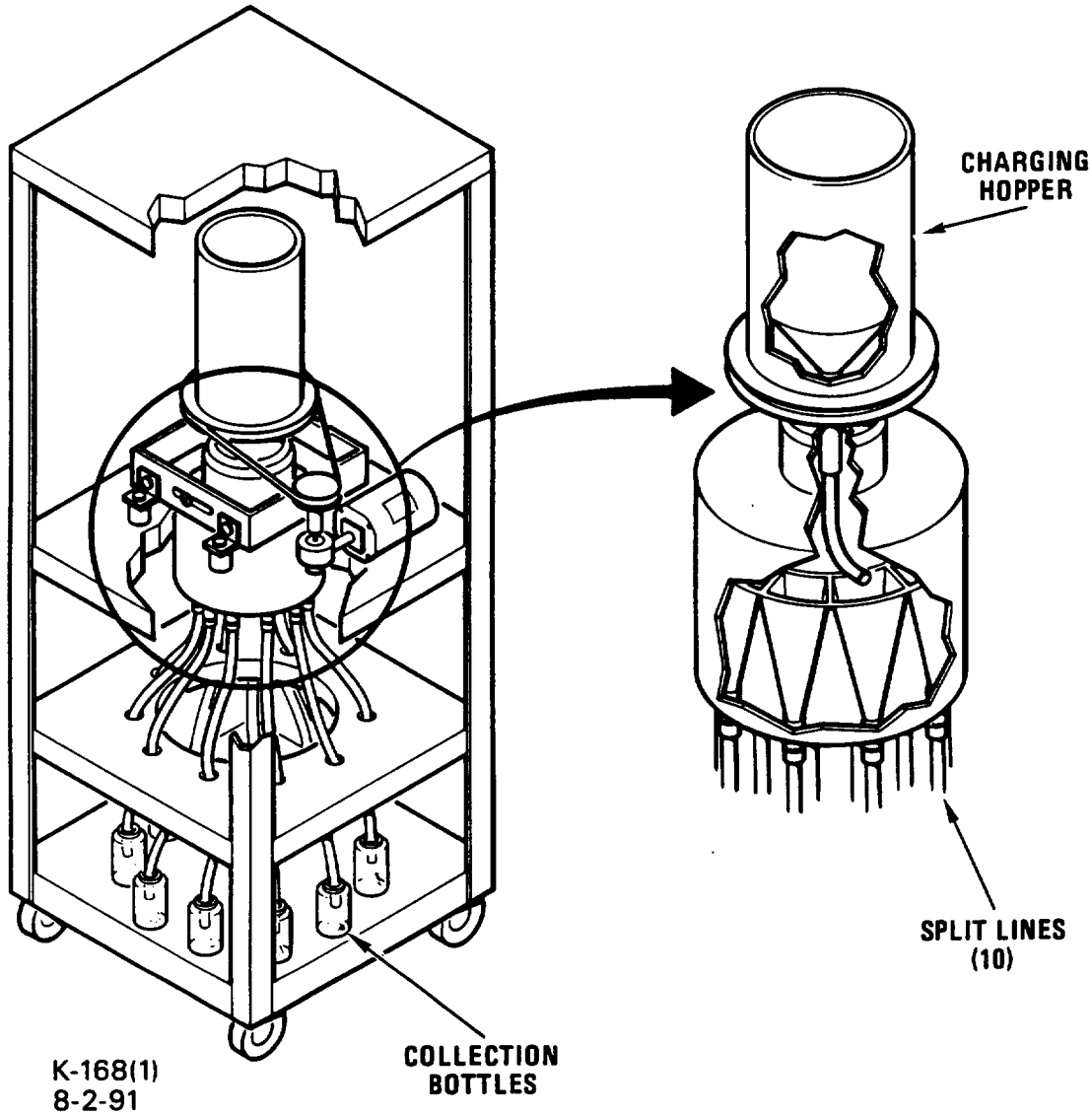

Fig. 9-5. Ten-way splitter

Particle composites are formed by putting the batches to be composited through the 10-way splitter. The resulting ten bottles of particles are set to one side, and ten empty bottles are loaded into the 10-way splitter. Each full bottle is then poured into the 10-way splitter. This process is repeated several times, resulting in a thorough mix of the particles in the composite.

9.2.3. Rotary Splitter

A rotary splitter (Fig. 9-6) is generally used to obtain large samples from kernel/coated particle batches or composites. Beneath the hopper of a rotary splitter is a rotating plate in a housing, with both the plate and housing tilted. This plate has a wedge-shaped slot running from the center to the edge, with the slot wider near the center and tapering to a point at the edge. The hose from the hopper can be positioned towards the center of the plate or towards the edge to adjust the size of the sample. As the particles fall from the hopper onto the plate, a few fall through the slot when it rotates past the hose, while most roll downward and off the edge of the plate. Those that fall through the slot are collected as the sample.

At the smallest setting, the width of the slot is several times the diameter of the particles. The usual practice is not to use the smallest setting so that the slot width does not bias the size of the selected particles in any way. The plate rotates at 60 to 70 revolutions per minute and it takes many minutes for the particles to pass through the splitter. A few particles are therefore selected from many parts of the particle population.

9.3. QUALITY CONTROL TEST METHODS

This section describes the quality control test methods listed in Tables 9-1 and 9-2. Nearly all are based on industry-accepted standard methods (i.e., ASTM methods). The exceptions are tests for which no standard method is available (for example, the burn-leach test).

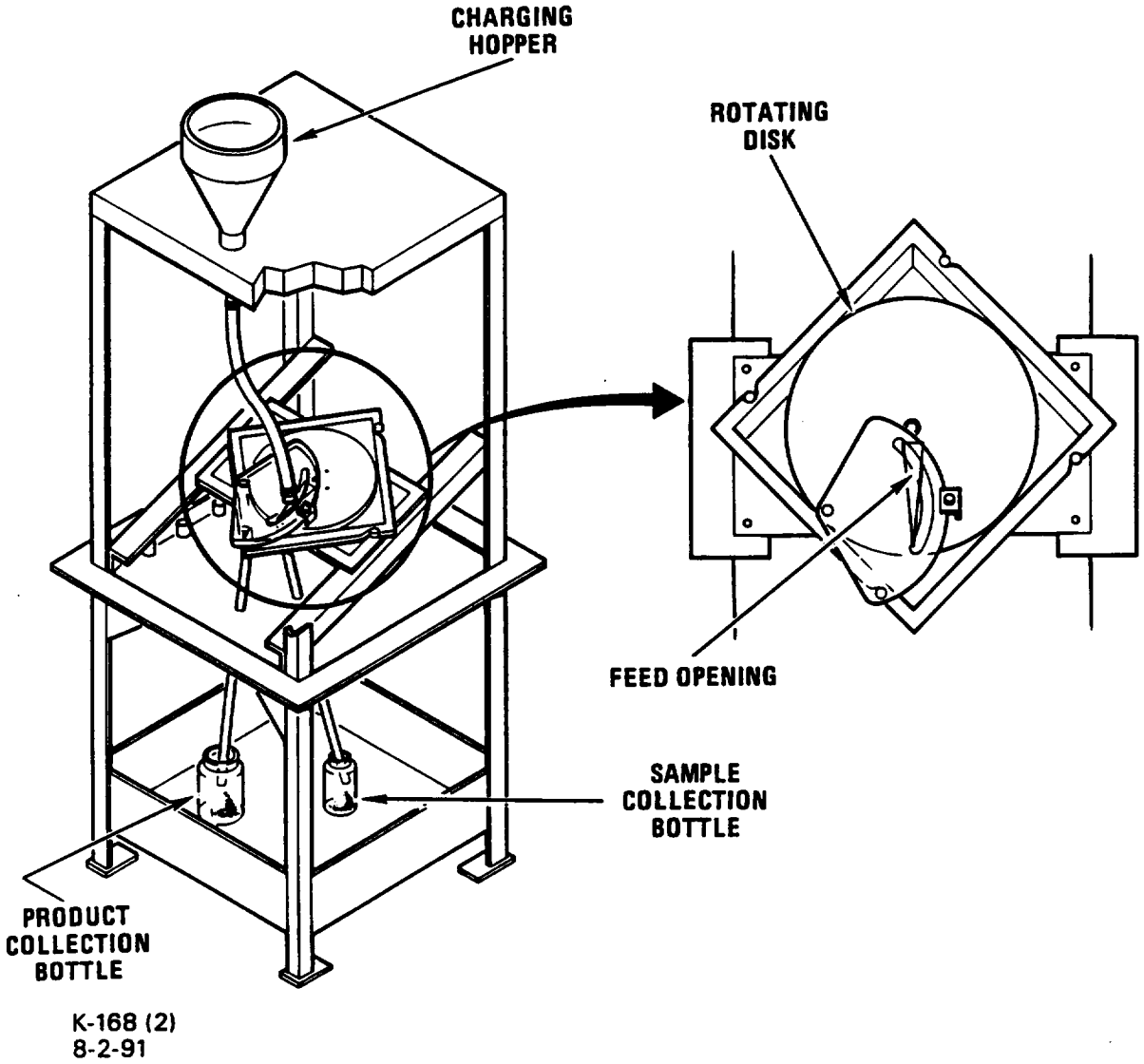

Fig. 9-6. Rotary splitter

9.3.1. Emission Spectrography

The presence and quantity of specified impurities in kernels or fuel compacts are determined by ionizing materials in a high-voltage electrical spark, optically measuring the characteristic emission spectrum, and comparing the result to known standards.

9.3.2. Atomic Absorption Spectrophotometry

Metallic impurities in kernels or fuel compacts are detected by ionizing materials in a high-temperature flame, transmitting light of a specific wavelength through the flame, and measuring its absorption. The absorption is compared to that of a series of standards to determine the concentration of the impurity.

9.3.3. Spectrophotometry

This technique to detect impurities chemically is based on producing a colored compound in solution. Light transmission through the solution is measured and compared to a series of standards.

9.3.4. LECO Combustion Analysis (Carbon)

This method is based on burning the analytical sample in O_2 in a closed system at a specified temperature, and collecting and measuring the resulting CO_2 to determine the carbon content of the sample.

9.3.5. Mass Spectrometry

This technique is based on deflecting ionized atoms in a magnetic field; the heavier nuclei deflect less than light nuclei.

9.3.6. Wet Chemistry

Kernels, fuel particles, or fuel compacts are first crushed and burned, then dissolved in nitric acid. The resulting solution is aliquoted and the uranium concentration is determined by the NBL-modified Davies-Gray potentiometric titration technique. The thorium concentration is determined by photometric titration.

9.3.7. LECO Fusion Analysis

The oxygen in UCO kernels is determined by an inert gas fusion technique. The sample is heated above 2700°C in a graphite crucible. Oxygen in the sample is released as carbon monoxide. Nitrogen carrier gas sweeps the CO through an ascarite trap and over hot copper oxide. Hydrogen is oxidized to water and absorbed in anhydrone, while CO is oxidized to CO_2 and measured in a thermal conductivity cell.

9.3.8. Mercury Pycnometry

This technique is used to measure the density of kernels and coated particles by determining the volume of mercury displaced by the particles at atmospheric pressure.

9.3.9. Mercury Intrusion

The OPyC coating microporosity determination is based on a mercury intrusion measurement at 68.9 MPa (10^4 psi). The amount of mercury intrusion defines the available surface-connected porosity, which is expressed as the volume of microporosity per unit area of OPyC outer surface.

9.3.10. Gradient Column

A density gradient column consisting of diodomethane and acetone or bromoform and acetone in a graduated column is used to measure IPyC and

SiC coating densities. Calibrated floats define the density gradients within a column, with each float sinking to a column level corresponding to its density. Fragments of coatings are introduced into the column and the level to which they sink is compared to the standards.

9.3.11. Bulk Density (Weight/Volume)

In the OPyC bulk density (weight/volume) determination, the density of the OPyC coated particles is determined by mercury pycnometry. A sample of the particles is weighed and the OPyC is removed by oxidation in air at an elevated temperature. The particles are allowed to cool and then reweighed. The density of the SiC coated substrate is then determined by mercury pycnometry. The OPyC density is calculated from the densities of the OPyC and SiC coated particles and the weight fraction of the OPyC coating.

The PPyC coating density is determined by measuring the OPyC coated particle density before depositing the PPyC layer and then determining the PPyC coated particle density. The weight fractions of the OPyC coating layer, and of the combined OPyC and PPyC coating layers, are determined by burning particles back to the SiC coating and noting the weight changes. The PPyC coating density (including the two adjacent seal coats) is calculated using the equation:

$$\text{Density} = \frac{(DP)(DS)\ (CP - CS)}{DS(1-CS) - DP(1 - CP)}\ , \qquad (9\text{-}1)$$

where DP = Density of PPyC coated particles,

DS = Density of OPyC coated particles used as the substrate for the PPyC coated-particle batch or composite,

CP = Weight fraction of pyrocarbon coatings external to the SiC coating,

CS = Weight fraction of the OPyC coating on the OPyC coated particles used as the substrate for the PPyC coated particle batch or composite.

The bulk density of the buffer coating is determined by an analogous method.

9.3.12. Coating Thickness and Kernel/Coated-Particle Diameter

9.3.12.1. Radiography. Coating thicknesses and particle diameter are measured by microscopic examination of high resolution X-radiographs. The digital output from these measurements is processed and printed by an on-line computer system. Individual values, averages, standard deviations, and other statistics are calculated by the computer program.

9.3.12.2. Particle Size Analyzer. Precise and rapid particle diameter measurements are obtained with a particle size analyzer. In addition to measuring diameter, the analyzer counts the number of particles measured. Such an analyzer is expected to be the major source of process control data for future particle coating operations. The unit operates using a light blockage principle (i.e., as a particle passes through a light beam, its shadow changes the current pass through a photodiode proportional to the cross-sectional area of the particle). Low particle count rates (<1200 particles/min) ensure that only one particle at a time is observed by the photodiode.

9.3.13. Detection of Defective Particles by Radiography

Particles with missing or incomplete coatings and/or excessive fuel dispersion are detected and quantified through examination of high-resolution x-radiographs.

9.3.14 Evaluation of OPyC-Oriented Porosity and Fuel Rod Macroporosity

Standard mounting and polishing procedures are used for fuel particles and fuel compacts. Comparative metallographic standards are used to define an acceptable OPyC-oriented porosity. Fuel compact macroporosity is determined by superimposing a grid upon a magnified field of view of the polished surface and determining the ratio of line intersections on the matrix and voids with major dimensions greater than 50 μm.

9.3.15. Optical Anisotropy Measurement on Seibersdorf Unit

Crystallite anisotropy in pyrocarbon structures is defined by a Bacon anisotropy factor, BAF, which is related to the integrated x-ray diffraction intensity of two planes. This factor can range from 1.0 for perfectly isotropic structures to ∞ for totally anisotropic structures. Characterization of pyrocarbon anisotropy by x-ray diffraction requires a planar specimen with a reference surface large enough to be aligned on a goniometer. Consequently, such measurements on spherical coating layers nominally 40 mm thick are impractical. As a result, a number of optical methods have been developed that take advantage of the bireflectant nature of pyrocarbons (i.e., a structure containing two principal directions of reflectivity). One such technique, based on a measuring device developed by the Austrian Research Center at Seibersdorf, relies on the observation that pyrocarbon coatings are preferentially oriented and possess different optical reflectivities parallel and perpendicular to the deposition plane. The technique is based on an empirical correlation between BAF_{x-ray} and an optically determined anisotropy (BAF_o).

9.3.16. Faceting Measurements by Radiography

The degree of faceting of a fuel particle is characterized in terms of an aspect ratio, the ratio of the maximum and minimum diameters of the particle. The diameters are measured on high resolution x-radiographs.

9.3.17. X-Ray Diffraction

X-ray diffraction is used to measure the apparent crystallite height (L_c) in the matrix filler particles. L_c is calculated from the half-height width of the (0002) diffraction peak using the following Scherrer relationship:

$$L_c = 0.89\ \lambda/B \cos\theta \quad , \qquad (9\text{-}2)$$

where λ = X-ray wavelength,

θ = Bragg angle,

B = half-height width of (0002) peak.

9.3.18. Coulter Count, Sartorius Sedimentation Balance and Tyler Screen

The graphite filler particle size distribution is defined by a Coulter counter or a Sartorius sedimentation balance. The shim particle size is defined by measuring the weight fraction of particles between a 28- and 14-mesh Tyler screen. An acceptable particle size distribution is necessary to achieve filler and shim particle homogeneity in the fired fuel rod.

9.3.19. Gamma Spectroscopy

Uranium and thorium homogeneity are determined by gamma counting both halves of a fuel compact at the green compact stage.

9.3.20. Burn-Leach

The defect fraction for the SiC layer in TRISO-coated fissile or fertile particles is measured by a burn-leach technique. This test burns off (oxidizes at approximately 750°C in air) the OPyC and PPyC layers on all particles and the IPyC and buffer layers on particles with defective SiC layers. After the burn treatment, the particles are

leached in nitric acid at approximately 100°C to dissolve any exposed uranium or thorium (i.e., any heavy metal not encapsulated by an intact SiC coating). The U or Th concentration in the leach solution is determined by neutron activation analysis, spectrophometry, or other method suitable for trace U or Th measurements. After subtracting the leached U or Th contributed by contamination, the number of defective particles is determined from the net U or Th leached and the defective particle fraction is calculated.

9.3.21. Combustion/Iodometric Titration

Sulfur is determined in graphite, coke, carbon, pitch, and fuel compacts by a direct combustion-iodometric titration method. The sample is burned at high temperatures to decompose any sulfates, such as sodium sulfate, and the sulfur is converted to sulfur dioxide. The sulfur dioxide is passed through an acidic potassium iodide-starch solution. In the presence of the free iodine formed by the reaction of potassium iodide and potassium iodate, the starch turns blue. As the iodine is consumed by the reaction with sulfur dioxide, the blue color of the solution fades. More potassium iodate solution is added to bring the solution back to its original color. The volume of the potassium iodate solution titrated to maintain the original color is a measure of the sulfur content of the sample.

9.3.22. Burn/Colorimetry

Fuel particles from burned-back fuel compacts are leached in HCl acid. The dissolved iron is reduced to ferrous iron with hydroxylamine hydrochloride, then reacted with 1,10-phenanthroline. The color intensity of the red ferrous complex is measured at approximately 510 nm using a suitable spectrophotometer. Beer's law is valid; consequently, color intensity is related to the amount of iron in solution.

9.3.23. Coke Content in Fired Fuel Compacts

The coke content in fired compacts is defined as the weight fraction of coke present in the carbonized matrix phase. It is calculated as follows:

$$\text{Coke Content} = \text{Coke Weight}/(\text{Coke Weight} + \text{Filler Weight}) \quad , \quad (9\text{-}3)$$

where Coke Weight = [Fired Compact Weight - (Fuel Particle + Shim + Filler Weight)].

If shim particles are impregnated with furfuryl alcohol, account must be taken for the expected weight loss in shim particles (furfuryl alcohol has a nominal char yield of about 50%). Typically, this results in a weight loss of 3 to 5 wt % in shim particles during carbonization.

9.3.24. Gaseous HCl Gas or Wet Acid Leach of Heavy Metal Contamination

One of the primary design criteria for the MHTGR core is to limit the fission gas release from the fuel to the helium coolant. A major contributor to the released fission gas is expected to be from contamination and defective particles incurred during fuel fabrication.

To measure heavy-metal contamination, uranium and thorium contamination is leached from the fuel compacts using a gaseous HCl leach or wet acid leach technique. The quantity of uranium and thorium leached from the compacts is measured spectrophotometrically. The spectrophotometric measurement of trace uranium and thorium standards uses bromo-PADAP and thorin as the chromogenic reagents. These reagents produce stable solutions that have linear absorbances with uranium or thorium concentration over the required range. Use of these reagents is advantageous because uranium is only a minor interference in the thorin-thorium method, and thorium does not react with bromo-PADAP at all.

9.4. IMPROVED QUALITY CONTROL TECHNIQUES

Three areas for potential improvement in quality control inspection/test techniques include: (1) SiC coating defect measurement, (2) use of image analysis technology for measuring physical properties and defective particle fractions, and (3) automation.

9.4.1. SiC Coating Defect Measurement

Evidence suggests that the burn/leach method is inadequate for detecting very small defects (< about 1 micron) in SiC coatings. This appears to result from the formation of an SiO_2 layer during the burn step. This layer seals very small defects, preventing oxygen from entering the particle interior and oxidizing the inner pyrocarbon and buffer layers. Two approaches to eliminate SiO_2 formation seem feasible. These are:

1. Removal of carbon and SiO_2 by glow discharge activation of H_2 to H^+ ion, followed by reaction with C and SiO_2 to form CH_4 and SiH_4 gas.

   Carbon and SiO_2 react with H^+ ions to form CH_4 and SiH_4, which can be used to remove carbon and SiO_2 from SiC coated particles.

   $$C + H_2 + 2\ H^+ = CH_4\ \text{gas} \quad , \qquad (9\text{-}4)$$

   $$SiO_2 + 4\ H_2 = SiH_4\ \text{gas} + 2\ H_2O \quad .$$

   These reactions can be used at ~400° to 500°C on previously burned-back TRISO coated fuel particles that have been acid leached to remove gross SiC defects. This allows small pores through the SiC coating to be accessed by the $H_2 + H^+$ reaction with the carbon to form CH_4 in defective particles. After

treatment, the HM from these additional SiC coating defects may be acid leached or injected with a detectable substance for x-ray examination.

2. Removal of SiO_2 by activated O_2 reaction followed by H_2 reaction.

   This approach consists of a low-temperature reaction (400°C) of the carbon with activated oxygen (ozone or O radical), followed by H_2 reduction of any SiO_2 formed. The low oxidation temperature will minimize SiO_2 surface migration to close SiC coatings. The acid leach of the treated particles will be the same as in 1 above.

   Another solution would be to replace the burn/leach method with an alternate technique. Potential methods that warrant consideration include high-pressure mercury intrusion/radiography, acoustic emission, and ion microtomography.

9.4.2. Image Analysis

The image analyzer system consists of an image camera, lens, and interface hardware; software for x-ray plate development, and a positioning table interface. The system can potentially employ state-of-the-art imaging techniques to determine particle diameters, coatings thicknesses, coating defects, and other properties.

9.4.3. Automation

In an automated, computer-controlled plant, fuel process variables and product characteristics would be continuously monitored using a computer network system to manage data input from (1) automated data-acquisition devices and (2) manual keyboard entry consoles. Graphical statistical process control (SPC) charts depicting consistency in process variables and product characteristics would be displayed on computer

monitors throughout the production cycle. This would provide real-time monitoring of MHTGR fuel quality and would allow production and quality control personnel to anticipate problems before discrepant material is produced.

9.5. STATISTICAL TEST METHODS

Acceptance testing of MHTGR fuel involves both attribute and variable sampling. Attribute sampling results in a single value representing the fuel property, whereas variable sampling provides a range of values with a mean and variance. The decision between variable and attribute sampling is based on the adequacy of the method to ensure that specification requirements are met within the economic constraints associated with sampling and product performance. For example, the SiC coating defect fraction is evaluated as an attribute for an entire fuel compact lot using a burn-leach test. The heavy metal leached (minus heavy-metal contamination) is divided by the total heavy metal present to give an effective SiC coating defect fraction for the entire compact lot. This test result is directly usable in fuel performance analysis. The attribute sampling approach is simpler and more direct than variable sampling, which defines a continuous distribution of defect fractions from unit to unit in a lot.

In contrast to SiC coating defect fractions, coating layer thicknesses are evaluated using variable sampling techniques that result in a determination of the mean value and the standard deviation for the population distribution. These statistical parameters allow an assessment to be made of the fraction of coating layers outside the specification limits. Variable sampling provides statistical parameters for correlation with TRISO coated particle pressure-induced failure calculations. The additional information obtained on variability allows manufacturing to make the same confidence level statement for a given fuel quality with much smaller samples than would be required for attribute sampling.

In cases where attribute sampling is selected, the specification is defined on either an upper (X_u) or lower (X_L) property value; i.e., if $X < X_L$ or $X > X_u$, the property is unacceptable, otherwise, it is acceptable. When variable sampling is selected, one or both of the following is specified:

1. The fraction of the population that can exceed given "critical limits" (control on population dispersion).
2. Upper and/or lower limits on the population mean.

The bases for attribute and variable sampling are described in Appendix A.

9.6. PROCESS CONTROL INSPECTION

Process control inspection is structured around real-time statistical process control (SPC) charting systems that graphically display production consistency and highlight abnormalities or adverse trends. Attribute sampling involves monitoring the fraction defective (referred to as a "P" chart). Variable sampling involves monitoring either the lot mean value ($\bar{X}_j$) and/or the standard deviation (S_x). This type of SPC monitoring is referred to as "X-bar/sigma" charting. X-bar/sigma monitoring can also be combined into a single SPC chart referred to as "tolerance factor" charting.

9.7. MHTGR SAMPLING PLANS

Process and product characteristics are monitored either as attribute or variable samples. The MHTGR fuel characteristics that are monitored as attributes are listed in Table 9-3. All other fuel properties are monitored using variable sampling.

The sampling plans to be used for MHTGR manufacturing will be based on a strategy of high average quality and sampling inspection which

TABLE 9-3
MHTGR FUEL PROPERTIES SAMPLED AS ATTRIBUTES

MHTGR Fuel Specification Category	Property Sampled	Criteria for Rejection
Fissile and fertile particles	OPyC coating Oriented porosity	Metallographic comparison to standard
	Defective SiC coating	Critically determined (burn-leach) value
	Missing or incomplete coatings and/or excessive fuel dispersion	Radiographic count of defects
	Faceting	Number of particles with aspect ratio above specification limit
Shim particles	Particle shape	Comparative visual standards
Fired compacts	Integrity	Visual standards
Fuel element assembly	See Table 9-2, Items 5-6 through 5-8, 62, 63, 65 through 67, 75, 77 through 79.	

results in a high product acceptance yield. This strategy relies on a manufacturing process capable of producing fuel that is well within specification limits. Under these conditions, the average quality level of the fuel delivered to the consumer (AOQL) is approximately equal to the average as-manufactured quality level (AQL) and the process is operating near 100% product acceptance. In the event the AQL approaches specification limits, the producer suffers a dramatic decrease in yield with only a marginal increase in the AOQL relative to the AQL.

Designing the optimum sampling plan (i.e., the minimum sampling required to assure conformance with specification requirements) will therefore require knowledge of the process capability under normal production conditions. An adequate margin between process capability and specification requirements will ensure that high-quality MHTGR fuel can be economically produced.

10. REFERENCES

2-1. Gas-Cooled Reactor Associates, "Utility/User Requirements for the Modular High Temperature Gas-Cooled Reactor Plant," GCRA 86-002, Rev. 5, 1989.

2-2. U.S. Department of Energy, "Top-Level Regulatory Criteria for the Standard MHTGR," DOE-HTGR-85002, Rev. 3, 1989.

2-3. Turner, R. F., et al., "Selection of LEU/Th Reference Fuel for the HTGR-SC/C Lead Plant," GA Report GA-A17123, May 1983.

2-4. "MHTGR Fuel/Fission Product Technology Development Plan," GA Document DOE-HTGR-86027, April 1987.

3-1. "Fuel Product Specification For MHTGR," GA Document DOE-HTGR-86081, Ref. F, June 1989.

3-2. "Technical Support Document of the MHTGR Fuel Product Specification," GA Document 903728, Rev. D, June 1989.

3-3. Stansfield, O. M., "Evolution of HTGR Coated Fuel Design," GA Report GA-A19685, September 1989.

3-4. Goodin, D. T., "MHTGR Fuel Performance and Supporting Data Base," GA Report GA-A19877, October 1989.

5-1. Brambilla, G., P. Gerontopulos, and D. Neri, "The SNAM Process for the Preparation of Ceramic Nuclear Fuel Microspheres: Laboratory Studies," Energia Nucleare, 17(4), 217 (1970).

5-2. Facchini, A. G., "The SNAM Process for the Preparation of Ceramic Nuclear Fuel Microspheres: Continuous Production Technique," Energia Nucleare, 17(4), 225 (1970).

5-3. Hardy, C. J., and E. S. Lane, "Gel Process Development in the United Kingdom," Symposium on Sol-Gel Processes and Reactor Fuel Cycle, Gatlinburg Tennessee, Conf-700502, 137 (1970).

5-4. Gallone, S., G. Schileo, and M. Zifferero, "Laboratory Studies and Pilot Plant Development of Sol-Gel Processes in Italy," Symposium on Sol-Gel Processes and Reactor Fuel Cycles, Gatlinburg Tennessee, Conf-700502, 150 (1970).

5-5. Zimmer, E., P. Naefe, and H. Ringl, "Aqueous Chemical Processes for the Preparation of High Temperature Reactor Fuel Kernels," Radiochemica Acta, 25, 161 (1978).

5-6. Dobson, J. C., and Brown, L. C., "Fissile Fuel Kernel Production Technology," GA Document 904401, August 6, 1980.

5-7. Winkler, E. O., "UCO Kernel Process Scale-Up Parameters," GA Document 907102, September 27, 1983.

5-8. Winkler, E. O., and Le, K. H., "Fissile Kernel GSP Process Summary," GA Document 906786, September 14, 1984.

5-9. Winkler, E. O., and DeVelasco, R. I., "UCO Fissile Kernel Process Scale-Up Parameters," U.S. DOE Report HTGR-85-143, GA Document 907102, 1985.

5-10. DeVelasco, R. I., and Montgomery, F. C., "Scale Up of UCO Fissile Kernel Process Parameter," GA Document 90857, September 25, 1986.

5-11. DeVelasco, R. I., "Critical Process Parameters for UCO Kernel Production," GA Document DOE-HTGR-88165, September 20, 1988.

5-12. Stinton, D. P., W. J. Lackey, and R. D. Spence, "Production of Spherical UO_2-UC_2 for Nuclear Fuel Applications Using Thermochemical Principles," USDOE report ORNL/TM-7651, 1981.

5-13. Ferguson, D. E., et al., "Preparation and Fabrication of ThO_2 Fuels," Oak Ridge National Laboratory, ORNL-3225, June 5, 1962.

5-14. Nelson, E. N., "Fluid Bed Denitrator of Thorium Nitrate," Mallinckrod Chemical Works, MCW-1511, January 1966.

5-15. Norman, et al., "Development of Liquid Gelling (Sol-Gel) Processes for HTGR Fuel Particle Fabrication," GAMD 6913, February 15, 1966.

5-16. McKorkle, K. A., "Steam Denitration of Thorium Nitrate in the SVA Fluid Bed Denitrator," KHM-033-PDD-74, July 29, 1974.

5-17. Rayleigh, J. W. S., Proceedings of London Math Soc. I.D. (1878).

5-18. Scott, P. D., et al., "Kinetics of Dissolution of B-Uranium Trioxide in Acid and Carbonate Solution," J. of the Chemical Soc., Dalton Transactions, 20, 1939 (1977).

5-19. Gmenlin Handbook of Inorganic Chemistry, Supplement Volume C7, Uranium Compounds with Nitrogen, 8th Edition, Springer Verlag, Berlin, 1981.

5-20. Photochemistry, J. G. Calvert, et al., p 787, John Wiley and Sons, Inc., New York, 1966.

5-21. Polyvinyl Alcohol, Basic Properties and Uses, J. G. Pritchard, Bordon and Breach Science Publishers, London, 1970.

5-22. Tsuchiya, Y., and K. Sumi, "Thermal Decomposition Products of Poly(vinyl Alcohol)," J. of Polymer Science, Part A-1, 7, 3151 (1969).

5-23. Price, G. H., "Self-Reduction in Ammonium Uranates," J. Inorg. and Nuclear Chemistry, 33, 4085 (1970).

5-24. El-Fekey, S. A., and N. H. Rofail, "The Thermal Decomposition of Ammonium Uranates Precipitated from Sulphate and Nitrate Media by Urea," Thermochimica Acta, 67, 137 (1986).

5-25. Woolfrey, J. L., "The Preparation of UO_2Powder: Effect of Ammonium Uranate Properties," J. of Nuclear Materials, 74, 123 (1978).

5-26. Woolfrey, J. L., "Surface Area Changes During the Thermal Decomposition of Ammonium Uranate," J. of Inorganic and Nuclear Chemistry, 38, 347 (1976).

5-27. Dobson, J. C., and L. C. Brown, "Fissile Fuel Kernel Production Technology," GA Document 90440, Rev. A, August 6, 1980.

6-1. LeFevre, R. L., and M. S. T. Price, "Coated Nuclear Fuel Particles: The Coating Process and Its Model," Nuclear Technology, September 1977.

6-2. Scheffel, W., and I. Tang, "Technical Support Document of the MHTGR Fuel Production Specification," GA Document 903728, Rev. D, June 1989.

7-1. Kovacs, W. J., and D. P. Harmon, "Irradiation Induced Dimensional Changes in HTGR Fuel Rods," GA Document 904308, Issue B, December 1979.

7-2. Johnson, W. R., "Thermal Conductivity of Large HTGR Fuel Rods," ERDA Report GA-A12910A (GA-LTR-9), January 1976.

7-3. DeVelasco, R. I., "Test Specification for Rod Fabrication Process Development," GA Document 909212, Rev. N/C, December 1986.

7-4. DeVelasco, R. I., "MHTGR Fuel Compact Process Specification," GA Document 909548, Issue 0, September 25, 1987.

7-5. Young, C. A., "Capsule HRB-21 Preirradiation Report," GA Document DOE-HTGR-88357, Issue B, February 8, 1991.

7-6. Scheffel, W. J., and I. M. Tang, "Fuel Product Specification for MHTGR," GA Document DOE-HTGR-86081, Rev. F, June 1989.

7-7. "Public Service Company of Colorado 330 MW(e) High-Temperature Gas-Cooled Reactor Research and Development Program - Quarterly Progress Report for the Period Ending June 30, 1969," USAEC Report GA-9440, July 31, 1969, pp. 67-123.

7-8. Scheffel, W. J., and I. M. Tang, "Technical Support Document of the MHTGR Fuel Production Specification," GA Document 903728, Rev. D, June 1989.

9-1. Juran, J. M., Quality Control Handbook, McGraw Hill Book Company, New York, 1962 (2nd Ed.).

9-2. U.S. Government Military Standard 105E, "Sampling Procedures and Tables for Inspection by Attributes," MIL-STD-105D, April 1985.

A-1. Hall, Peter, Rates of Conversions in the Central Limits Thorem, Pitman Publishing Company, Massachusetts, 1982.

A-2. U.S. Government Military Standard 414, "American National Standard Sampling Procedure and Tables for Inspection by Variables for Percent Defective," MIL-STD-414, June 1957.

APPENDIX A
ATTRIBUTE AND VARIABLE SAMPLING

A.1. ATTRIBUTE SAMPLING

A.1.1. Application

Attribute sampling is based on random sampling of a discrete quantity that is classed as either defective or nondefective; e.g., the selection of black versus white, or cracked versus uncracked. This type of inspection defines a sharp division as to what constitutes a defective property. A continuous range of values is not considered. Attribute sampling can be applied to any property provided a definition of what constitutes a defective item is made. No assumption is made as to the distribution of a property. Attribute sampling represents a truly general approach.

The easiest type of sampling plan to design is a lot-by-lot inspection of attributes. A lot is defined as N_T similar items, and the plan is to randomly select a single sample of N items ($N < N_T$) from the lot. The N items are inspected, and the number of defectives, a, is noted. This number is compared with a preestablished level of acceptable defects $a_{(d)}$, and the following decisions are made:

If $a < a_{(d)}$, accept the lot,
If $a > a_{(d)}$, reject the lot.

The best estimate of the fraction defective in a lot (P) is a/N. However, since $N < N_T$, there are manufacturer and consumer risks associated with the above decisions. Namely, there are probabilities associated with the rejection of good material (termed manufacturer's risk) and acceptance of bad material (termed consumer's risk). These

risks are quantified through construction of an operating characteristic (OC) curve. Figure A-1 highlights the critical parameters in an OC curve. The parameters β and P_2 are stipulated in the product specification, where β is the probability of accepting a batch with the fraction P_2 of the population defective. The quantities α and P_1 are determined by the manufacturer, where α is the probability of rejecting a batch with the fraction P_1 defective and $P_1 < P_2$. The manufacturer determines α and P_1 based on an economic analysis of his risk.

Given these parameters, the objective of an attribute sampling plan is to determine appropriate (a,N) combinations for lot acceptance. The OC curve for attribute sampling is defined from the cumulative binomial distribution (Ref. 9-1) as follows:

$$L(p) = \sum_{a=0}^{a(d)} \frac{N!}{a!\ (N - a)!} P^a \cdot (1 - P)^{N - a} \quad ,$$

where L(p) is the probability of observing $a_{(d)}$ or fewer defects in a sample size N from a very large population N_T, i.e., $N_T >> N$. Given P and $a_{(d)}$, one can solve the above relationship for the sample size N, corresponding to a given probability of acceptance, L(p).

A.1.2. Attribute Sampling Plans

Statistical quality control inspection based on attribute sampling involves setting an acceptance limit on the number of defects observed in a given sample size. This is equivalent to defining the probability of acceptance that no more than a certain percentage of material is defective, termed the lot tolerance percent defective (LTPD). Attribute sampling plans are inspection screens which define the probability of accepting (termed the consumer's risk) a given LTPD. This inspection screen is termed an operating characteristic curve (see Fig. A-1). In contrast, the probability that a given percentage of defective material exists is determined by statistical process control (SPC) charting of process capability. This is illustrated in Fig. A-2, which depicts the

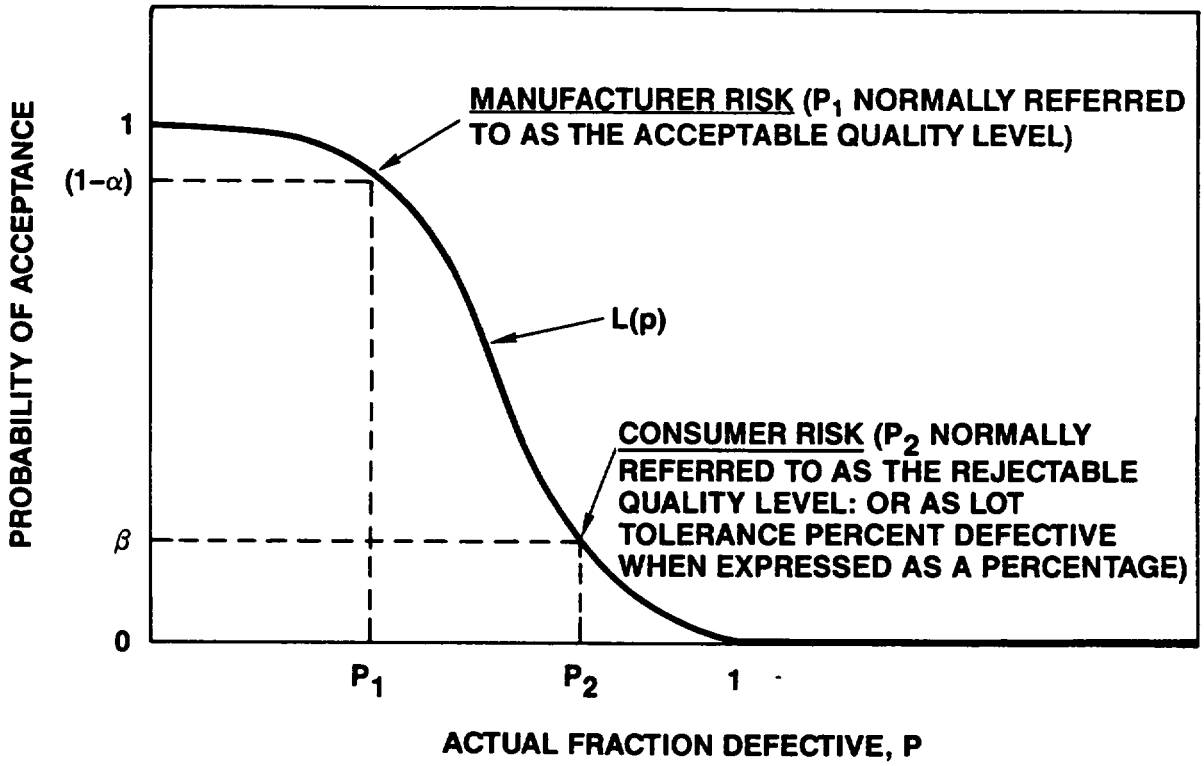

K-176(9)
8-6-91

The OC curve is determined if the distribution is known, i.e., binominal or normal, and by specifying (α, P_1) and (β, P_2) or (β, P_2) plus N (sample size).

Fig. A-1. An operating characteristic curve defines the consumer and manufacturer risks

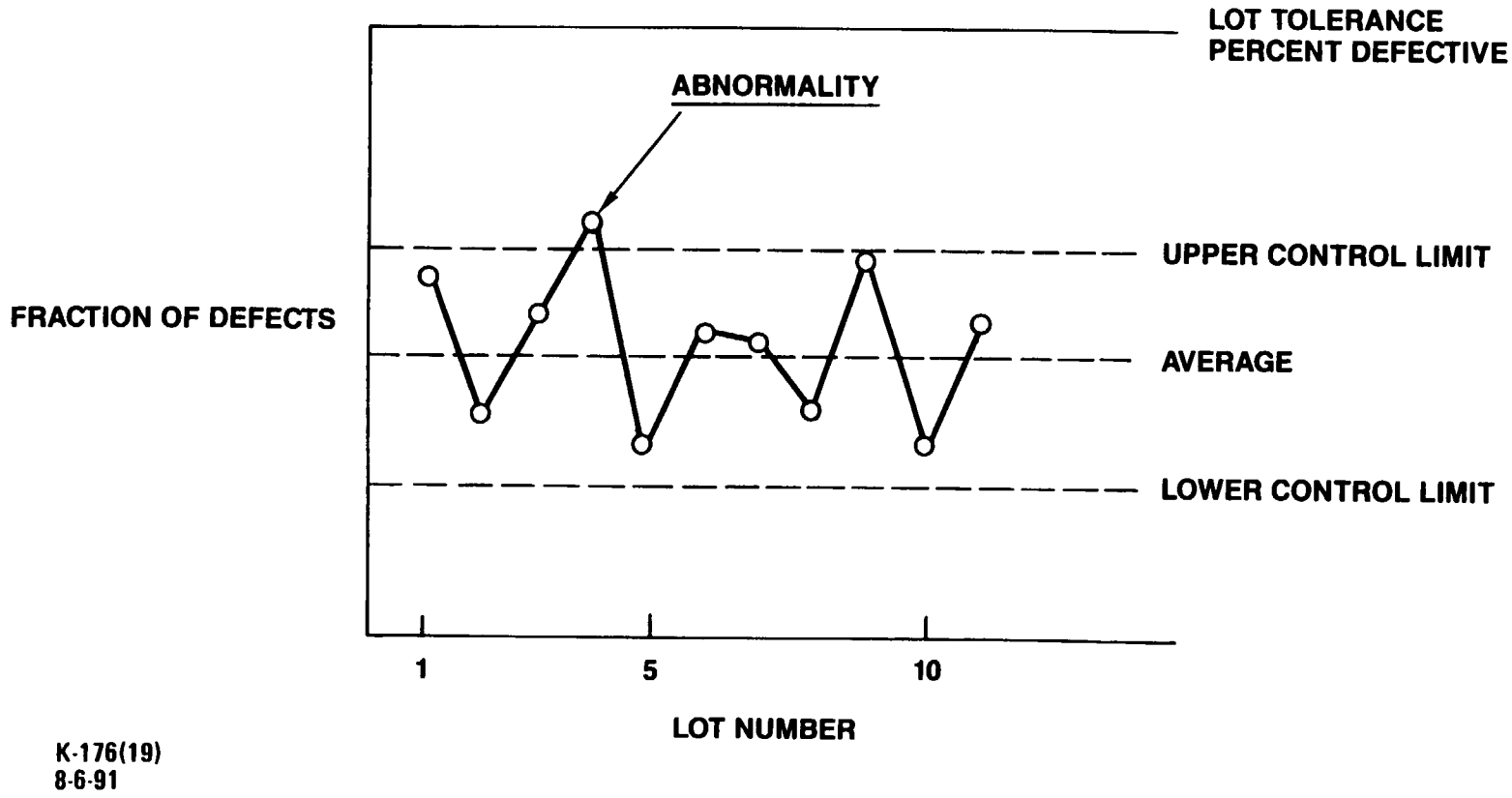

Fig. A-2. Statistical process control charting defines the probability that a given fraction of defective material exists

random lot variation of a defect fraction about the population average value. The dashed lines in this figure define a statistical boundary of acceptable variation under normal operating conditions; namely, a value such as 99.7% (3 σ) of lot defect fractions would be expected to be within these boundaries. Consequently, if a lot measurement is outside of these boundaries, a process abnormality is assumed to exist. This type of attribute SPC control chart provides a means to anticipate and correct problems before producing fuel which has a defect fraction outside the LTPD.

The average defect function is referred to as the acceptable quality level (AQL). For reduced statistical quality control inspection to be effective, the AQL generally should be less than or equal to one-fifth the LTPD. This requirement implies that statistical sampling plans are structured to verify a given quality level and not to improve quality. Specifically, as the average defect fraction increases above the expected value (AQL), the sampling plan penalizes the producer by progressively rejecting a higher percentage of lots submitted for inspection.

A.2. VARIABLE SAMPLING

A.2.1. Application

Variable sampling is used when the discrete nature of a sample property such as defective or nondefective is not of interest, but rather a continuous distribution of values such as for coating thickness is desired. In variable sampling, properties such as weight, dimensions, or density have measured values which are defined by continuous variations within a sample.

One could easily apply attribute inspection procedures by simply measuring the fraction of the population falling outside an acceptable range, but to do so would mean that some important information on variations within the acceptable range is being ignored. Having obtained

several measured values of a continuous variable, one can make statistical interferences about the distribution of the variable. The fraction outside the acceptable range can be inferred more accurately from calculations based on a measured distribution in a sample than by measuring the fraction outside acceptable limits in a sample. Consequently, variable sampling is preferred from a quality control standpoint as being more efficient and economical.

The statistical analysis is concerned mainly with a distribution function. This involves defining the distribution parameters of a continuous variable, i.e., the mean and variance. Variable sampling on a lot-by-lot basis involves measuring N items in the sample and calculating the following sample statistics:

$$\bar{X}_j = \frac{1}{N} \sum_{i=1}^{N} X_i \quad ,$$

$$(S_x)_j = \left[\frac{1}{(N - 1)} \sum_{i=1}^{N} (X_i - \bar{X}_j)^2 \right]^{1/2} \quad ,$$

where $\bar{X}_j$ and $(S_x)_j$ are the average value and standard deviation, respectively, for the jth lot, and X_i is the ith measured value of a continuous random variable X within the jth lot. Central Limit Theorems (Ref. A-1) in statistics dictate that the variable $\bar{X}_j$ is normally distributed about property mean, μ, with variance, $\simeq (S_x)^2/N$. Furthermore, the Central Limit Theorems dictate that properties will be normally distributed, provided a large number of independent variables control each property value, and no single variable dominates the property value to the exclusion of other variables. For example, in the coating of pyrocarbon and SiC layers on TRISO coated particles, the following variables affect coating thickness:

- Temperature.
- Coating rate.

- Gas composition.
- Gas pressure.
- Coating batch size.
- Particle size distribution during coating.
- Particle weight distribution during coating.
- Levitating gas flow path.

These multiple, independent variables assure that coating layer thicknesses are normally distributed.

Bounds on the mean value and variance of a population are referred to as confidence limits. These limits are determined such that the interval between limits will bound values determined from a certain fraction of samples taken from the population. Confidence limit bounds provide the framework for constructing statistical process control charts for variable measurements of mean values and standard deviations. Figure A-3 depicts random lot variations of mean values and standard deviations about their respective population averages. The dashed lines define a statistical boundary of acceptable variation under normal operating conditions; namely, 99.7% (3 σ) of lot means and standard deviations would be expected to be within these boundaries. Consequently, if a lot mean value and/or standard deviation is outside of these boundaries, the natural conclusion is that a process abnormality exists. This strategy provides a means for anticipating and correcting problems before producing fuel that is outside of specification limits.

A.2.2. Variable Sampling Plans

Two types of specifications are used to control variable properties; specifications on the mean value and specifications on the population dispersion (i.e., population variance).

A specification on a mean value is defined in terms of 95% confidence that the mean value is greater than or equal to a lower limit $\overline{X}_L$

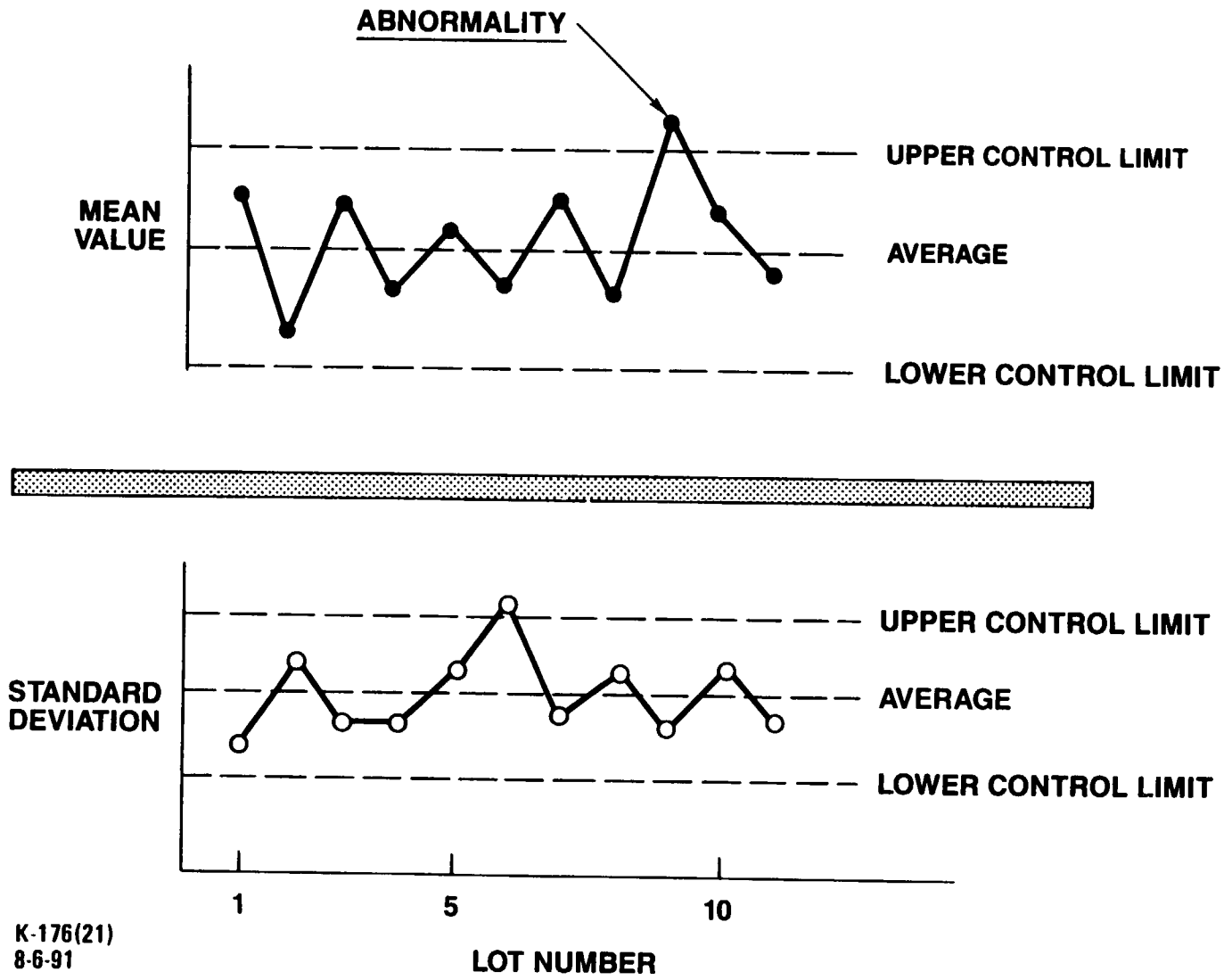

Fig. A-3. Statistical process control charting provides a method to determine if population mean values and standard deviations are within expected ranges

and/or less than or equal to an upper limit $\overline{X}_u$. (The 95% value has been selected as industry practice for nuclear fuels.) The parameters for the statistical acceptance test used in determining the acceptability of the population based on sample information are the sample size (n), the sample average value ($\overline{X}$), the sample standard deviation (S_x), and the student's t factor (t). The appropriate value of t is based on the specified confidence level, the sample size, and whether the test is one-tailed or two-tailed.

Values A and/or B are calculated, where

$$A = \overline{X} - tS_x/\sqrt{n} \quad ,$$

and

$$B = \overline{X} + tS_x/\sqrt{n} \quad .$$

If $A \geq \overline{X}_L$ and $B \leq \overline{X}_u$, as applicable, the population is accepted; otherwise, it is rejected.

The specification on population dispersion is defined in terms of 95% confidence that no more than Y% of the population is beyond either a lower critical limit X_L or an upper critical limit X_u. The parameters for the statistical acceptance test are the sample size (n), the sample mean value ($\overline{X}$), the sample standard deviation (S_x), and the tolerance factor K. The appropriate value of K is based on the specified confidence level, the fraction allowed outside the critical limit, the sample size, and whether the test is one-tailed or two-tailed. The values C and/or D are calculated where

$$C = \overline{X} - KS \quad ,$$

and

$$D = \overline{X} + KS \quad .$$

If $C \geq X_L$ and $D \leq X_u$, as applicable, the population is accepted; otherwise, it is rejected.

Figure A-4 is a plot of tolerance factor versus rejectable quality level for 95% confidence levels and sample sizes between 20 and 500 units. The figure shows a decrease in tolerance factor for an increase in the sample size or the rejectable quality level. As sample sizes increase above 500, the tolerance factors rapidly converge to the standard normal deviate factors for a known population. The tolerance factors shown in Fig. A-4 are consistent with those determined for variable sampling plans determined from MIL-STD-414 (Ref. A-2).

The values of t and K to be used in the statistical tests described above are obtained from standard statistical tables.

A.2.3. Restrictions of Normality on Variable Sampling

Variable sampling is based on the assumption of a normally distributed property. Consequently, when variable sampling is employed, a statistical test should be used to verify this assumption. If normality is rejected, the type of departure from normality and the effect on the statistical methods must be evaluated. The effect of departure from normality is discussed below with emphasis on whether or not a normal distribution is conservative. The following distributions are compared to a normal distribution:

- Rectangular distribution (equal frequency of occurrence over the entire property range).

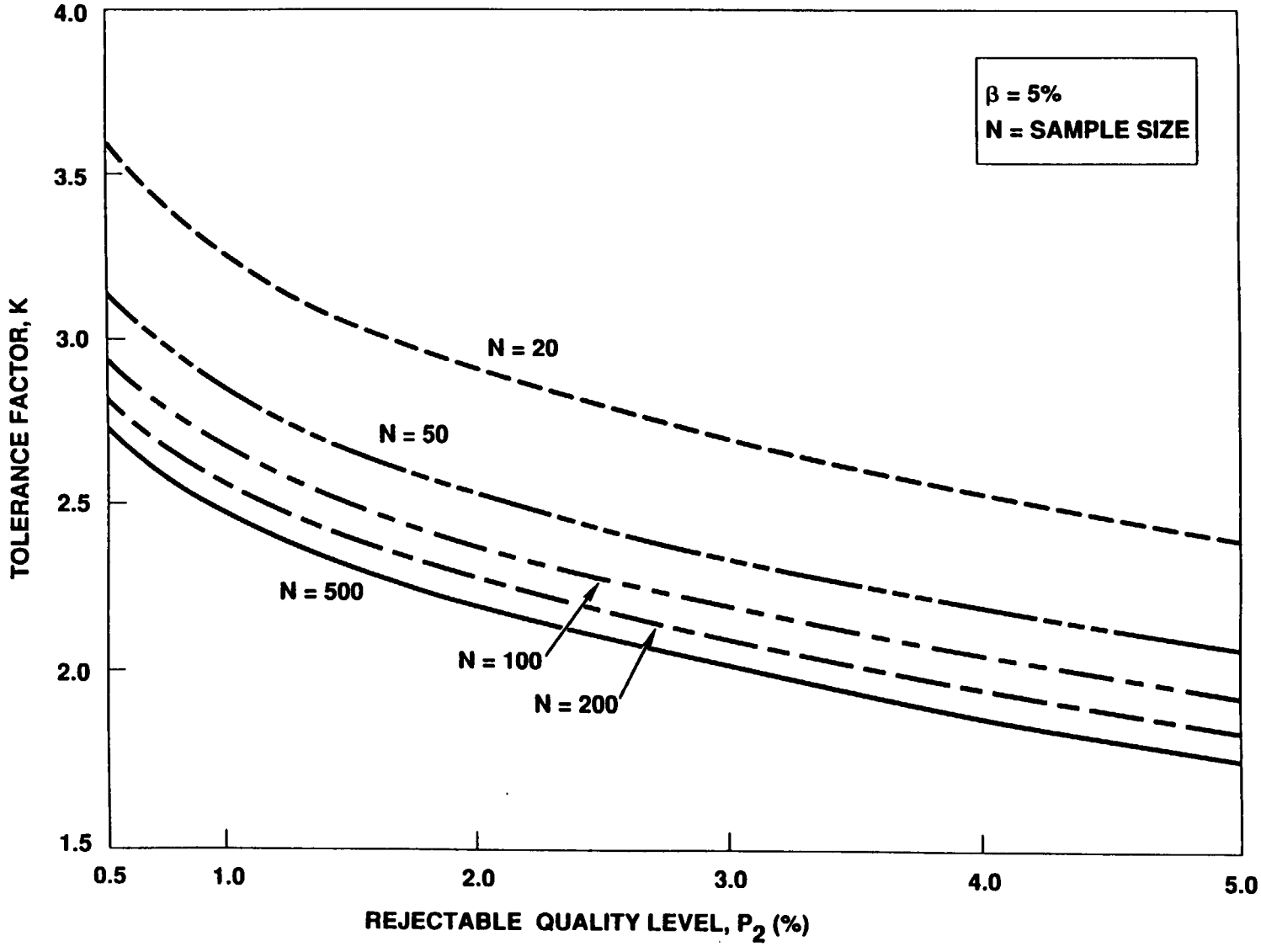

Fig. A-4. Tolerance factor versus rejectable quality level for a 95% confidence bound

- Triangular distribution (symmetric frequency distribution with a linear decrease in frequency from the mean value for either an increase or decrease in the property value).

- Bimodal distribution (a secondary frequency peak offset from the primary peak).

Figure A-5 shows the property frequencies for these distributions (solid curves) compared to the assumption that the property is normally distributed. This figure shows that the normal distribution has tails beyond the property ranges of either the rectangular or triangular distribution. Quantitatively, it can be shown that the normal distribution will estimate a fraction defective equal to or greater than the true fraction defective for defective fractions up to approximately 0.0125.

This results in the conclusion that variable sampling is adequate to detect batches with excessive defects for distributions which are actually rectangular or triangular, provided the rejectable quality level (p_2) is specified at <0.0125.

The bimodal distribution represents a different case. This is illustrated in Fig. A-5, which shows that the tail of the normal distribution (dashed line) does not extend beyond the secondary peak of the bimodal distribution. A decision on whether the normal distribution estimates a fraction defective equal to or greater than the actual defect fraction depends on: (1) the rejectable quality level (p_2) and (2) the actual fraction defective in the secondary peak (γ).

It can be shown that variable sampling is adequate to detect batches with excessive defects for bimodal distributions where the actual defects in secondary peak are less than or equal to the

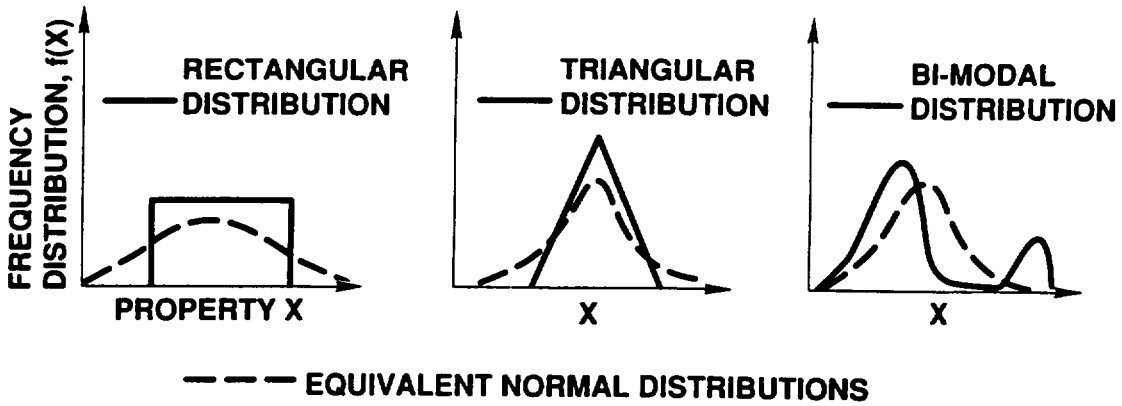

Fig. A-5. Comparative evaluation of non-normal and equivalent normal distributions

rejectable quality level, P_2. If the above condition is not met, then the producer may exercise one of the following options.

1. Apply variable sampling exclusively to that fraction of the population in the secondary peak of the bimodal distribution. For example, if the secondary peak contains X fraction of the population, then the producer may want to specify that no more than Y fraction of the secondary peak population is outside the critical limit. This would have the overall effect of assuring that the total population contains $<X \cdot Y$ fraction defects, provided the primary peak does not contribute to defects. If this option is selected, standard variable sampling techniques are applied to the secondary peak population, i.e., the producer defines an acceptable property range around the secondary peak and calculates the mean and variance. The rejectable quality level imposed on this population is then multiplied by a weighting factor equal to the fraction of the total population in the secondary population.

2. Apply an empirical correction factor to the normal distribution to assure that it encompasses an acceptable fraction of defects in the outlying secondary peak. For example, the standard deviation of the normal distribution could be multiplied by a factor greater than one to assure that the estimated fraction defects are greater than or equal to the actual fraction defects. This empirical factor is determined by a trial and error approach. The producer than applies standard variable sampling techniques for the normal distribution with an empirically corrected standard deviation.

The rectangular, triangular, and bimodal distribution are the most likely nonnormal property distributions that might be encountered during production. However, with rare exceptions under steady-state, well-controlled production operating conditions, the normal distribution of properties is to be expected.

A.3. STATISTICAL PROCESS CONTROL

Figure A-6 illustrates how SPC production control charts are defined. Individual data points on the chart represent separate lots, composites, or batches with measured values of P, $\overline{X}$, S, or ($\overline{X} \pm k\ S$). Upper and lower control limits are assessed to assure that 99.7% of all future measured values will be between these limits (dashed lines), and that the control limits are well within the specification limits for normal production. Consequently, if a measured lot, composite or batch is beyond these limits, a potential production abnormality is assumed to exist and corrective action is taken before violation of a MHTGR fuel specification limit.

This approach is illustrated in Fig. A-7, which shows process and product SPC charting for TRISO coated fissile or fertile fuel. A variable SPC control chart is used to monitor coating rate process consistency. In turn, coating rate for a TRISO layer is dependent on gas concentration and pressure, batch size, and the time of coating. Consequently, if there is consistency in these process parameters (process sampling in Fig. A-8), coating rate would be expected to vary within the statistical process control envelope of acceptability. Control of coating rate provides high assurance that the coating layer thickness and density are within the established normal boundary of variation of these product characteristics. This is illustrated by variable SPC charting (product sampling) of these characteristics in Fig. A-7.

The important point is that consistency of process parameters needed to assure product quality levels is independently verified by monitoring product characteristics; for example, high coating rates for a fixed batch coating time would reproduce higher than average coating thicknesses. Consequently,, analytical cross-checks can be developed in the computerized quality control data acquisition inspection system to verify self-consistency between the process and product characteristics being monitored.

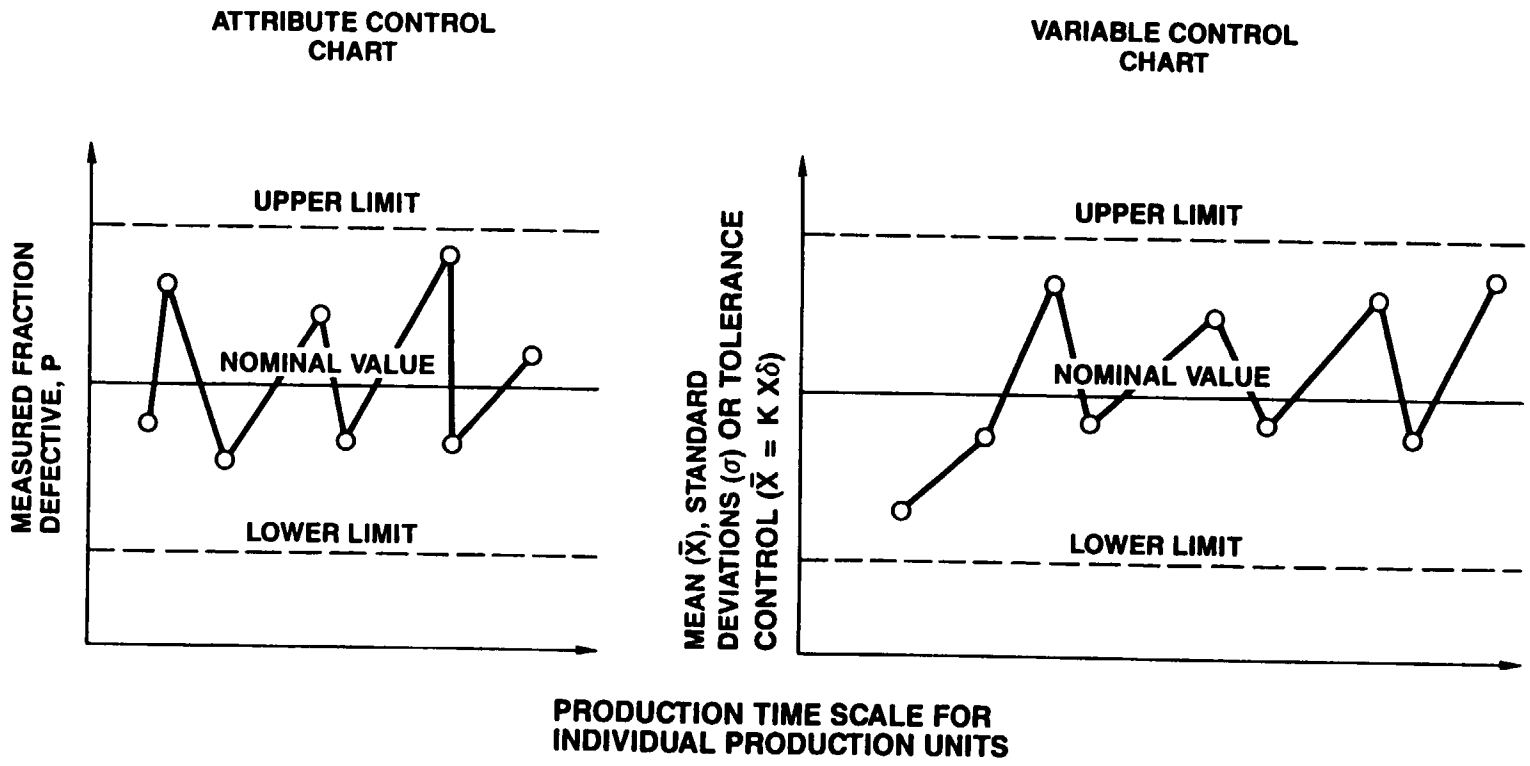

Fig. A-6. SPC control charts for attribute or variable sampling measurements

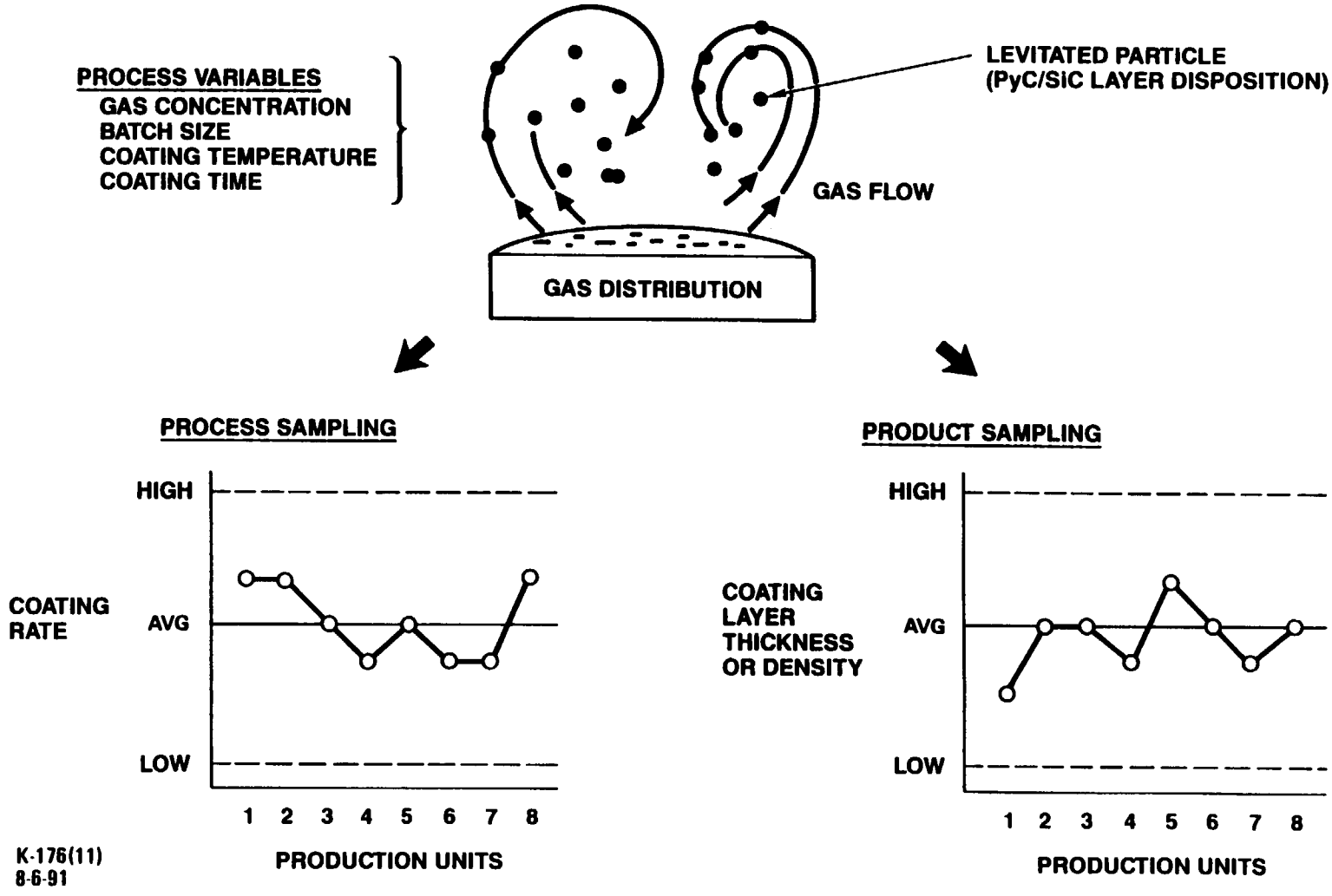

Fig. A-7. Real-time SPC charting monitors process and product characteristics

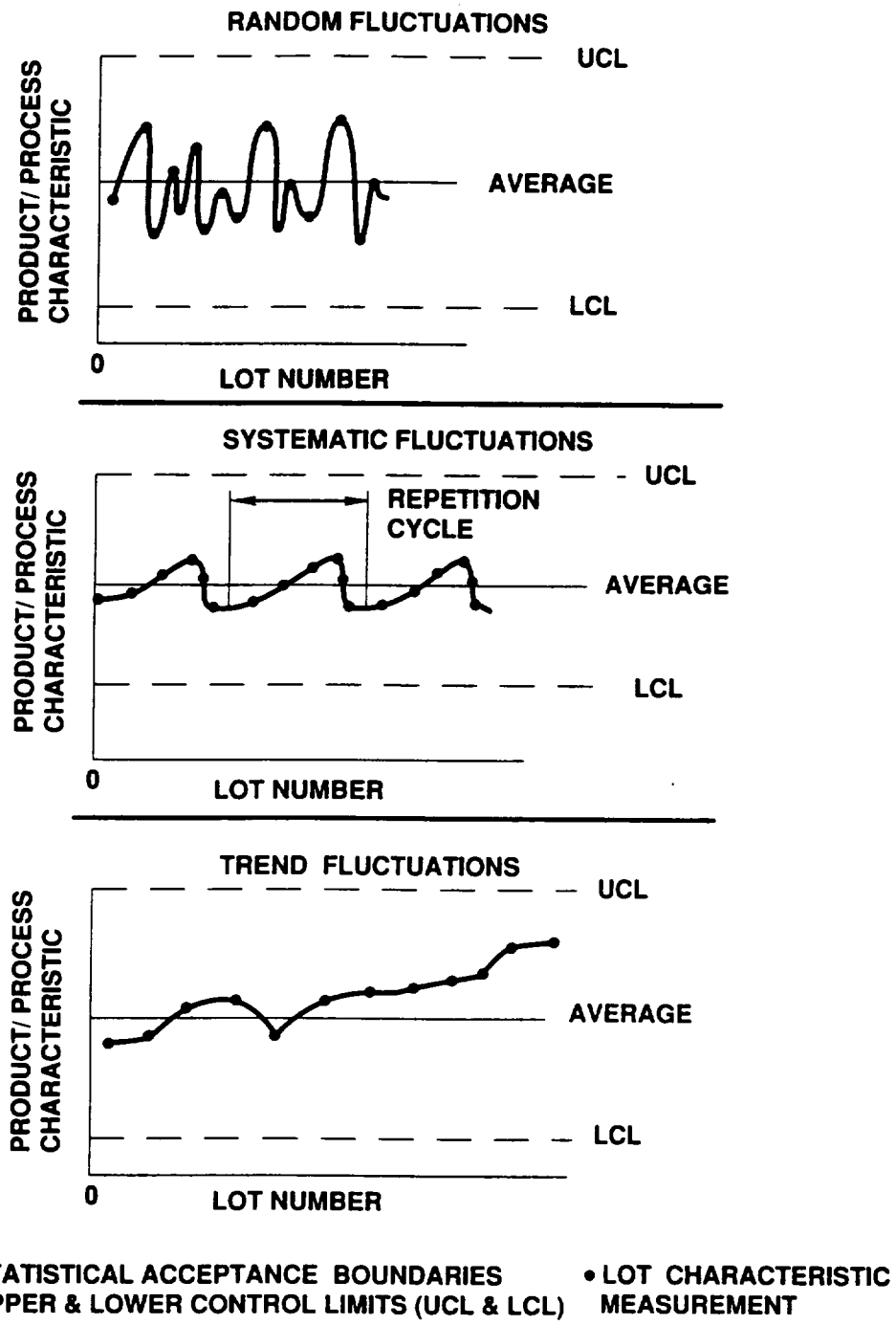

Fig. A-8. SPC charts show process and product characteristic variations

The real-time SPC monitoring system also provides the ability to distinguish between different process and product characteristic patterns that may develop during normal production. These patterns are graphically illustrated in Fig. A-8, which shows random, systematic, and trend fluctuations. The ability to quickly react to these trends during production provides a real-time process control system that anticipates and corrects process abnormalities before producing discrepant material.

APPENDIX B
LIST OF ACRONYMS AND ABBREVIATIONS

ADU	ammonium diuranate
ADUN	acid deficient uranyl nitrate
AOQL	average outgoing quality limit
AQL	acceptable quality level
AU	ammonium uranate
AVR	Arbeitsgemeinschaft Vesuch Reaktor
CVD	chemical vapor deposited (coating)
DoD	Department of Defense
DOE	Department of Energy
DU	depleted uranium
EAB	exclusion area boundary
EPZ	emergency planning zone
FHT	final heat treatment
FRG	Federal Republic of Germany
FSV	Fort St. Vrain
GA	General Atomics
GSP	gel-supported precipitation
HEU	high-enriched uranium
HM	heavy metal
HOBEG	Hochtemperaturreaktor Brennelement Gressellshaft (Hanau, Germany)
HTGR	high-temperature gas-cooled reactor
HVAC	heating, ventilating, and air conditioning
IPA	isopropyl alcohol
IPyC	inner pyrocarbon coating
ISI	in-service inspection
LBE	licensing base event
LEL	low level explosive limit
LTPD	lot tolerance percent defective

MHTGR	Modular High-Temperature Gas-Cooled Reactor
MTS	metyltricholorosilane
NEPA	National Environmental Protection Act
NPR	New Production Reactor
NQA	nuclear quality assurance
OPyC	outer pyrocarbon coating
OSHA	Occupational Safety and Health Act
PAG	protective action guide
PPyC	protective low-density pyrocarbon coating
PVA	polyvinyl alcohol
PyC	pyrocarbon coating
QAPD	Quality Assurance Program Document
QAR	Quality Assurance Requirements Document
R/B	release-to-birth ratio or fission gas release
SNM	special nuclear material
SPC	statistical process control
THFA	tetrayhydrofurfuryl alcohol
TRISO	multilayered fuel-particle coating of pyrolytic carbon and silicon carbide
UCO	uranium oxycarbide
UNH	uranyl nitrate
WA	work authorization